THE UNIVERSITY OF CALGARY

Group-Blind Multiuser Detection for CDMA Systems

by

Jae-Chon Yu

A THESIS

SUBMITTED TO THE FACULTY OF GRADUATE STUDIES

IN PARTIAL FULFILLMENT OF THE REQUIREMENTS FOR THE

DEGREE OF MASTER OF SCIENCE

DEPARTMENT OF ELECTRICAL AND COMPUTER ENGINEERING

CALGARY, ALBERTA

JANUARY, 2001

Abstract

We will discuss group-blind multiuser detectors which can reduce intra-cell and inter-cell interference efficiently. These detectors have better performance compared to conventional multiuser detectors and combat the near-far problem. Estimated group-blind multiuser detectors which use blind channel estimation and subspace tracking algorithm are proposed for real time implementation in DS-CDMA systems. These estimated group-blind multiuser detectors have reasonable performance with low calculation complexity.

Due to the asymmetric allocation of uplink and downlink time slots in Universal Mobile Telecommunications System Terrestrial Radio Access Time Division Duplex (UTRA-TDD), the performance of mobile stations can be degraded seriously by inter-cell interference. Group-blind multiuser detectors are therefore proposed to mitigate this problem.

Acknowledgments

The author would like to thank Dr. Anders Høst-Madsen for his supervision and guidance of the work presented in this thesis. The author would also like to thank TRLabs and the University of Calgary for their funding support. Finally, this work would never have been completed without the encouragement, understanding, and love of my dear wife, So-Young.

To So-Young

Contents

List of Figures

List of Tables

Chapter 1

Direct Sequence Code Division Multiple Access (DS-CDMA)

1.1 Introduction

Over the last decade, the demand for wireless communications has increased dramatically. To meet the demand for wireless communications, many techniques have been developed. People want to communicate with anyone, at any time, and anywhere. To meet these goals, better communications techniques should be developed. Wireless communications technology is generally more expensive, and its quality is generally inferior to wired communications technology. In addition, as bandwidth is at a premium, spectral efficiency is increasingly important. Therefore, research is needed to improve wireless communications technology.

Among varieties of code division multiple access (CDMA) technology, direct sequence code division multiple access (DS-CDMA) is a popular and new wireless technology. The basic concept of CDMA is to multiplex users by unique spreading codes. This is unlike frequency division multiple access (FDMA) and time division multiple access (TDMA). The significant improvement in performance and capacity is the most attractive property of DS-CDMA systems.

Multiple access interference (MAI) is the most significant capacity limiting factor in a conventional DS-CDMA system. To mitigate MAI, many multiuser detectors have been introduced such as the optimum multiuser detector, suboptimum multiuser detectors, and blind multiuser detectors.

1.2 CDMA Systems

1.2.1 History of CDMA

Spread spectrum communications originated in the military field. Due to the anti-jamming property, spread spectrum communications is well suited for telecommunications applications where there exist dispersive channels in cellular systems.

CDMA developed from the Shannon theorem [1]. In 1949, the basic ideas of CDMA were introduced by Claude Shannon and Robert Pierce. They described the interference averaging effect and graceful degradation of CDMA [2]. A direct

sequence spread spectrum system was proposed by Tosa-Rogoff in 1950, and the processing gain equation and noise multiplexing idea were introduced [3]. In 1956, Price and Green patented the anti-multipath "Rake" receiver, which can resolve signals from different propagation paths. Magnuski first mentioned the near-far problem, i.e., a high power interference degrading a weak signal [3]. In 1978, Cooper and Nettleton introduced spread spectrum communications for cellular applications [4]. Qualcomm developed DS-CDMA techniques during the 1980s, which made the commercialization of cellular spread spectrum communications possible. In 1996, commercial operation of narrowband CDMA IS-95 systems began. Verdu introduced optimum multiuser detection in an additive white Gaussian noise channel in 1986 and extensive research followed [5].

During the 1990s, wideband CDMA was developed over the world: cdma2000 and W-CDMA/NA in the United States, UTRA in Europe, W-CDMA in Japan, TD-SCDMA in China, and CDMA I and CDMA II in Korea. Commercial operation of wideband CDMA is expected to commence in 2001.

1.2.2 CDMA concept

In CDMA, each user is allocated a unique spreading code to spread his information bits. At the receiver, the unique spreading code is used to despread the information bits. Small correlation between this unique spreading code and that of other users make this possible. CDMA is also known spread spectrum

communications because it spreads the information bit with a unique spreading code and makes the bandwidth of the information bit larger. CDMA is often called spread spectrum multiple access (SSMA).

Spread spreading techniques make multiple access possible because of the unique spreading sequence. A spread spectrum technique must satisfy following properties:

- The bandwidth of the transmitted signal must be larger that the bandwidth of the information bits.
- The radio-frequency bandwidth does not depend on the bandwidth of the information bits.

The processing gain is the ratio of the bandwidth of the spread signal to the bandwidth of information bits:

$$PG = \frac{B_s}{B_i}$$

Where B_s is the bandwidth of the spread signal and B_i is the bandwidth of the information bit. Since a spread spectrum signal has a much larger bandwidth than the narrow bandwidth signal, there are many features characterizing a spread spectrum signal. The features of the spread spectrum technique are described as follows.

- **Multiple Access:** Spread spectrum techniques have multiple access ca-

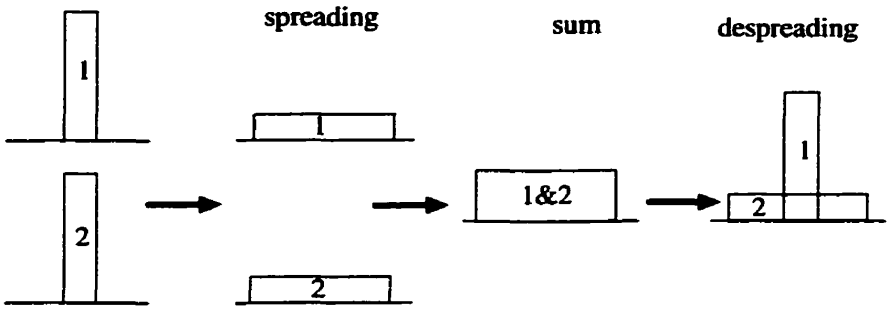

Figure 1.1: Principle of spread spectrum multiple access

pability. Although multiple users transmit their signals at the same time and with the same frequency, the receiver can recognize desired users signal exactly because it uses a unique spreading code. Figure 1.1 shows that the multiple access capability of spread spectrum technique. Each spread signal was sent through channels and the received signal is the summation of two spread signals (1&2). At the receiver, the signal of user 1 can be extracted by despreading the spread signal remaining the signal of user 2 spread. This is the principle of spread spectrum multiple access.

- **Multipath Interference Resistance:** There are some different paths between transmitter and receiver in a radio channel because of reflections, diffraction, and scattering. The signals from different paths are all copies of the same transmitted signal with different amplitudes, phases, delays, and arrival angles. At the receiver, the sum of these signals result in a dispersed signal. Spread spectrum technique can combat this multipath interference well.

- **Interference Rejection:** Interference can be reduced by despreading at the receiver. Cross-correlating interference will spread the power of interference over the noise level.

- **Anti-Jamming:** If interference was made by an enemy on purpose in a military scenario, cross-correlating this interference will reduce the power of interference. This is very attractive in military field.

- **Privacy:** The transmitted signal can only be despread with its own spreading code.

There are many techniques to generate the spread spectrum signals: direct sequence spread spectrum, frequency hopping spread spectrum, time hopping spreading spectrum, and hybrid spread spectrum. In next section, we will discuss direct sequence spread spectrum briefly.

1.2.3 DS-CDMA

In DS-CDMA systems, the data signal is directly spread by a digital spreading code. In most cases, the data signal is digital. Figure 1.2(a) depicts a block diagram of a DS-CDMA transmitter. The data signal is spread by a spreading code consisting of a number of code bits called "chips". Then the spread signal modulates a radio frequency carrier. The chip rate of the spreading code should be much higher than that of information bits to obtain the desired spreading

of the signal. For the spreading modulation, various modulation techniques are used such as binary phase shift keying (BPSK), differential binary phase shift keying (D-BPSK), quadrature phase shift keying (QPSK), or minimum shift keying (MSK). In Figure 1.2(b), the receiver employ demodulation first and uses coherent demodulation to despread the spread spectrum signal. The receiver must not only generate the spreading code but also synchronize the spreading code with the received signal. After synchronization, the tracking is used to maintain the synchronization. After despread, the transmitted data signal is obtained.

We have discussed the features of spread spectrum signals in previous section, Now, we describe some advantages and drawbacks. First of all, the advantages are as follows:

- It is possible to demodulate coherently.
- No synchronization is needed among many users
- By simple multiplication, spreading can be implemented easily
- All users share the same frequency. So, the frequency synthesizer is simple.

Second of all, the drawbacks are as follows.

- There exists the near-far problem. If we assume that all users transmit the same power, the received power of the users close to the base station

are much higher than the users far from the base station. The users close to the base station may seriously interfere with the users far from the base station. This near-far problem can be solved by power control or multiuser detection.

- It is difficult to acquire and maintain the synchronization of the received signal and the spreading code.

1.3 Summary of the Literature

Over the last decade, many alternative receivers to improve DS-CDMA systems have been studied. For cases in which the spreading codes of other users are not available, single-user detectors which improve upon the conventional detector have been proposed [6, 7, 8]. Verdu first introduced the optimum multiuser detector, which consists of a bank of matched filters followed by a Viterbi algorithm [5]. This detector uses maximum likelihood sequence detection which has exponential calculation complexity with respect to the number of users. With this detector, performance increases dramatically at the risk of calculation complexity. For the trade-off between calculation complexity and performance, many suboptimum multiuser detectors have been studied.

We can classify most of the proposed detectors in one of two categories: linear multiuser detectors and subtractive interference cancellation detectors.

The basic idea of subtractive interference cancellation detection is the creation of separate estimates of the MAI in order to subtract out the MAI seen by each user. The successive interference cancellation (SIC) detector was introduced in [9, 10]. This detector subtracts out the MAI successively. The parallel interference cancellation (PIC) detector was introduced in [10, 11]. This detector subtracts out the MAI in parallel. For linear multiuser detection, a linear mapping is applied to the soft outputs matched filters or to the received signal directly so as to reduce the MAI. Since the MAI is time varying, this strategy involves the difficulty of computing the linear mapping in real time.

The decorrelating detector (zero-forcing detector) was introduced in [12] and was analyzed by Lupas and Verdu for synchronous [13] and asynchronous [14] channels. The basic idea of the decorrelating detector is to map the inverse matrix $\mathbf{R}$ (cross-correlation matrix of spreading codes) so as to decorrelate the users. This detector has substantial performance gains over the conventional detector and near-far problem resistance while maintaining lower complexity than the optimum detector. However, it has the drawback of enhancing the noise. Another suboptimum multiuser detector is the minimum mean square error (MMSE) detector, which applies a modified the inverse matrix of $\mathbf{R}$ to the matched filter outputs [15]. This detector has near-far problem resistance and better performance than the decorrelating detector in the presence of noise.

The blind MMSE multiuser detection was introduced by M. Honig [16]. This

detector can reduce the MAI with the prior knowledge of only the signature waveform. A blind MMSE multiuser detector based on signal subspace estimation, which has a high-resolution, was introduced by Wang and Poor [17]. Semi-blind multiuser detectors using the subspace method were proposed by Høst-Madsen in [19]. The name of these detectors were changed to group-blind multiuser detectors because they group known users and unknown users from adjacent cells. These detectors are well suited for base stations and use blind techniques to suppress the inter-cell interference from adjacent cells and zero-forcing/MMSE techniques to eliminate intra-cell interference of known users. The group-blind multiuser detector has extended for asynchronous DS-CDMA system with multipath channels in [20]. For real time systems, subspace tracking algorithms in group-blind multiuser detectors were considered in [21, 22, 23]. As well, the performance of blind and group-blind multiuser detectors were recently studied [24].

1.4 Objectives

The objective of this thesis is to make some further developments of the group-blind multiuser detector for applications in practical CDMA systems. We will make two developments in this direction: development of subspace tracking algorithms and analyzing application of the group-blind multiuser detector to UTRA-TDD.

First, we will make two developments of subspace tracking algorithms: FASIR and NA-CSVD. Due to changing multipath and moving mobile stations in wireless communications, the channel is non-stationary. In addition, using SVD for subspace decomposition in non-stationary channel is too complex and time-consuming. Therefore, a tracking algorithm tracking the exact channel and reducing the calculation complexity for the non-stationary channel is needed.

Second, we will analyze the application of the group-blind multiuser detector to UTRA-TDD. UTRA-TDD systems have a serious inter-cell interference problem because of asymmetric uplink and downlink allocation. An application of the group-blind multiuser detector, which has a good performance in the presence of inter-cell interference, will be analyzed.

1.5 Outline

In Chapter 2, multiuser detectors in synchronous DS-CDMA systems will be introduced and evaluated by performance analysis. Chapter 3 introduces multiuser detectors in asynchronous DS-CDMA systems and analyzes their performance. In Chapter 4, multiuser detectors using the estimated correlation matrix will be discussed. Channel estimation and the subspace tracking algorithm is introduced. In Chapter 5, we discuss the group-blind multiuser detection for UTRA-TDD. Chapter 6 discusses some final considerations.

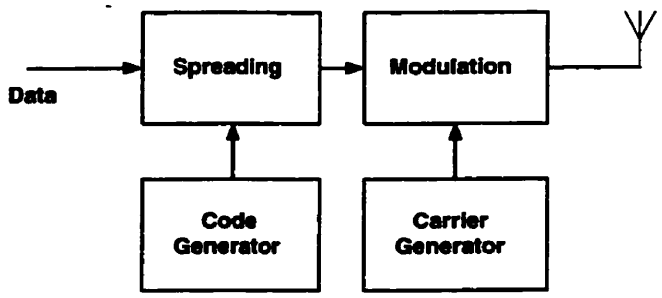

(a) Transmitter of DS-CDMA

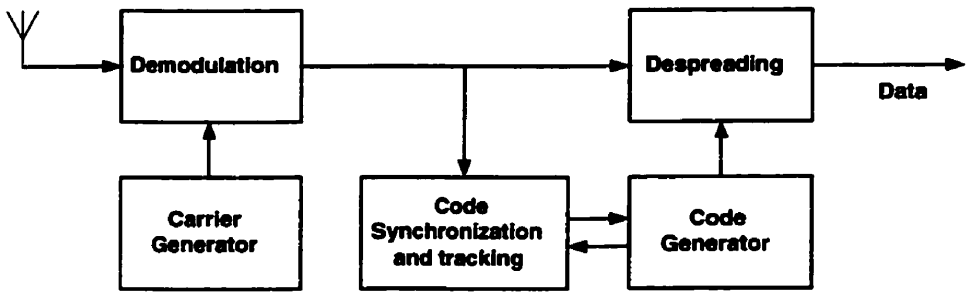

(b) Receiver of DS-CDMA

Figure 1.2: Block diagram of a DS-CDMA system

Chapter 2

Multiuser Detection for Synchronous DS-CDMA Systems

There are two types of system models in DS-CDMA systems: a synchronous system model, and an asynchronous system model. The synchronous system model is well suited for mobile stations because the received signal at the mobile stations is synchronous. The asynchronous system model is well suited for base stations because the transmitted signals from the mobile stations is asynchronous. Multiuser detectors for synchronous systems are introduced in this chapter. In chapter 3, multiuser detectors for asynchronous systems will be introduced.

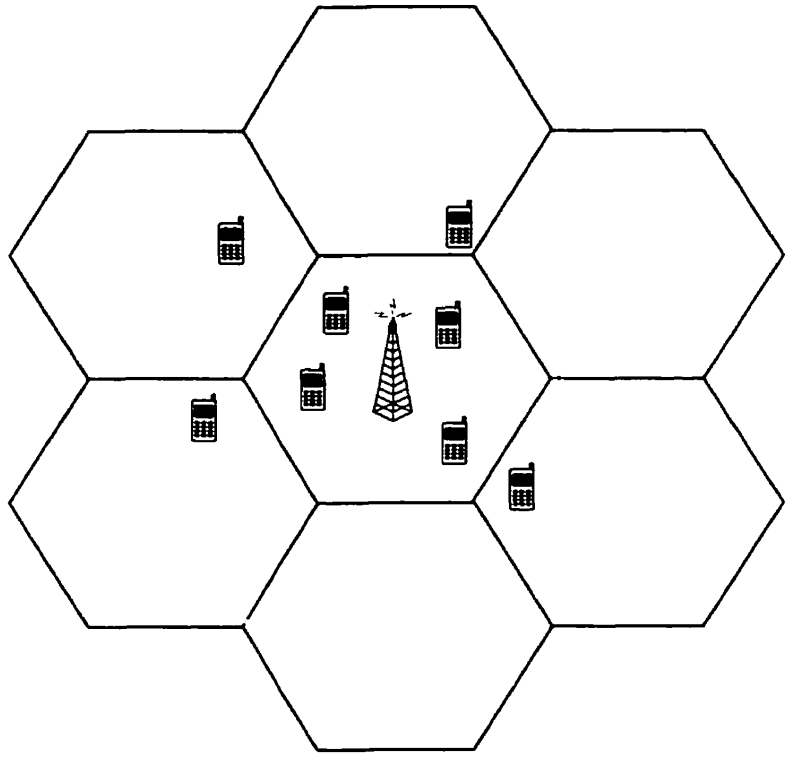

Figure 2.1: A cellular system model with intra-cell and inter-cell interference

2.1 Synchronous System Model

We first consider multiuser detectors in synchronous DS-CDMA systems. Although system models for base stations should be asynchronous in practice, we will start with a simple synchronous system model for easy understanding. Figure 2.1 shows a cellular system which has 4 users in one cell and inter-cell interference of 4 unknown users from adjacent cells. Consider a synchronous DS-CDMA system with $\bar{K}$ known users within the cell , inter-cell interference of $\tilde{K}$ users from adjacent cells, and white Gaussian noise. The received signal

from all users can be described as

$$r(t) = \sum_{k=1}^{\bar{K}} \bar{b}_k \bar{A}_k \bar{s}_k(t) + \sum_{j=1}^{\tilde{K}} \tilde{b}_j \tilde{A}_j \tilde{s}_j(t) + \sigma n(t) \tag{2.1}$$

where $\bar{b}_k$ is the information bit of the known users, $\tilde{b}_j$ the information bit of inter-cell interference, $\bar{A}_k$, $\tilde{A}_j$ are the received amplitude, $\bar{s}_k$, $\tilde{s}_k$ are the spreading sequences, and $n(t)$ is the white Gaussian noise with unit power. In DS-CDMA systems, spreading sequences can be expressed as

$$\bar{s}_k(t) = \tilde{s}_j(t) = \sum_{i=0}^{N-1} c_k^i \psi(t - iT/N) \tag{2.2}$$

where c is the code information, ± 1, ψ is the chip pulse waveform, T is the symbol duration, and N is the processing gain.

For a simple calculation, we suggest a vector communications system model where the received signal is a vector at time t. The received signal in vector form is

$$\begin{aligned} \mathbf{r} &= \sum_{k=1}^{\bar{K}} \bar{b}_k \bar{A}_k \bar{\mathbf{s}}_k + \sum_{j=1}^{\tilde{K}} \tilde{b}_j \tilde{A}_j \tilde{\mathbf{s}}_j + \sigma \mathbf{n} \\ &= \mathbf{S}\mathbf{A}\mathbf{b} + \sigma \mathbf{n} = \bar{\mathbf{S}}\bar{\mathbf{A}}\bar{\mathbf{b}} + \tilde{\mathbf{S}}\tilde{\mathbf{A}}\tilde{\mathbf{b}} + \sigma \mathbf{n} \end{aligned} \tag{2.3}$$

where $\bar{\mathbf{S}}$ is the matrix consisting of column vectors $\bar{\mathbf{s}}_k$, i.e., $\bar{\mathbf{S}} = [\bar{\mathbf{s}}_1\, \bar{\mathbf{s}}_2 \cdots \bar{\mathbf{s}}_K]$, $\tilde{\mathbf{S}}$ is the matrix consisting of column vectors $\tilde{\mathbf{s}}_k$, i.e., $\tilde{\mathbf{S}} = [\tilde{\mathbf{s}}_1\, \tilde{\mathbf{s}}_2 \cdots \tilde{\mathbf{s}}_K]$, $\bar{\mathbf{A}}, \tilde{\mathbf{A}}$ are

the diagonal matrices consisting of $\bar{A}_k, \tilde{A}_k$ respectively:

$$\begin{aligned} \bar{\mathbf{A}} &= \mathbf{diag}\left(\bar{A}_1, \bar{A}_2, \ldots, \bar{A}_K\right) \\ \tilde{\mathbf{A}} &= \mathbf{diag}\left(\tilde{A}_1, \tilde{A}_2, \ldots, \tilde{A}_{\tilde{K}}\right), \end{aligned} \tag{2.4}$$

and $\bar{\mathbf{b}}, \tilde{\mathbf{b}}$ are the information symbols for known users and unknown users. The matrices, $\mathbf{S}$ and $\mathbf{A}$, including the property of both known users and unknown users can be expressed as

$$\begin{aligned} \mathbf{S} &= [\bar{\mathbf{S}}\,\tilde{\mathbf{S}}], \\ \mathbf{A} &= \begin{bmatrix} \bar{\mathbf{A}} & \mathbf{0} \\ \mathbf{0} & \tilde{\mathbf{A}} \end{bmatrix} \\ \mathbf{b} &= \begin{bmatrix} \bar{\mathbf{b}} \\ \tilde{\mathbf{b}} \end{bmatrix}. \end{aligned} \tag{2.5}$$

For the derivation of multiuser detectors, there are two useful lemmas. The correlation matrix of the received signal can be expressed with the matrices of the spreading codes and the received amplitudes.

Lemma 1 *The correlation matrix of the received signal* $\mathbf{r}$ *can be described as*

$$\begin{aligned}\mathbf{R} = E[\mathbf{r}\mathbf{r}^T] &= \mathbf{S}\mathbf{A}^2\mathbf{S}^T + \sigma^2\mathbf{I} \\ &= \bar{\mathbf{S}}\bar{\mathbf{A}}^2\bar{\mathbf{S}}^T + \tilde{\mathbf{S}}\tilde{\mathbf{A}}^2\tilde{\mathbf{S}}^T + \sigma^2\mathbf{I} \qquad (2.6)\end{aligned}$$

□

Proof: The correlation matrix of the received signal can be written as

$$\begin{aligned}\mathbf{R} &= E[\mathbf{r}\mathbf{r}^T] = E\left[\left(\bar{\mathbf{S}}\bar{\mathbf{A}}\bar{\mathbf{b}} + \tilde{\mathbf{S}}\tilde{\mathbf{A}}\tilde{\mathbf{b}} + \sigma\mathbf{n}\right)\left(\bar{\mathbf{S}}\bar{\mathbf{A}}\bar{\mathbf{b}} + \tilde{\mathbf{S}}\tilde{\mathbf{A}}\tilde{\mathbf{b}} + \sigma\mathbf{n}\right)^T\right] \\ &= \bar{\mathbf{S}}\bar{\mathbf{A}}E[\mathbf{b}\mathbf{b}^T]\bar{\mathbf{A}}^T\bar{\mathbf{S}}^T + \bar{\mathbf{S}}\bar{\mathbf{A}}E[\mathbf{b}\tilde{\mathbf{b}}^T]\tilde{\mathbf{A}}^T\tilde{\mathbf{S}}^T + \bar{\mathbf{S}}\bar{\mathbf{A}}E[\mathbf{b}\mathbf{n}^T]\sigma \\ &+ \tilde{\mathbf{S}}\tilde{\mathbf{A}}E[\tilde{\mathbf{b}}\mathbf{b}^T]\bar{\mathbf{A}}^T\bar{\mathbf{S}}^T + \tilde{\mathbf{S}}\tilde{\mathbf{A}}E[\tilde{\mathbf{b}}\tilde{\mathbf{b}}^T]\tilde{\mathbf{A}}^T\tilde{\mathbf{S}}^T + \tilde{\mathbf{S}}\tilde{\mathbf{A}}E[\tilde{\mathbf{b}}\mathbf{n}^T]\sigma \\ &+ \sigma E[\mathbf{n}\mathbf{b}^T]\bar{\mathbf{A}}^T\bar{\mathbf{S}}^T + \sigma E[\mathbf{n}\tilde{\mathbf{b}}^T]\tilde{\mathbf{A}}^T\tilde{\mathbf{S}}^T + \sigma^2 E[\mathbf{n}\mathbf{n}^T]. \qquad (2.7)\end{aligned}$$

From the assumption that the information bits of users are independent and the information bits and noise are independent, we can obtain following equations:

$$\begin{aligned}E[\mathbf{b}\mathbf{b}^T] &= E[\tilde{\mathbf{b}}\tilde{\mathbf{b}}^T] = E[\mathbf{n}\mathbf{n}^T] = \mathbf{I} \\ E[\mathbf{b}\tilde{\mathbf{b}}^T] &= E[\tilde{\mathbf{b}}\mathbf{b}^T] = E[\mathbf{b}\mathbf{n}^T] = E[\tilde{\mathbf{b}}\mathbf{n}^T] = E[\mathbf{n}\mathbf{b}^T] = E[\mathbf{n}\tilde{\mathbf{b}}^T] = \mathbf{0}. \qquad (2.8)\end{aligned}$$

From (2.8), the correlation matrix of the received signal can be derived as

$$\mathbf{R} = \bar{\mathbf{S}}\bar{\mathbf{A}}^2\bar{\mathbf{S}}^T + \tilde{\mathbf{S}}\tilde{\mathbf{A}}^2\tilde{\mathbf{S}}^T + \sigma^2\mathbf{I}. \qquad (2.9)$$

Q.E.D.

For the high resolution of calculation, the correlation matrix of the received signal should be decomposed by eigenvalue decomposition or singular value decomposition.

Lemma 2 ***(Subspace concept 1):*** *The correlation matrix* $\mathbf{R}$ *can be decomposed into a signal subspace and noise subspace as*

$$\begin{aligned} \mathbf{R} &= \mathbf{S}\mathbf{A}^2\mathbf{S}^T + \sigma^2\mathbf{I} = \mathbf{U}\Lambda\mathbf{U}^T \\ &= [\mathbf{U}_s\mathbf{U}_n] \begin{bmatrix} \Lambda_s & \mathbf{0} \\ \mathbf{0} & \sigma^2\mathbf{I} \end{bmatrix} \begin{bmatrix} \mathbf{U}_s^T \\ \mathbf{U}_n^T \end{bmatrix} \\ &= \mathbf{U}_s\Lambda_s\mathbf{U}_s^T + \sigma^2\mathbf{U}_n\mathbf{U}_n^T \end{aligned} \tag{2.10}$$

where $\mathbf{U}_s$ *is the signal subspace eigenvector matrix,* $\mathbf{U}_n$ *is the noise subspace eigenvector matrix,* Λ_s *is the signal subspace eigenvalue matrix, and* Λ_n *is the noise subspace eigenvalue matrix.*

□

As depicted in Figure 2.2, the bases of signal space are the column vectors of $\mathbf{S}$ or $\mathbf{U}_s$ and the bases of noise space are $\mathbf{U}_n$. As well, the signal subspace and noise subspace are orthogonal.

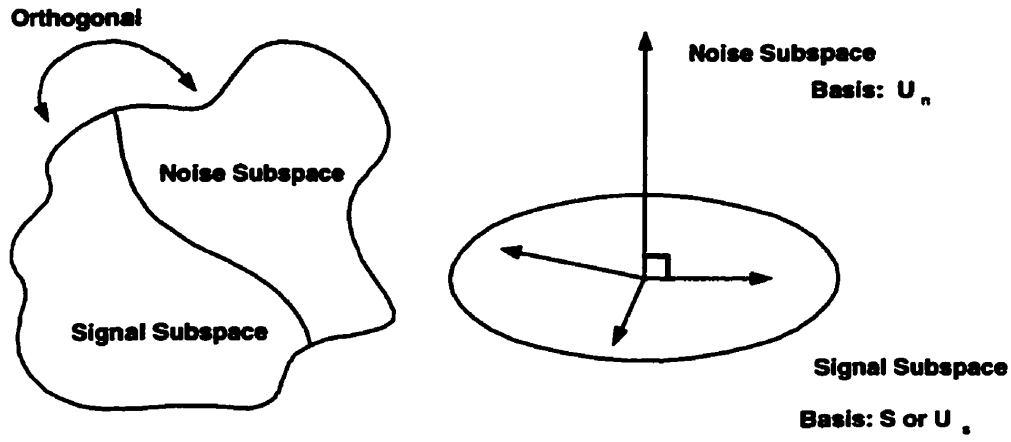

Figure 2.2: Subspace Concept 1

2.2 Linear Detectors

In this thesis, all multiuser detectors are linear detectors which use simple mapping to estimate the information bits. The estimated information bit of linear detectors for user k is given by

$$\hat{\tilde{b}}_k = \mathbf{sgn}\left(\mathbf{w}_k^T \mathbf{r}\right) \tag{2.11}$$

where $\mathbf{w}_k$ is the vector for user k and $\hat{\tilde{b}}_k$ is the estimated information bit for user k. Simple linear detectors have lower complexity and worse performance than the optimum detector.

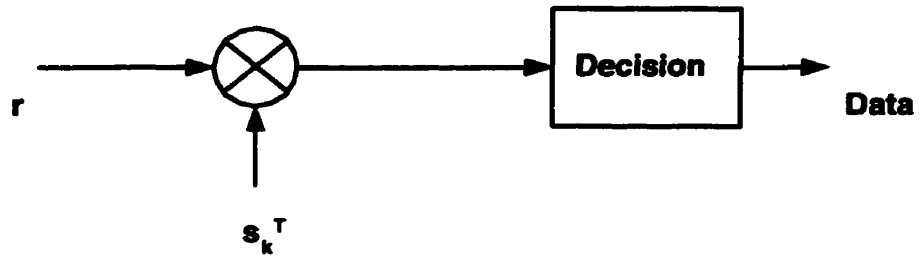

Figure 2.3: The conventional detector for DS-CDMA

2.3 Conventional Detector

In IS-95 DS-CDMA systems, the conventional detector, single user detector, is employed. The conventional detector consists of a matched filter which can despread the data signal as depicted in Figure 2.3. The regenerated spreading code is correlated with the received signal. After correlation, the decision of data is made by either hard decision or soft decision. The received signal is given in a vector form as

$$\mathbf{r} = \sum_{k=1}^{\tilde{K}} \tilde{b}_k \tilde{A}_k \tilde{\mathbf{s}}_k + \sum_{j=1}^{\tilde{K}} \tilde{b}_j \tilde{A}_j \tilde{\mathbf{s}}_j + \sigma \mathbf{n}. \tag{2.12}$$

The estimated information bit of the conventional detector is given by

$$\hat{b}_k = \mathbf{sgn}(\tilde{\mathbf{s}}_k \mathbf{r}). \tag{2.13}$$

The conventional detector is easy to implement with a matched filter (correlator). Although the conventional detector is used in IS-95 DS-CDMA systems,

it has poor performance when there exists interference from other users.

2.4 Problem of MAI

The conventional detector has a problem of MAI due to the nonorthogonality of spreading codes of users. From the fact that $\bar{\mathbf{s}}_k^T \bar{\mathbf{s}}_k = 1$, the output of the conventional detector for user 1 can be expressed as

$$A_1 b_1 + \underbrace{\sum_{k=2}^{\bar{K}} \bar{b}_k \bar{A}_k \bar{\mathbf{s}}_1^T \bar{\mathbf{s}}_k}_{intra-cell\ MAI} + \underbrace{\sum_{j=1}^{\bar{K}} \bar{b}_j \bar{A}_j \bar{\mathbf{s}}_1^T \tilde{\mathbf{s}}_j}_{inter-cell\ MAI} + \sigma \bar{\mathbf{s}}_1^T \mathbf{n}. \tag{2.14}$$

In (2.14), the first term represents the desired data for the user, the second term represents intra-cell interference from the other users of a cell, the third term represents inter-cell interference from the users of adjacent cells, and the last term represents noise multiplied by $\bar{\mathbf{s}}_1^T$.

MAI is the most significant problem in DS-CDMA systems. To reduce MAI, some approaches, such as a good cross-correlation spreading code, power control, and multiuser detection, have been introduced. In this thesis, we concentrate on multiuser detection to reduce both intra-cell and inter-cell interference.

2.5 Blind Linear Multiuser Detectors

Since base stations do not send the spreading codes of other users to mobile stations, the mobile stations should suppress interference blindly. In multiuser detection, 'blind' means that detectors know only their spreading codes and do not know the spreading codes of other users. There are two types of blind linear detectors: the blind linear minimum mean square error (MMSE) detector and the blind linear zero-forcing detector. The blind linear MMSE detector can reduce interference from all users without the spreading codes of interfering users from a MMSE perspective. The blind linear zero-forcing detector can suppress interference from all users without the spreading codes of interfering users in the sense that it forces the other users interference to zero.

2.5.1 Blind Linear MMSE Multiuser Detectors

Blind linear MMSE detectors can be defined in the sense that they minimize the mean squared error between a real information bit and an estimated information bit, as depicted in Figure 2.4. The problem is to find the mapping which minimizes the MSE.

Definition 1 *The vector of blind linear MMSE detectors can be obtained by*

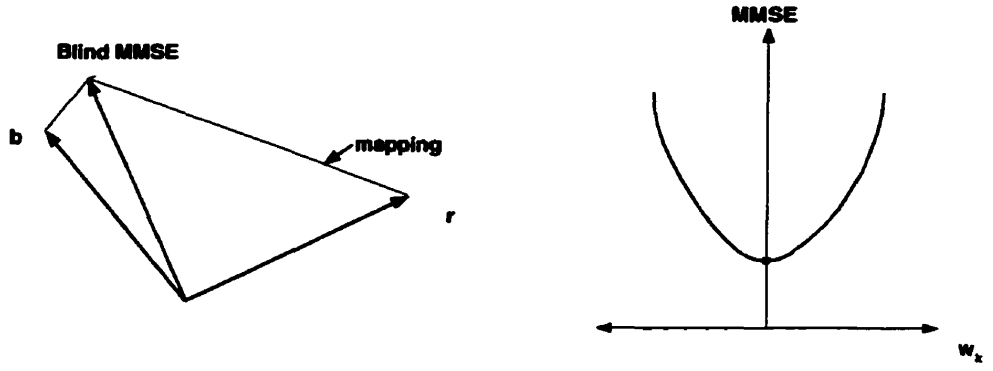

Figure 2.4: Blind MMSE detector

solving the minimization problem of the Mean Squared Error:

$$\mathbf{w}_k = \arg \min_{\mathbf{w}_k \in R^N} E\left[(\bar{b}_k - \mathbf{w}_k^T \mathbf{r})^2\right]. \tag{2.15}$$

□

There are two types of methods applicable to blind linear MMSE detectors: the direct method, using the correlation matrix directly, and the subspace method, using the signal subspace for high resolution of calculations.

Proposition 1 ***(Direct method for the blind Linear MMSE detector):*** *The estimated information bit of the blind Linear MMSE detector using the direct method can be written as*

$$\hat{\bar{b}}_k = \mathbf{sgn}\left(\bar{\mathbf{s}}_k^T \mathbf{R}^{-1} \mathbf{r}\right). \tag{2.16}$$

□

Proof: The mean squared error between the real information bit and the estimated bit is

$$\begin{aligned} & E\left[(\bar{b}_k - \mathbf{w}_k^T\mathbf{r})^2\right] \\ = \; & E\left[(\bar{b}_k - \mathbf{w}_k^T\mathbf{r})(\bar{b}_k - \mathbf{w}_k^T\mathbf{r})^T\right] \\ = \; & E\left[(\bar{b}_k - \mathbf{w}_k^T\mathbf{r})(\bar{b}_k - \mathbf{r}^T\mathbf{w}_k)\right] \\ = \; & E\left[(\bar{b}_k^2 + \mathbf{w}_k^T\mathbf{r}\mathbf{r}^T\mathbf{w}_k - 2\bar{b}_k\mathbf{w}_k^T\mathbf{r})\right] \end{aligned} \tag{2.17}$$

$$\begin{aligned} = \; & E\left[(\bar{b}_k^2 + \mathbf{w}_k^T\mathbf{r}\mathbf{r}^T\mathbf{w}_k - 2\bar{b}_k\mathbf{w}_k^T(\bar{\mathbf{S}}\bar{\mathbf{A}}\bar{\mathbf{b}} + \tilde{\mathbf{S}}\tilde{\mathbf{A}}\tilde{\mathbf{b}} + \sigma\mathbf{n}))\right] \\ = \; & (E[\bar{b}_k^2] + \mathbf{w}_k^T E[\mathbf{r}\mathbf{r}^T]\mathbf{w}_k - 2\mathbf{w}_k^T(\bar{\mathbf{S}}\bar{\mathbf{A}}E[\bar{\mathbf{b}}\bar{b}_k] + \tilde{\mathbf{S}}\tilde{\mathbf{A}}E[\tilde{\mathbf{b}}\bar{b}_k] + \sigma E[\mathbf{n}\bar{b}_k])) \end{aligned} \tag{2.18}$$

From the assumption that the information bits of users are independent and the information bits and noise are independent, we can obtain following expectations:

$$E\left[(\bar{b}_k - \mathbf{w}_k^T\mathbf{r})^2\right] = (1 + \mathbf{w}_k^T\mathbf{R}\mathbf{w}_k - 2\mathbf{w}_k^T\bar{A}_k\bar{\mathbf{s}}_k). \tag{2.19}$$

Since $\mathbf{R}$ is positive definite, the above function is convex and the vector minimizing the above function can be expressed as

$$\begin{aligned} \nabla(1 + \mathbf{w}_k^T \mathbf{R}\mathbf{w}_k - 2\mathbf{w}_k^T \bar{A}_k \bar{\mathbf{s}}_k) &= 2\mathbf{R}\mathbf{w}_k - 2\bar{A}_k\bar{\mathbf{s}}_k = 0 \\ \mathbf{R}\mathbf{w}_k &= \bar{A}_k\bar{\mathbf{s}}_k \\ \mathbf{w}_k &= \mathbf{R}^{-1}\bar{A}_k\bar{\mathbf{s}}_k. \end{aligned} \tag{2.20}$$

In this detector, we did not consider A_k because the detector uses a hard decision method.

Q.E.D.

Proposition 2 ***(Subspace method for the blind MMSE detector):*** *The estimated information bit of the blind linear MMSE detector using the subspace method can be written as*

$$\hat{\bar{b}}_k = \mathbf{sgn}\left(\bar{\mathbf{s}}_k^T \mathbf{U}_s \Lambda_s^{-1} \mathbf{U}_s^T \mathbf{r}\right). \tag{2.21}$$

□

Proof: The solution of the subspace method for the blind linear MMSE detector can be derived by substituting the result of Lemma 2 for $\mathbf{R}$ and using the fact

that $\bar{\mathbf{s}}_k^T \mathbf{U}_n = \mathbf{0}$ from Proposition 1. The inverse matrix of $\mathbf{R}$ can be derived as

$$\begin{aligned}
\mathbf{R}^{-1} &= (\mathbf{S}\mathbf{A}^2\mathbf{S}^T + \sigma^2\mathbf{I})^{-1} \\
&= \left([\mathbf{U}_s \mathbf{U}_n] \begin{bmatrix} \Lambda_s & \mathbf{0} \\ \mathbf{0} & \sigma^2\mathbf{I} \end{bmatrix} \begin{bmatrix} \mathbf{U}_s^T \\ \mathbf{U}_n^T \end{bmatrix} \right)^{-1} \\
&= [\mathbf{U}_s \mathbf{U}_n] \begin{bmatrix} \Lambda_s^{-1} & \mathbf{0} \\ \mathbf{0} & \sigma^{-2}\mathbf{I} \end{bmatrix} \begin{bmatrix} \mathbf{U}_s^T \\ \mathbf{U}_n^T \end{bmatrix} \\
&= \mathbf{U}_s \Lambda_s^{-1} \mathbf{U}_s^T + \sigma^{-2} \mathbf{U}_n \mathbf{U}_n^T
\end{aligned} \tag{2.22}$$

from Lemma 2.

Q.E.D.

2.5.2 Blind Linear Zero-forcing Multiuser Detector

Blind linear zero-forcing detectors can be defined in the sense of the minimization problem with a constraint as depicted in Figure 2.5.

Definition 2 *The vector of the blind linear zero-forcing detector can be defined as*

$$\mathbf{w}_k = \arg \min_{\mathbf{w}_k \in \Re^K} \left[(\mathbf{w}_k^T (\mathbf{S}\mathbf{A}))^2 \right] \; s.t. \; \mathbf{w}_k^T \bar{\mathbf{s}}_k = 1. \tag{2.23}$$

□

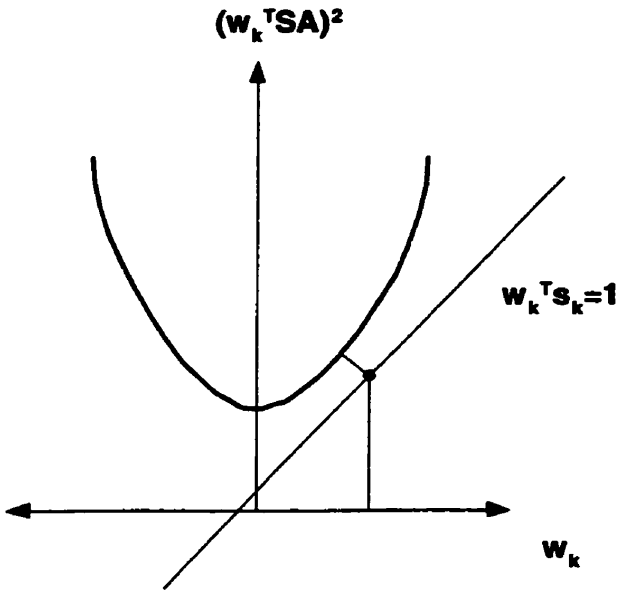

Figure 2.5: Blind zero-forcing detector

By using above definition and Lemma 2, the blind linear zero-forcing detector using the subspace method can be derived.

Proposition 3 ***(Subspace method for the blind zero-forcing detector):*** *From (2.23) and Lemma 2, the estimated information bit of the blind linear zero-forcing detector using subspace method is*

$$\hat{\bar{b}}_k = \mathbf{sgn}\left(\bar{\mathbf{s}}_k^T \mathbf{U}_s (\Lambda_s - \sigma^2 \mathbf{I})^{-1} \mathbf{U}_s^T \mathbf{r}\right). \tag{2.24}$$

□

Proof: Since vector $\mathbf{w}_k \in range(\mathbf{U}_s)$, we can write $\mathbf{w}_k = \mathbf{U}_s\mathbf{c}$. By inserting $\mathbf{w}_k$ into (2.23), we obtain the minimization problem with a constraint:

$$\begin{aligned}
\mathbf{c} &= \arg \min_{\mathbf{c}\in\Re^K} \left[((\mathbf{U}_s\mathbf{c})^T(\mathbf{SA}))^2\right] \ s.t.\ (\mathbf{U}_s\mathbf{c})^T\bar{\mathbf{s}}_k = 1 \\
&= \arg \min_{\mathbf{c}\in\Re^K} \left[(\mathbf{U}_s\mathbf{c})^T(\mathbf{SA}^2\mathbf{S}^T)(\mathbf{U}_s\mathbf{c})\right] \ s.t.\ \mathbf{c}^T\mathbf{U}_s^T\bar{\mathbf{s}}_k = 1 \\
&= \arg \min_{\mathbf{c}\in\Re^K} \mathbf{c}^T\left[\mathbf{U}_s^T(\mathbf{SA}^2\mathbf{S}^T)\mathbf{U}_s\right]\mathbf{c} \ s.t.\ \mathbf{c}^T\mathbf{U}_s^T\bar{\mathbf{s}}_k = 1. \qquad (2.25)
\end{aligned}$$

From Lemma 2, this problem can be written as

$$\begin{aligned}
\mathbf{c} &= \arg \min_{\mathbf{c}\in\Re^K} \mathbf{c}^T\left[\mathbf{U}_s^T(\mathbf{U}_s\Lambda_s\mathbf{U}_s^T + \sigma^2\mathbf{U}_n\mathbf{U}_n^T - \sigma^2\mathbf{I}_K)\mathbf{U}_s\right]\mathbf{c} \ s.t.\ \mathbf{c}^T\mathbf{U}_s^T\bar{\mathbf{s}}_k = 1 \\
&= \arg \min_{\mathbf{c}\in\Re^K} \mathbf{c}^T(\Lambda_s - \sigma^2\mathbf{I}_K)\mathbf{c} \ s.t.\ \mathbf{c}^T\mathbf{U}_s^T\bar{\mathbf{s}}_k = 1. \qquad (2.26)
\end{aligned}$$

By the Lagrange multiplier method, the minimization problem with a constraint (2.26) can be solved as

$$\begin{aligned}
\mathcal{L}(\mathbf{c}) &= \mathbf{c}^T(\Lambda_s - \sigma^2\mathbf{I}_K)\mathbf{c} - 2\mu\mathbf{c}^T\left[\mathbf{U}_s^T\bar{\mathbf{s}}_k - 1\right] \\
\nabla\mathcal{L}(\mathbf{c}) &= 2(\Lambda_s - \sigma^2\mathbf{I}_K)\mathbf{c} - 2\mu\mathbf{U}_s^T\bar{\mathbf{s}}_k = \mathbf{0} \\
\mathbf{c} &= \mu(\Lambda_s - \sigma^2\mathbf{I}_K)^{-1}\mathbf{U}_s^T\bar{\mathbf{s}}_k \qquad (2.27)
\end{aligned}$$

Thus,

$$\mathbf{w}_k = \mu\mathbf{U}_s(\Lambda_s - \sigma^2\mathbf{I}_K)^{-1}\mathbf{U}_s^T\bar{\mathbf{s}}_k \qquad (2.28)$$

and μ can be omitted because of the **sgn** processing for the detection.

Q.E.D.

2.6 Group-Blind Multiuser Detection

Consider a synchronous DS-CDMA cellular system which uses the same channel for all users. Due to the nonorthogonality of spreading codes in the uplink of DS-CDMA systems, there exist two types of interference: intra-cell interference from the cell where the desired user is located and inter-cell interference from adjacent cells. Although a base station knows all spreading codes of the users within the cell, it typically does not know the spreading codes of the interfering users from adjacent cells. So far, many multiuser detectors consider only intra-cell interference because they only know the spreading codes of the users in the cell. Therefore, they have shown a poor performance when there exists unknown users' interference, i.e., inter-cell interference because inter-cell interference can not be suppressed by traditional multiuser detectors. To overcome this problem, blind multiuser detectors that suppress intra-cell interference and inter-cell interference with only its own spreading code were developed. But, these have not been sufficient because they do not use the other users' spreading codes in the cell where the desired user is located. Therefore, to improve performance efficiency, group-blind multiuser detectors were introduced by Anders Høst-Madsen in 1998 [19]. These detectors use the spreading codes of known users to eliminate intra-cell interference and use a blind technique to suppress inter-cell interference.

There is another subspace concept for group-blind multiuser detectors. The

basic idea is that after projecting the correlation matrix onto the orthogonal subspace of $\bar{\mathbf{S}}$, we can decompose the orthogonally projected correlation matrix to signal subspace of $\tilde{\mathbf{S}}$ and noise subspace.

Lemma 3 ***(Subspace concept 2):*** *The orthogonally projected correlation matrix of received signal can be expressed as*

$$\bar{\mathbf{P}}^{\perp}\mathbf{R}\bar{\mathbf{P}}^{\perp} = \tilde{\mathbf{U}}_s\tilde{\mathbf{\Lambda}}_s\tilde{\mathbf{U}}_s^T + \sigma^2\tilde{\mathbf{U}}_n\tilde{\mathbf{U}}_n^T. \tag{2.29}$$

□

Proof: The projection matrix of $\bar{\mathbf{S}}$ is

$$\bar{\mathbf{P}} = \bar{\mathbf{S}}(\bar{\mathbf{S}}^T\bar{\mathbf{S}})^{-1}\bar{\mathbf{S}}^T, \tag{2.30}$$

and the orthogonal projection matrix is

$$\bar{\mathbf{P}}^{\perp} = \mathbf{I} - \bar{\mathbf{P}}. \tag{2.31}$$

Since $\bar{\mathbf{P}}^{\perp}$ projects $\mathbf{R}$ onto orthogonal subspace of $\bar{\mathbf{S}}$, only subspace of $\tilde{\mathbf{S}}$ and noise space are remained. Hence, the orthogonally projected correlation matrix

can be decomposed as

$$\begin{aligned}\bar{\mathbf{P}}^{\perp}\mathbf{R}\bar{\mathbf{P}}^{\perp} &= \left[\tilde{\mathbf{U}}_s\tilde{\mathbf{U}}_n\tilde{\mathbf{U}}_o\right]\begin{bmatrix}\tilde{\Lambda}_s & \mathbf{0} & \mathbf{0}\\ \mathbf{0} & \sigma^2\mathbf{I} & \mathbf{0}\\ \mathbf{0} & \mathbf{0} & \mathbf{0}\end{bmatrix}\begin{bmatrix}\tilde{\mathbf{U}}_s^T\\ \tilde{\mathbf{U}}_n^T\\ \tilde{\mathbf{U}}_o^T\end{bmatrix}\\ &= \tilde{\mathbf{U}}_s\tilde{\Lambda}_s\tilde{\mathbf{U}}_s^T+\sigma^2\tilde{\mathbf{U}}_n\tilde{\mathbf{U}}_n^T \qquad (2.32)\end{aligned}$$

Q.E.D.

The following multiuser detectors were derived for the synchronous case from the original works by Høst-Madsen and Wang in 1999, and these detectors have the best performance in the environment where the inter-cell interference exists.

There are two forms of multiuser detectors. Form I uses subspace concept 2 and form II uses subspace concept 1. Although the form I and form II detector have the same performance, the calculation complexity in eigenvalue decomposition (EVD) or singular value decomposition (SVD) of form I is lower than that of form II. Form II detectors are efficient if we must estimate the channel response because the estimation of the channel response needs the SVD or EVD of Lemma 2. In the case of form I detectors, two iterations of SVD or EVD should be implemented for Lemma 2 and Lemma 3.

2.6.1 Group-Blind Linear Zero-forcing Multiuser Detection

The group-blind linear zero-forcing detector can be defined as eliminating intra-cell interference and minimizing inter-cell interference with a zero-forcing technique.

Definition 3 ***(Group-blind Linear Zero-forcing Detector:)*** *The vector of the group-blind linear zero-forcing detector can be defined as*

$$\mathbf{w}_k = \arg \min_{\mathbf{w}_k \in \mathbf{range(S)}} \left[(\mathbf{w}_k^T(\mathbf{SA}))^2 \right], \text{ subject to } \mathbf{w}_k^T \bar{\mathbf{S}} = \mathbf{1}_k. \tag{2.33}$$

□

The group-blind linear zero-forcing detector has two forms. First, it uses subspace concept 2 (Lemma 3) with a lower calculation complexity.

Proposition 4 ***(Form I of the Group-blind Linear Zero-forcing Detector)*** *The estimated information bit of the group-blind linear zero-forcing detector can be written as*

$$\hat{\tilde{b}}_k = \mathbf{sgn}\left(\mathbf{1}_k^T (\bar{\mathbf{S}}^T \bar{\mathbf{S}})^{-1} \bar{\mathbf{S}}^T [\mathbf{I} - \mathbf{R}\tilde{\mathbf{U}}_s (\tilde{\Lambda}_s - \sigma^2 \mathbf{I})^{-1} \tilde{\mathbf{U}}_s^T] \mathbf{r} \right). \tag{2.34}$$

□

Proof: Assume that $\mathbf{w}_k$ has two components, $\bar{\mathbf{w}}_k \in \text{range}(\bar{\mathbf{S}})$ and $\tilde{\mathbf{w}}_k \in \text{range}(\tilde{\mathbf{U}}_s)$. Then $\mathbf{w}_k$ can be expressed as the summation of two components , i.e., $\mathbf{w}_k = \tilde{\mathbf{w}}_k + \bar{\mathbf{w}}_k$. $\bar{\mathbf{w}}_k$ can be obtained from the constraint of (2.33) using the pseudo inverse of $\bar{\mathbf{S}}$:

$$\bar{\mathbf{w}}_k = \bar{\mathbf{S}} \left(\bar{\mathbf{S}}^T \bar{\mathbf{S}}\right)^{-1} \mathbf{1}_k. \tag{2.35}$$

Then $\mathbf{w}_k = \tilde{\mathbf{U}}_s \mathbf{c}_k + \bar{\mathbf{w}}_k$, for some $\mathbf{c}_k \in \Re^{\tilde{K}}$. $\mathbf{c}_k$ can be found by inserting $\mathbf{w}_k$ to the minimization of (2.33):

$$\begin{aligned} \mathbf{c}_k &= \arg\min_{\mathbf{c}\in\Re^{\tilde{K}}} \left\{ \left(\tilde{\mathbf{U}}_s \mathbf{c} + \bar{\mathbf{w}}_k\right)^T \mathbf{S}\mathbf{A} \right\}^2 \\ &= \arg\min_{\mathbf{c}\in\Re^{\tilde{K}}} \left(\tilde{\mathbf{U}}_s \mathbf{c}_k + \bar{\mathbf{w}}_k\right)^T \left(\mathbf{S}\mathbf{A}^2\mathbf{S}^T\right) \left(\tilde{\mathbf{U}}_s \mathbf{c}_k + \bar{\mathbf{w}}_k\right) \\ &= \arg\min_{\mathbf{c}\in\Re^{\tilde{K}}} \left(\tilde{\mathbf{U}}_s \mathbf{c}_k + \bar{\mathbf{w}}_k\right)^T \left(\mathbf{R} - \sigma^2\mathbf{I}\right) \left(\tilde{\mathbf{U}}_s \mathbf{c}_k + \bar{\mathbf{w}}_k\right). \end{aligned} \tag{2.36}$$

The derivative of (2.36) is

$$\nabla = 2\tilde{\mathbf{U}}_s^T \left(\mathbf{R} - \sigma^2\mathbf{I}\right) \left(\tilde{\mathbf{U}}_s \mathbf{c}_k + \bar{\mathbf{w}}_k\right) = 0. \tag{2.37}$$

By solving the above equation, we see

$$\mathbf{c}_k = -\left[\tilde{\mathbf{U}}_s^T \left(\mathbf{R} - \sigma^2\mathbf{I}\right) \tilde{\mathbf{U}}_s\right]^{-1} \tilde{\mathbf{U}}_s^T \left(\mathbf{R} - \sigma^2\mathbf{I}\right) \bar{\mathbf{w}}_k. \tag{2.38}$$

From $\bar{\mathbf{P}} + \bar{\mathbf{P}}^{\perp} = \mathbf{I}$, $\tilde{\mathbf{U}}_s^T \bar{\mathbf{P}} = \mathbf{0}$, $\mathbf{c}_k$ can be written as

$$\mathbf{c}_k = -\left[\tilde{\mathbf{U}}_s^T \bar{\mathbf{P}}^{\perp} \left(\mathbf{R} - \sigma^2 \mathbf{I}\right) \bar{\mathbf{P}}^{\perp} \tilde{\mathbf{U}}_s\right]^{-1} \tilde{\mathbf{U}}_s^T \left(\mathbf{R} - \sigma^2 \mathbf{I}\right) \bar{\mathbf{w}}_k. \tag{2.39}$$

By using Lemma 3 and $\tilde{\mathbf{U}}_s^T \bar{\mathbf{w}}_k = \mathbf{0}$, $\mathbf{c}_k$ can be obtained from

$$\begin{aligned} \mathbf{c}_k &= -\left(\tilde{\Lambda}_s - \sigma^2 \mathbf{I}\right)^{-1} \tilde{\mathbf{U}}_s^T \left(\mathbf{R} - \sigma^2 \mathbf{I}\right) \bar{\mathbf{w}}_k \\ &= -\left(\tilde{\Lambda}_s - \sigma^2 \mathbf{I}\right)^{-1} \tilde{\mathbf{U}}_s^T \mathbf{R} \bar{\mathbf{w}}_k. \end{aligned} \tag{2.40}$$

Finally $\mathbf{w}_k$ can be written as

$$\mathbf{w}_k = \tilde{\mathbf{U}}_s \mathbf{c}_k + \bar{\mathbf{w}}_k = [\mathbf{I} - \tilde{\mathbf{U}}_s (\tilde{\Lambda}_s - \sigma^2 \mathbf{I})^{-1} \tilde{\mathbf{U}}_s^T \mathbf{R}] \bar{\mathbf{S}} (\bar{\mathbf{S}}^T \bar{\mathbf{S}})^{-1} \mathbf{1}_k. \tag{2.41}$$

Q.E.D.

Second, form II of the group-blind linear zero-forcing detector uses subspace concept 1 (Lemma 2).

Proposition 5 ***(Form II of the Group-blind Linear Zero-forcing Detector):*** *The estimated information bit of the group-blind linear zero-forcing detector can be written as*

$$\hat{\bar{b}}_k = \mathbf{sgn}\left(\mathbf{1}_k^T \left[\bar{\mathbf{S}}^T \mathbf{U}_s \left(\Lambda_s - \sigma^2 \mathbf{I}\right)^{-1} \mathbf{U}_s^T \bar{\mathbf{S}}\right]^{-1} \bar{\mathbf{S}}^T \mathbf{U}_s \left(\Lambda_s - \sigma^2 \mathbf{I}\right)^{-1} \mathbf{U}_s^T \mathbf{r}\right) \tag{2.42}$$

□

Proof: We utilize the Lagrange multiplier method to solve the constrained optimization problem (2.33). Therefore, $\mathbf{w}_k$ is

$$\begin{aligned} \mathbf{w}_k &= \arg \min_{\mathbf{w}_k \in \text{range(S)}} \mathbf{w}_k^T \mathbf{S}\mathbf{A}^2\mathbf{S}^T\mathbf{w}_k + \underline{\lambda}^T \left(\bar{\mathbf{S}}^T\mathbf{w}_k - \mathbf{1}_{+k}\right) \\ &= \left(\mathbf{S}\mathbf{A}^2\mathbf{S}^T\right)^\dagger \bar{\mathbf{S}}\underline{\lambda}. \end{aligned} \tag{2.43}$$

By substituting (2.43) into $\bar{\mathbf{S}}^T\mathbf{w}_k = \mathbf{1}_k$, we obtain $\underline{\lambda} = [\bar{\mathbf{S}}^T(\mathbf{S}\mathbf{A}^2\mathbf{S}^T)^\dagger\bar{\mathbf{S}}]^{-1}\mathbf{1}_k$. Thus, the solution for group-blind linear zero-forcing detector for user k is

$$\begin{aligned} \mathbf{w}_k &= \left(\mathbf{S}\mathbf{A}^2\mathbf{S}^T\right)^\dagger \bar{\mathbf{S}} \left[\bar{\mathbf{S}}^T \left(\mathbf{S}\mathbf{A}^2\mathbf{S}^T\right)^\dagger \bar{\mathbf{S}}\right]^{-1} \mathbf{1}_k \\ &= \mathbf{U}_s \left(\Lambda_s - \sigma^2\mathbf{I}\right)^{-1} \mathbf{U}_s^T\bar{\mathbf{S}} \left[\bar{\mathbf{S}}^T\mathbf{U}_s \left(\Lambda_s - \sigma^2\mathbf{I}\right)^{-1} \mathbf{U}_s^T\bar{\mathbf{S}}\right]^{-1} \mathbf{1}_k, \end{aligned} \tag{2.44}$$

from Lemma 2 and the fact that $\mathbf{U}_n^T\bar{\mathbf{S}} = \mathbf{0}$.

Q.E.D.

2.6.2 Group-Blind Linear Hybrid Multiuser Detection

The group-blind linear hybrid detector can be defined in the sense that it minimizes inter-cell interference with the MMSE method and minimizes intra-cell interference with the zero-forcing technique.

Definition 4 ***(Group-blind Linear Hybrid Detector):*** *The vector of the*

group-blind Linear hybrid detector can be defined as

$$\mathbf{w}_k = \arg \min_{\mathbf{w} \in \text{range}(\bar{\mathbf{S}})} E\left\{ \left| b_k[i] - \mathbf{w}_k^T \mathbf{r}[i] \right|^2 \right\}, \qquad \textit{subject to} \quad \mathbf{w}^T \bar{\mathbf{S}} = \mathbf{1}_k^T. \tag{2.45}$$

□

There are two forms of detector for the group-blind linear hybrid detector. Form I of the detector uses projection method and can be expressed as follows:

Proposition 6 ***(Form I of the Group-blind Linear Hybrid Detector):*** *The estimated information bit of the group-blind linear hybrid detector can be written as*

$$\hat{\bar{b}}_k = \mathbf{sgn}\left(\mathbf{1}_k^T (\bar{\mathbf{S}}^T \bar{\mathbf{S}})^{-1} \bar{\mathbf{S}}^T (\mathbf{I} - \mathbf{R} \tilde{\mathbf{U}}_s \tilde{\Lambda}_s^{-1} \tilde{\mathbf{U}}_s^T) \mathbf{r} \right). \tag{2.46}$$

□

Proof: Assume that $\mathbf{w}_k$ has two components, $\bar{\mathbf{w}}_k \in \text{range}(\bar{\mathbf{S}})$ and $\tilde{\mathbf{w}}_k \in \text{range}(\tilde{\mathbf{U}}_s)$. Then $\mathbf{w}_k$ can be expressed as the summation of two components , i.e., $\mathbf{w}_k = \bar{\mathbf{w}}_k + \tilde{\mathbf{w}}_k$. $\bar{\mathbf{w}}_k$ can be obtained from the constraint of (2.45) using the pseudo inverse of $\bar{\mathbf{S}}$:

$$\bar{\mathbf{w}}_k = \bar{\mathbf{S}} \left(\bar{\mathbf{S}}^T \bar{\mathbf{S}} \right)^{-1} \mathbf{1}_k. \tag{2.47}$$

Then the vector for user k is $\mathbf{w}_k = \tilde{\mathbf{U}}_s \mathbf{c}_k + \bar{\mathbf{w}}_k$, for some $\mathbf{c}_k \in \Re^{\tilde{K}}$. $\mathbf{c}_k$ can be found by inserting $\mathbf{w}_k$ to the minimization of (2.45):

$$\begin{aligned}
\mathbf{c}_k &= \arg\min_{\mathbf{c}\in\Re^{\tilde{K}}} E\left\{\left|b_k[i] - \left(\tilde{\mathbf{U}}_s\mathbf{c} + \bar{\mathbf{w}}_k\right)^H \mathbf{r}[i]\right|^2\right\} \\
&= \arg\min_{\mathbf{c}\in\Re^{\tilde{K}}} \left(\tilde{\mathbf{U}}_s\mathbf{c} + \bar{\mathbf{w}}_k\right)^H \mathbf{R}\left(\tilde{\mathbf{U}}_s\mathbf{c} + \bar{\mathbf{w}}_k\right) - 2\mathbf{c}^H\tilde{\mathbf{U}}_s^H\bar{\mathbf{h}}_k \\
&= -\left(\tilde{\mathbf{U}}_s^H\mathbf{R}\tilde{\mathbf{U}}_s\right)^{-1}\tilde{\mathbf{U}}_s^H\mathbf{R}\bar{\mathbf{w}}_k. \qquad (2.48)
\end{aligned}$$

From the fact, $\bar{\mathbf{P}} + \bar{\mathbf{P}}^{\perp} = \mathbf{I}$, $\tilde{\mathbf{U}}_s^T\bar{\mathbf{P}} = \mathbf{0}$, and Lemma 3, $\mathbf{c}_k$ is

$$\begin{aligned}
\mathbf{c}_k &= -\left(\tilde{\mathbf{U}}_s^H\bar{\mathbf{P}}^{\perp}\mathbf{R}\bar{\mathbf{P}}^{\perp}\tilde{\mathbf{U}}_s\right)^{-1}\tilde{\mathbf{U}}_s^H\mathbf{R}\bar{\mathbf{w}}_k \\
&= -\tilde{\Lambda}_s^{-1}\tilde{\mathbf{U}}_s^H\mathbf{R}\bar{\mathbf{w}}_k. \qquad (2.49)
\end{aligned}$$

Hence, the $\bar{\mathbf{w}}_k$ cab be written as

$$\begin{aligned}
\bar{\mathbf{w}}_k &= \tilde{\mathbf{U}}_s\mathbf{c}_k + \bar{\mathbf{w}}_k \\
&= (\mathbf{I}_{Pm} - \tilde{\mathbf{U}}_s\tilde{\Lambda}_s^{-1}\tilde{\mathbf{U}}_s^H\mathbf{R})\bar{\mathbf{w}}_k \\
&= (\mathbf{I}_{Pm} - \tilde{\mathbf{U}}_s\tilde{\Lambda}_s^{-1}\tilde{\mathbf{U}}_s^H\mathbf{R})\bar{\mathbf{S}}(\bar{\mathbf{S}}^T\bar{\mathbf{S}})^{-1}\mathbf{1}_k. \qquad (2.50)
\end{aligned}$$

Q.E.D.

Form II of the detector uses Lemma 2.

Proposition 7 ***(Form II of the Group-blind Linear Hybrid Detector):***

The estimated information bit of the group-blind linear hybrid detector can be expressed as

$$\hat{\tilde{b}}_k = \mathbf{sgn}\left(\mathbf{1}_k^T \left[\bar{\mathbf{S}}^T \mathbf{U}_s \Lambda_s^{-1} \mathbf{U}_s^T \bar{\mathbf{S}}\right]^{-1} \bar{\mathbf{S}}^T \mathbf{U}_s \Lambda_s^{-1} \mathbf{U}_s^T \mathbf{r}\right). \tag{2.51}$$

□

Proof: The constrained optimization problem (2.45) can be solved by Lagrange multiplier method. Thus the problem (2.45) can be written as

$$\begin{aligned}
\mathbf{w}_k &= \arg\min_{\mathbf{w}\in\Re^{\tilde{K}}} E\left\{\left|b_k[i] - \mathbf{w}^T\mathbf{r}[i]\right|^2\right\} + \tilde{\underline{\lambda}}^T\left(\bar{\mathbf{S}}^T\mathbf{w} - \mathbf{1}_k\right) \\
&= \arg\min_{\mathbf{w}\in\Re^{\tilde{K}}} \mathbf{w}^T\mathbf{R}\mathbf{w} - 2\bar{\mathbf{s}}_k^T\mathbf{w} + \tilde{\underline{\lambda}}^T\left(\bar{\mathbf{S}}^T\mathbf{w} - \mathbf{1}_k\right) \\
&= \arg\min_{\mathbf{w}\in\Re^{\tilde{K}}} \mathbf{w}^T\mathbf{R}\mathbf{w} + \underline{\lambda}^T\left(\bar{\mathbf{S}}^T\mathbf{w} - \mathbf{1}_k\right) \;=\; \mathbf{R}^{-1}\bar{\mathbf{S}}\underline{\lambda},
\end{aligned} \tag{2.52}$$

where $\underline{\lambda} \triangleq \tilde{\underline{\lambda}} - 2\mathbf{1}_k$. Substituting (2.52) into the constraint that $\bar{\mathbf{S}}^T\mathbf{w}_k = \mathbf{1}_k$, we obtain $\underline{\lambda} = (\bar{\mathbf{S}}^T\mathbf{R}^{-1}\bar{\mathbf{S}})^{-1}\mathbf{1}_k$. Hence, $\mathbf{w}_k$ can be written as

$$\mathbf{w}_k \;=\; \mathbf{R}^{-1}\bar{\mathbf{S}}\left[\bar{\mathbf{S}}^T\mathbf{R}^{-1}\bar{\mathbf{S}}\right]^{-1}\mathbf{1}_k = \mathbf{U}_s\Lambda_s^{-1}\mathbf{U}_s^T\bar{\tilde{\mathbf{S}}}\left[\bar{\tilde{\mathbf{S}}}^T\mathbf{U}_s\Lambda_s^{-1}\mathbf{U}_s^T\bar{\tilde{\mathbf{S}}}\right]^{-1}\mathbf{1}_k, \tag{2.53}$$

using the fact that $\mathbf{U}_n^T\bar{\mathbf{S}} = \mathbf{0}$ and Lemma 2.

Q.E.D.

2.6.3 Group-Blind Linear MMSE Multiuser Detection

The group-blind linear MMSE detector can be defined in the sense that it minimizes inter-cell interference and intra-cell interference with MMSE method. Let $\bar{\mathbf{r}}[i] = \bar{\mathbf{S}}\bar{\mathbf{A}}\bar{\mathbf{b}}[i] + \mathbf{v}[i]$ be the component of $\mathbf{r}[i]$, i.e., known users' signal and noise of $\mathbf{r}[i]$. Then the group-blind linear MMSE detector can be defined as follows.

Definition 5 ***(Group-blind Linear MMSE Detector)*** *The vector of the group-blind linear MMSE detector for user k can be defined using the fact that $\mathbf{w}_k = \bar{\mathbf{w}}_k + \tilde{\mathbf{w}}_k$, where $\bar{\mathbf{w}}_k \in \bar{\mathbf{S}}$ and $\tilde{\mathbf{w}}_k \in \tilde{\mathbf{U}}_s$, such that*

$$\bar{\mathbf{w}}_k = \arg \min_{\mathbf{w} \in \text{range}(\bar{\mathbf{S}})} E\left\{ \left| b_k[i] - \mathbf{w}^T \bar{\mathbf{r}}[i] \right|^2 \right\}, \tag{2.54}$$

$$\tilde{\mathbf{w}}_k = \arg \min_{\mathbf{w} \in \text{range}(\tilde{\mathbf{U}}_s)} E\left\{ \left| b_k[i] - (\mathbf{w} + \bar{\mathbf{w}}_k)^T \mathbf{r}[i] \right|^2 \right\}. \tag{2.55}$$

□

Form I of the group-blind linear MMSE detector uses Lemma 3, and form II of this detector uses Lemma 2.

Proposition 8 ***(Form I of the Group-blind Linear MMSE Detector):*** *The estimated information bit of the group-blind linear MMSE detector can be derived as follows:*

$$\hat{\bar{b}}_k = \mathbf{sgn}\left(\mathbf{1}_k^T \left(\bar{\mathbf{S}}^T \bar{\mathbf{S}} + \sigma^2 \mathbf{I} \right)^{-1} \bar{\mathbf{S}}^T \left(\mathbf{I} - \mathbf{R}\tilde{\mathbf{U}}_s \tilde{\Lambda}_s^{-1} \tilde{\mathbf{U}}_s^T \right) \mathbf{r} \right). \tag{2.56}$$

□

Proof: From the (2.54), we can find $\bar{\mathbf{w}}_k$. We assume $\bar{\mathbf{w}}_k = \bar{\mathbf{S}}\bar{\mathbf{c}}_k$ because $\bar{\mathbf{w}}_k \in \bar{\mathbf{S}}$, and $\bar{\mathbf{S}}$ has full column rank $\bar{\mathbf{r}}$. We can get $\mathbf{c}_k$ by substituting $\bar{\mathbf{w}}_k$ into (2.54):

$$\begin{aligned}
\bar{\mathbf{c}}_k &= \arg\min_{\mathbf{c}\in\Re^{\bar{K}}} E\left\{\left|b_k[i] - \mathbf{c}^T\bar{\mathbf{S}}^T\bar{\mathbf{r}}[i]\right|^2\right\} \\
&= \arg\min_{\mathbf{c}\in\Re^{\bar{K}}} \mathbf{c}^T\left[\bar{\mathbf{S}}^T\left(\bar{\mathbf{S}}\bar{\mathbf{S}}^T + \sigma^2\mathbf{I}\right)\bar{\mathbf{S}}\right]\mathbf{c} - 2\mathbf{1}_{\bar{K}\iota+k}^T\bar{\mathbf{S}}^T\bar{\mathbf{S}}\mathbf{c} \\
&= \left[\left(\bar{\mathbf{S}}^T\bar{\mathbf{S}}\right)\left(\bar{\mathbf{S}}^T\bar{\mathbf{S}}\right) + \sigma^2\bar{\mathbf{S}}^T\bar{\mathbf{S}}\right]^{-1}\left(\bar{\mathbf{S}}^T\bar{\mathbf{S}}\right)\mathbf{1}_k = \left(\bar{\mathbf{S}}^T\bar{\mathbf{S}} + \sigma^2\mathbf{I}\right)^{-1}\mathbf{1}_k. \quad (2.57)
\end{aligned}$$

From the same derivation as (2.49), we can write $\tilde{\mathbf{w}}_k = \tilde{\mathbf{U}}_s\tilde{\mathbf{c}}_k = -\tilde{\Lambda}_s^{-1}\tilde{\mathbf{U}}_s^T\mathbf{R}\bar{\mathbf{w}}_k$, and $\mathbf{w}_k$ is thus the summation of these two results:

$$\begin{aligned}
\mathbf{w}_k &= \tilde{\mathbf{U}}_s\tilde{\mathbf{c}}_k + \bar{\mathbf{w}}_k = \left(\mathbf{I} - \tilde{\mathbf{U}}_s\tilde{\Lambda}_s^{-1}\tilde{\mathbf{U}}_s^T\mathbf{R}\right)\bar{\mathbf{S}}\bar{\mathbf{c}}_k \\
&= \left(\mathbf{I} - \tilde{\mathbf{U}}_s\tilde{\Lambda}_s^{-1}\tilde{\mathbf{U}}_s^T\mathbf{R}\right)\bar{\mathbf{S}}\left(\bar{\mathbf{S}}^T\bar{\mathbf{S}} + \sigma^2\mathbf{I}\right)^{-1}\mathbf{1}_k. \quad (2.58)
\end{aligned}$$

Q.E.D.

Proposition 9 ***(Form II of the Group-blind Linear MMSE Detector):*** *The estimated information bit of the group-blind linear MMSE detector can be written as*

$$\begin{aligned}
\hat{\bar{b}}_k = \mathbf{sgn}\Big(&\mathbf{1}_k^T\left(\bar{\mathbf{S}}^T\bar{\mathbf{S}} + \sigma^2\mathbf{I}\right)^{-1}\bar{\mathbf{S}}^T \\
&\times\left[\mathbf{I} - \left(\mathbf{Q}_s\mathbf{R}_s^{-T}\right)\left(\Pi\Lambda_s\Pi^T\right)^{-1}\left(\mathbf{Q}_s\mathbf{R}_s^{-T}\right)^T\mathbf{R}\right]\mathbf{r}\Big). \quad (2.59)
\end{aligned}$$

□

Proof: By using $\mathbf{U}_s$, we need to find a basis for the range$(\tilde{\mathbf{U}}_s)$. As well, from Lemma 3, range $\left(\bar{\mathbf{P}}^{\perp}\mathbf{U}_s\right)$ = range$(\tilde{\mathbf{U}}_s)$. Consider the (rank-deficient) QR factorization of the matrix $\left(\bar{\mathbf{P}}^{\perp}\mathbf{U}_s\right)$:

$$\bar{\mathbf{P}}^{\perp}\mathbf{U}_s = \begin{bmatrix} \mathbf{Q}_s & \mathbf{Q}_o \end{bmatrix} \begin{bmatrix} \mathbf{R}_s & \mathbf{R}_o \\ \mathbf{0} & \mathbf{0} \end{bmatrix} \Pi. \tag{2.60}$$

Then the columns of the matrix $\mathbf{Q}_s$ are the bases of the range$(\tilde{\mathbf{U}}_s)$. The solution of this detector can thus be derived from (2.58) and the vector can be written as

$$\mathbf{w}_k = \left[\mathbf{I} - \mathbf{Q}_s \left(\mathbf{Q}_s^T \mathbf{R} \mathbf{Q}_s\right)^{-1} \mathbf{Q}_s^T \mathbf{R}\right] \bar{\mathbf{S}} \left(\bar{\mathbf{S}}^T \bar{\mathbf{S}} + \sigma^2 \mathbf{I}\right)^{-1} \mathbf{1}_k. \tag{2.61}$$

For the high-resolution calculation, $\mathbf{Q}_s^T\mathbf{R}\mathbf{Q}_s$ can be changed with $\mathbf{U}_s$ and Lemma 2:

$$\mathbf{Q}_s^T \mathbf{R} \mathbf{Q}_s \;=\; \mathbf{Q}_s^T \left(\mathbf{U}_s \Lambda_s \mathbf{U}_s^T + \sigma^2 \mathbf{U}_n \mathbf{U}_n^T\right) \mathbf{Q}_s \tag{2.62}$$

From $\mathbf{U}_s\mathbf{Q}_s = 0$, $\bar{\mathbf{P}} + \bar{\mathbf{P}}^{\perp} = \mathbf{I}$, and $\bar{\mathbf{P}}\mathbf{Q}_s = 0$, $\mathbf{Q}_s^T\mathbf{R}\mathbf{Q}_s$ can be written as

$$\begin{aligned}\mathbf{Q}_s^T\mathbf{R}\mathbf{Q}_s &= \mathbf{Q}_s^T\left(\mathbf{U}_s\Lambda_s\mathbf{U}_s^T\right)\mathbf{Q}_s \\ &= \mathbf{Q}_s^T\left(\bar{\mathbf{P}}^{\perp}\mathbf{U}_s\Lambda_s\mathbf{U}_s^T\bar{\mathbf{P}}^{\perp}\right)\mathbf{Q}_s = \mathbf{Q}_s^T\left(\bar{\mathbf{P}}^{\perp}\mathbf{U}_s\right)\Lambda_s\left(\bar{\mathbf{P}}^{\perp}\mathbf{U}_s\right)^T\mathbf{Q}_s \\ &= \mathbf{Q}_s^T\left[\begin{array}{cc}\mathbf{Q}_s & \mathbf{Q}_o\end{array}\right]\left[\begin{array}{cc}\mathbf{R}_s & \mathbf{R}_o \\ 0 & 0\end{array}\right]\Pi\Lambda_s\Pi^T\left[\begin{array}{cc}\mathbf{R}_s & \mathbf{R}_o \\ 0 & 0\end{array}\right]^T\left[\begin{array}{cc}\mathbf{Q}_s & \mathbf{Q}_o\end{array}\right]^T\mathbf{Q}_s \\ &= \mathbf{R}_s\Pi\Lambda_s\Pi^T\mathbf{R}_s^T. \end{aligned} \tag{2.63}$$

By inserting (2.63) to (2.61), we obtain the result (2.59)

Q.E.D.

2.7 Performance Analysis

In this section, we analyze the performance of multiuser detectors. The estimated information data of a linear detector for user 1 can be given by

$$\hat{\bar{b}}_1[i] = \mathbf{sgn}\left(\mathbf{w}_1^T\mathbf{r}[i]\right). \tag{2.64}$$

From (2.3), the received signal is

$$\mathbf{r}[i] = \sum_{k=1}^{K}\bar{b}_k[i]\bar{A}_k\bar{\mathbf{s}}_k + \sum_{j=1}^{\tilde{K}}\tilde{b}_j[i]\tilde{A}_j\tilde{\mathbf{s}}_j + \sigma\mathbf{n}. \tag{2.65}$$

Thus the output of the linear detector can be written as

$$\mathbf{w}_1^T\mathbf{r}[i] = \bar{b}_1[i]\bar{A}_1\mathbf{w}_1^T\bar{\mathbf{s}}_1 + \underbrace{\sum_{k=2}^{K}\bar{b}_k[i]\bar{A}_k\mathbf{w}_1^T\bar{\mathbf{s}}_k}_{intra-cell\ MAI} + \underbrace{\sum_{j=1}^{\tilde{K}}\tilde{b}_j[i]\tilde{A}_j\mathbf{w}_1^T\tilde{\mathbf{s}}_j}_{inter-cell\ MAI} + \underbrace{\sigma\mathbf{w}_1^T\mathbf{n}}_{noise} \tag{2.66}$$

Assuming that the user information data are independent and that the noise is independent of user information data, the signal-to-interference-plus-noise ratio(SINR) at the output of the linear detector is obtained using

$$\begin{aligned} SINR(\mathbf{w}_1) &= \frac{E\left\{\mathbf{w}_1^T\mathbf{r}[i]|\bar{b}_1[i]\right\}^2}{Var\left\{\mathbf{w}_1^T\mathbf{r}[i]|\bar{b}_1[i]\right\}} \\ &= \frac{\bar{A}_1^2\left(\mathbf{w}_1^T\bar{\mathbf{s}}_1\right)^2}{\sum_{k=2}^{K}\bar{A}_k^2\left(\mathbf{w}_1^T\bar{\mathbf{s}}_k\right)^2+\sum_{j=1}^{\tilde{K}}\tilde{A}_j^2\left(\mathbf{w}_1^T\tilde{\mathbf{s}}_j\right)^2+\sigma^2||\mathbf{w}_1||^2} \end{aligned} \tag{2.67}$$

In this thesis, we assume that there are 6 users in the cell of interest and 4 inter-cell interfering users from adjacent cells. For simplicity, the BPSK modulation scheme is used. The processing gain is 31, the received amplitude of in-cell users is 1, and the received amplitude of out-cell users is $1/\sqrt{2}$. Randomly generated spreading codes are used for comparison with different cross-correlation of spreading codes. SINR for each multiuser detector is obtained from (2.67). From the evaluation of minimum SINR of the detectors, we can find the performance in the worst case, i.e., high cross-correlation between spreading codes in synchronous systems. The bit error rate can be obtained by $Q(\sqrt{SINR})$ where Q is the Q function of the Gaussian probability density function.

Figure 2.6 shows the performance of the hybrid group-blind multiuser detector in the case of high and low cross-correlation of spreading codes. In this figure, 'single' means that the conventional detector is using a matched filter, 'partial' means that it uses the spreading codes of known users, and 'full' means

that it uses the spreading codes of known and unknown users, i.e., the ideal case. The minimum SINR of the hybrid group-blind multiuser detector is better than that of the conventional detector at SNR$\geq$ $2dB$ and the partial-MMSE detector at SNR$\geq$ $6dB$. However, the hybrid group-blind multiuser detector has a lower SINR than the conventional detector and the partial-MMSE detector at low SNRs. The maximum SINRs of the hybrid group-blind multiuser detector have almost the same values as the full MMSE detector at all SNRs. In Figure 2.7, the SINRs of the group-blind MMSE multiuser detector have almost the same values as the ideal full MMSE detector and the subspace based blind MMSE detector. Due to the high cross-correlation of spreading codes, the minimum SINRs of the group-blind MMSE detector have lower SINR difference than maximum SINRs. Figure 2.8 shows a performance comparison of group-blind multiuser detectors. We can see that the group-blind MMSE multiuser detector has the best performance compared to other group-blind multiuser detectors in the worst case (high cross-correlation of spreading codes). However, group-blind multiuser detectors have almost the same performance in the best case (low cross-correlation of spreading codes).

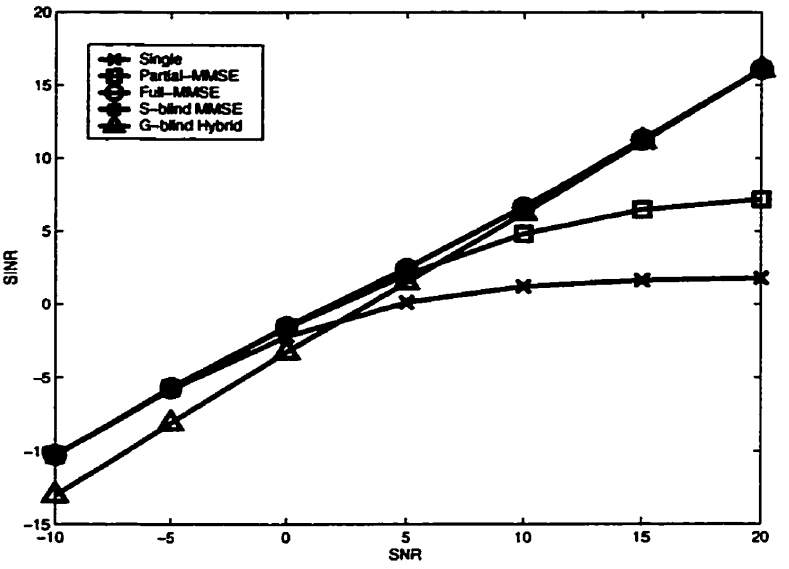

(a) Minimum SINR

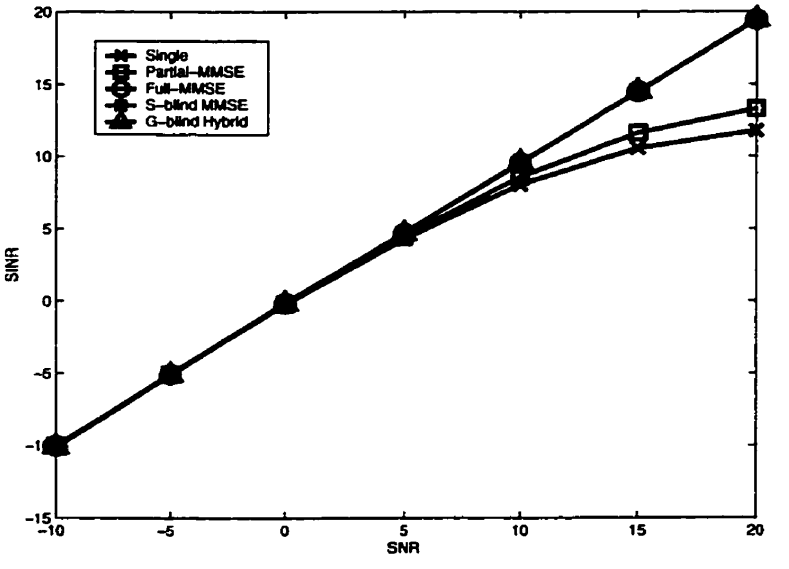

(b) Maximum SINR

Figure 2.6: Performance of the hybrid group-blind multiuser detector compared to conventional multiuser detectors (Synchronous system, N=31, 6 known users, 4 unknown users, SIR(intra-cell)=0dB, SIR(inter-cell)=3dB, 100 ensemble)

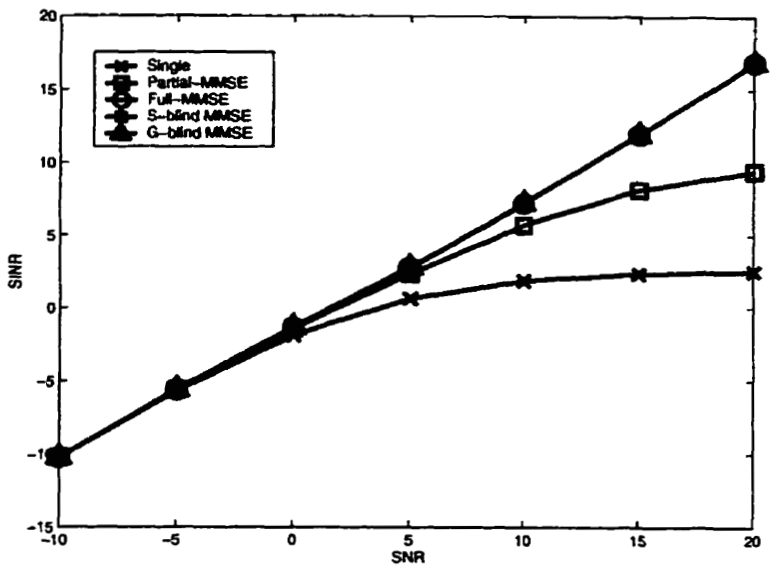

(a) Minimum SINR

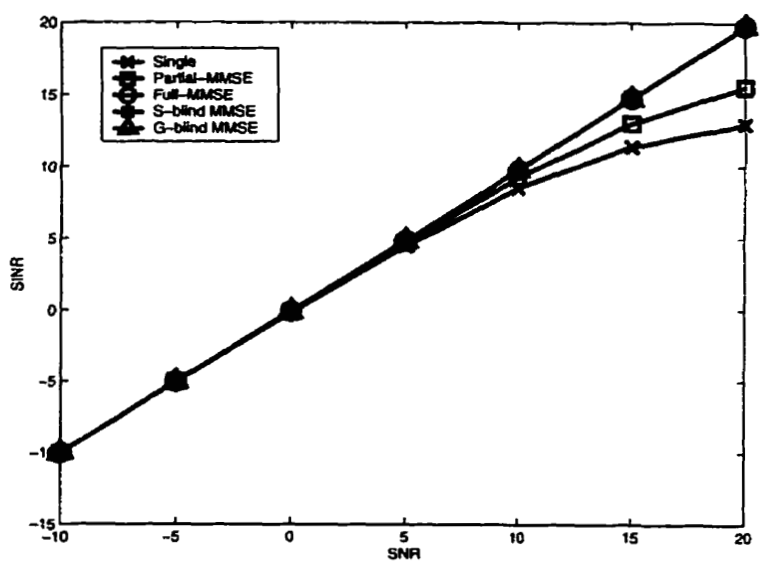

(b) Maximum SINR

Figure 2.7: Performance of the group-blind MMSE multiuser detector compared to conventional multiuser detectors (Synchronous system, N=31, 6 known users, 4 unknown users, SIR(intra-cell)=0dB, SIR(inter-cell)=3dB, 100 ensemble)

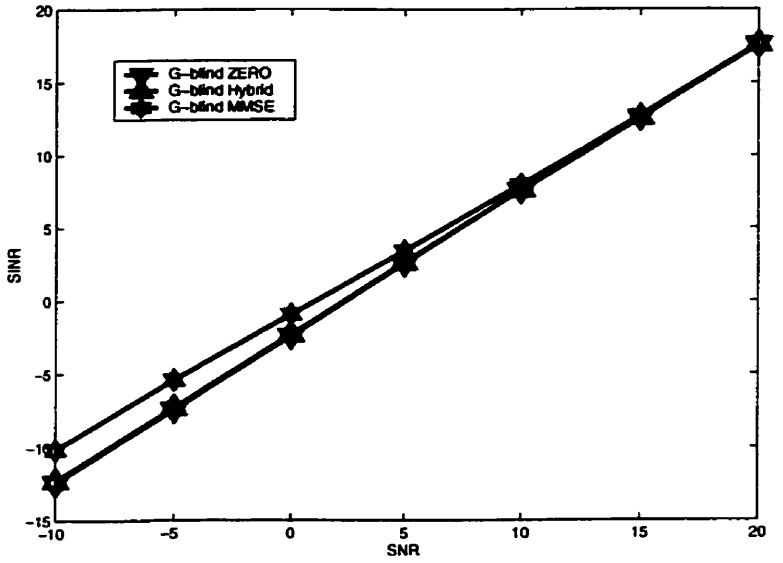

(a) Minimum SINR

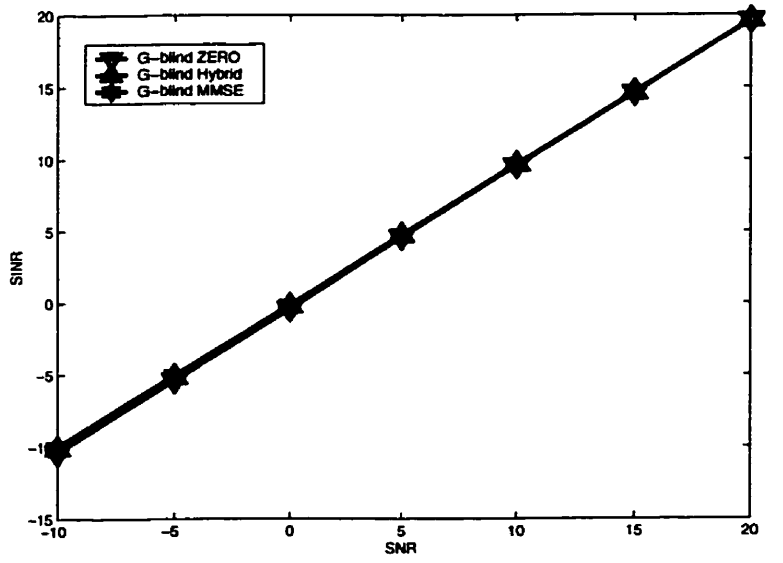

(b) Maximum SINR

Figure 2.8: Performance comparison of group-blind multiuser detectors (Synchronous system, N=31, 6 known users, 4 unknown users, SIR(intra-cell)=0dB, SIR(inter-cell)=3dB, 100 ensemble)

Chapter 3

Multiuser Detection for Asynchronous DS-CDMA Systems

In cellular systems, the transmitted signals from mobile stations are asynchronous. Even if they transmit their signals synchronously, the transmitted signals are delayed by multipath caused by reflection, diffraction, and scattering as depicted in Figure 3.2. In addition, each user has his own delay as described in Figure 3.1. Therefore, asynchronous system models are well suited for base stations. In this chapter, we consider an asynchronous system model that includes multipaths, the propagation delay of each user, and fading. In Chapter 4 and 5, we will discuss many multiuser detectors for an asynchronous system model.

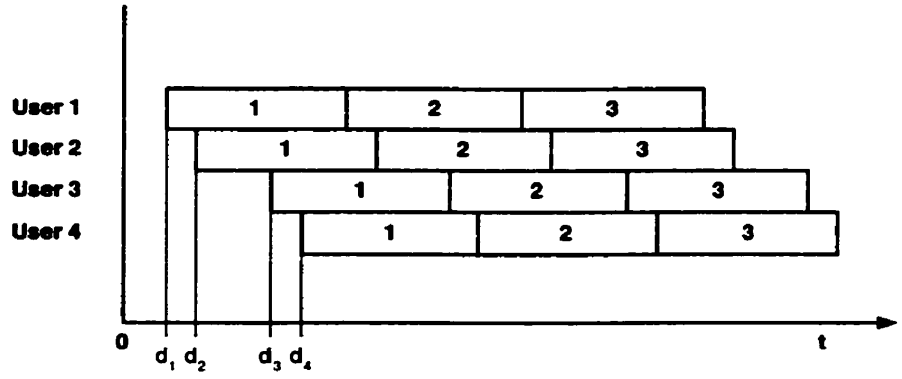

Figure 3.1: Timing diagram for asynchronous systems

3.1 Asynchronous Signal Model

Consider an asynchronous DS-CDMA system with intra-cell interference of $\bar{K}$ known users within a cell and inter-cell interference of $\tilde{K}$ unknown users from adjacent cells. The transmitted signals from all users pass through their multipath channels with additive Gaussian noise. The transmitted signal from the k-th user can be written as

$$x_k(t) = A_k \sum_{i=0}^{M-1} b_k[i]\, s_k(t - iT - d_k), \tag{3.1}$$

where d_k is the delay of the k-th user, T denotes the duration of symbol, s_k is the spreading sequence, b_k is the symbol stream, M is the frame length, and A_k denotes amplitude. The spreading sequence for k-th user is given by

$$s_k(t) = \sum_{j=0}^{N-1} c_k[j]\, \psi(t - jT_c), \quad 0 \le t \le T, \tag{3.2}$$

where N is the processing gain, T_c is the chip duration ($T_c = \frac{T}{N}$), ψ is the chip waveform, and c_k is the ± 1 signature sequence. The impulse response of multipath channel for user k can be written as

$$g_k(t) = \sum_{l=1}^{L} \alpha_{kl} \delta(t - \tau_{kl}), \tag{3.3}$$

where α_{kl} is the complex path gain, τ_{kl} denotes the delay of k-th user's l-th path, and L is the number of paths. The impulse response of multipath channel is depicted in Figure 3.2. The transmitted signals of raised cosine shape go through each path and are summed at the receiver. By using (3.1) and (3.3), the component of the received signal from the k-th user can be obtained from

$$y_k(t) = x_k(t) * g_k(t) = \sum_{i=0}^{M-1} b_k[i] \underbrace{[A_k s_k(t - iT - d_k) * g_k(t)]}_{h_k(t-iT)}, \tag{3.4}$$

where $*$ denotes the convolution. From (3.2), $h_k(t)$ can be rewritten as

$$\begin{aligned} h_k(t) &\triangleq A_k s_k(t - d_k) * g_k(t) \\ &= \sum_{j=0}^{N-1} c_k[j] \underbrace{\left[A_k \sum_{l=1}^{L} \alpha_{kl} \psi\left(t - jT_c - d_k - \tau_{kl}\right) \right]}_{\bar{g}_k(t - jT_c)}. \end{aligned} \tag{3.5}$$

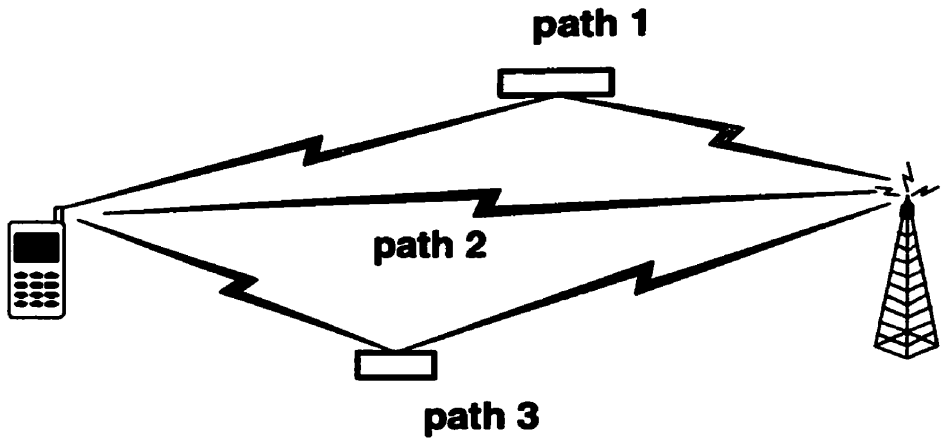

(a) Multi-path channel

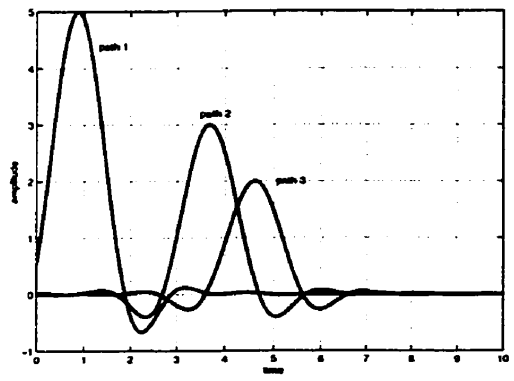

(b) Response of each path

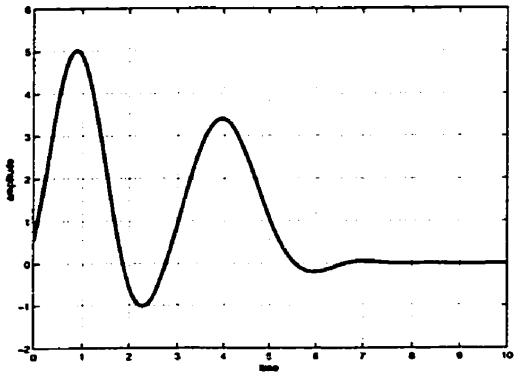

(c) total response of all paths

Figure 3.2: Response of multi-path channel

In (3.5), $\bar{g}_k(t)$ is the composite channel response, considering the transmitted amplitude, the waveform of the chip pulse, and the multipath channel:

$$\bar{g}_k(t) \triangleq A_k \sum_{l=1}^{L} \alpha_{kl} \psi\left(t - d_k - \tau_{kl}\right). \tag{3.6}$$

Finally, the received signal of the $\bar{K}$ known users and $\tilde{K}$ unknown users can be described as

$$\begin{aligned} r(t) &= \sum_{k=1}^{K=\bar{K}+\tilde{K}} y_k(t) + v(t) \\ &= \sum_{k=1}^{\bar{K}} y_k(t) + \sum_{j=1}^{\tilde{K}} y_j(t) + v(t), \end{aligned} \tag{3.7}$$

where $v(t)$ is a complex Gaussian noise process with zero-mean. The sampling time interval of the received signal is $\Delta = \frac{T_c}{p} = \frac{T}{P}$, where $P \triangleq pN$. Therefore, the n-th sample of i-th symbol for the received signal is given by

$$\begin{aligned} r[i,n] &\triangleq r\left((iP+n)\Delta\right) = r(iT+n\Delta) \\ &= \sum_{k=1}^{K} \underbrace{y_k(iT+n\Delta)}_{y_k[i,n]} + \underbrace{v(iT+n\Delta)}_{v[i,n]}. \end{aligned} \tag{3.8}$$

Denote $\iota_k \triangleq \lceil \frac{d_k+\tau_{kL}+T_c}{T} \rceil$. From (3.4), the component of each user, $y_k[i,n]$ can be expressed in the form

$$\begin{aligned} y_k[i,n] &\triangleq y_k(iT+n\Delta) = \sum_{j=0}^{M-1} b_k[j]\, h_k(iT+n\Delta-jT) \\ &= \sum_{j=i-\iota_k}^{i} b_k[j]\, \underbrace{h_k(iT+n\Delta-jT)}_{h_k[i-j,n]} = \sum_{j=0}^{\iota_k} h_k[j,n]\, b_k[i-j], \end{aligned} \tag{3.9}$$

by using the fact that $h_k(t)$ is zero outside the interval $[0,(\iota_k+1)T]$. For the k-th user, the received signal can be expressed as

$$r[i,n] = h_k[0,n]b_k[i] + \underbrace{\sum_{j=1}^{\iota_k} h_k[j,n]b_k[i-j]}_{\text{ISI}} + \underbrace{\sum_{k'\neq k} y_{k'}[i,n]}_{\text{MAI}} + v[i,n], \quad (3.10)$$

where the second term is the inter symbol interference (ISI) from the previous symbol of the k-th user and the third term is the multiple-access interference (MAI) from the other users. For the convenience of the calculation, we use the vector form of the received signal. Let

$$\underbrace{\underline{r}[i]}_{P\times 1} \triangleq \begin{bmatrix} r[i,0] \\ \vdots \\ r[i,P-1] \end{bmatrix}, \quad \underbrace{\underline{v}[i]}_{P\times 1} \triangleq \begin{bmatrix} v[i,0] \\ \vdots \\ v[i,P-1] \end{bmatrix}, \quad \underbrace{\underline{b}[i]}_{K\times 1} \triangleq \begin{bmatrix} b_1[i] \\ \vdots \\ b_K[i] \end{bmatrix},$$

$$\underbrace{\underline{H}[j]}_{P\times K} \triangleq \begin{bmatrix} h_1[j,0] & \cdots & h_K[j,0] \\ \vdots & \vdots & \vdots \\ h_1[j,P-1] & \cdots & h_K[j,P-1] \end{bmatrix}, \quad j=0,1,\cdots,\iota_k.$$

Then from (3.8) and(3.9) we can express the received signal in the form of the convolution:

$$\underline{r}[i] = \underline{H}[i] * \underline{b}[i]. \quad (3.11)$$

Define $\iota \triangleq \max_{1\le k\le K}\{\iota_k\}$. From the assumption that the i-th symbol is spread over the previous symbol and next symbol, we must consider the m received signal vectors. Define

$$\underbrace{\mathbf{r}[i]}_{Pm\times 1} \triangleq \begin{bmatrix} \underline{r}[i] \\ \vdots \\ \underline{r}[i+m-1] \end{bmatrix}, \quad \underbrace{\mathbf{v}[i]}_{Pm\times 1} \triangleq \begin{bmatrix} \underline{v}[i] \\ \vdots \\ \underline{v}[i+m-1] \end{bmatrix},$$

$$\underbrace{\mathbf{b}[i]}_{r\times 1} \triangleq \begin{bmatrix} \underline{b}[i-\iota] \\ \vdots \\ \underline{b}[i+m-1] \end{bmatrix}, \quad \underbrace{\mathbf{H}}_{Pm\times r} \triangleq \begin{bmatrix} \underline{H}[\iota] & \cdots & \underline{H}[0] & \cdots & \mathbf{0} \\ \vdots & \ddots & \ddots & \ddots & \vdots \\ \mathbf{0} & \cdots & \underline{H}[\iota] & \cdots & \underline{H}[0] \end{bmatrix},$$

where $r \triangleq K(m+\iota)$. We can then write (3.11) in matrix form:

$$\mathbf{r}[i] = \mathbf{H}\,\mathbf{b}[i] + \mathbf{v}[i]. \tag{3.12}$$

In (3.12), the smoothing factor m is chosen from the fact that $m = \lceil \frac{P+K}{P-K} \rceil \iota$. Note the matrix $\mathbf{H}$ is a "tall" matrix, which means $Pm \geq r \triangleq K(m+\iota)$.

For the high resolution of calculation, the correlation matrix of the received signal should be decomposed using eigenvalue decomposition or singular value decomposition.

Lemma 4 ***(Subspace concept 3):*** *The correlation matrix* $\mathbf{R}$ *can be decomposed into signal subspace and noise subspace as*

$$\begin{aligned} \mathbf{R} &= \mathbf{H}\mathbf{H}^H + \sigma^2\mathbf{I} = \mathbf{U}\Lambda\mathbf{U}^T \\ &= [\mathbf{U}_s\mathbf{U}_n] \begin{bmatrix} \Lambda_s & \mathbf{0} \\ \mathbf{0} & \sigma^2\mathbf{I} \end{bmatrix} \begin{bmatrix} \mathbf{U}_s^T \\ \mathbf{U}_n^T \end{bmatrix} \\ &= \mathbf{U}_s\Lambda_s\mathbf{U}_s^T + \sigma^2\mathbf{U}_n\mathbf{U}_n^T \end{aligned} \tag{3.13}$$

where $\mathbf{U}_s$ *is the signal subspace eigenvector matrix,* $\mathbf{U}_n$ *is the noise subspace eigenvector matrix,* Λ_s *is the signal subspace eigenvalue matrix, and* Λ_n *is the noise subspace eigenvalue matrix.*

□

3.2 Linear Detectors

Linear detectors which have linear calculation complexity with respect to the number of users for the asynchronous system can be written as

$$\hat{\tilde{b}}_k = sgn\left(\mathbf{w}_k^H \mathbf{r}\right) \tag{3.14}$$

where $\mathbf{w}_k$ is the vector for user k. Although linear detectors have lower complexity than the optimum detector, they have performance inferior to the optimum detector.

3.3 Blind Linear Multiuser Detectors

There are two blind linear detectors, the blind linear MMSE detector and the blind linear zero-forcing detector. The blind linear MMSE detector can reduce the interference from all users with the knowledge of its own spreading code in terms of Minimum Mean Squared Error (MMSE). The blind linear zero-forcing detector can suppress the interference from all users with the knowledge of its own spreading code in the sense that it forces the other users interference to zero.

3.3.1 Blind Linear MMSE Multiuser Detector

There are two types of method for blind linear MMSE detector: direct method, using the correlation matrix directly, and subspace method, using the signal subspace.

Definition 6 *The vector of blind linear MMSE detectors can be defined as a minimization of Mean Squared Error;*

$$\mathbf{w}_k = \arg \min_{\mathbf{w}_k \in C^{Pm}} E\left[(\bar{b}_k - \mathbf{w}_k^H \mathbf{r})^2\right]. \tag{3.15}$$

□

Proposition 10 ***(Direct Method for the Blind Linear MMSE detector):*** *The estimated information bit of the blind linear MMSE detector with direct method can be written as*

$$\hat{\bar{b}}_k = \mathbf{sgn}\left(\bar{\mathbf{h}}_k^H \mathbf{R}^{-1} \mathbf{r}\right) \tag{3.16}$$

□

Proof: The mean squared error between the real information bit and the estimated information bit is

$$\begin{aligned} & E\left[(\bar{b}_k - \mathbf{w}_k^H \mathbf{r})^2\right] \\ = \; & E\left[(\bar{b}_k - \mathbf{w}_k^H \mathbf{r})(\bar{b}_k - \mathbf{w}_k^H \mathbf{r})^H\right] \end{aligned}$$

$$\begin{aligned} = \; & E\left[(\bar{b}_k - \mathbf{w}_k^H \mathbf{r})(\bar{b}_k - \mathbf{r}^H \mathbf{w}_k)\right] \\ = \; & E\left[(\bar{b}_k^2 + \mathbf{w}_k^H \mathbf{r}\mathbf{r}^H \mathbf{w}_k - 2\bar{b}_k \mathbf{w}_k^H \mathbf{r})\right] \\ = \; & E\left[(\bar{b}_k^2 + \mathbf{w}_k^H \mathbf{r}\mathbf{r}^H \mathbf{w}_k - 2\bar{b}_k \mathbf{w}_k^H (\bar{\mathbf{H}}\bar{\mathbf{b}} + \tilde{\mathbf{H}}\tilde{\mathbf{b}} + \sigma \mathbf{n}))\right] \\ = \; & (E[\bar{b}_k^2] + \mathbf{w}_k^H E[\mathbf{r}\mathbf{r}^H]\mathbf{w}_k - 2\mathbf{w}_k^H (\bar{\mathbf{H}} E[\bar{\mathbf{b}}\bar{b}_k] + \tilde{\mathbf{H}} E[\tilde{\mathbf{b}}\bar{b}_k] + \sigma E[\mathbf{n}\bar{b}_k])) \\ = \; & (1 + \mathbf{w}_k^H \mathbf{R}\mathbf{w}_k - 2\mathbf{w}_k^H \bar{\mathbf{h}}_k). \end{aligned}$$

Since $\mathbf{R}$ is positive definite, the above function is convex and the vector minimizing the above function can be found using

$$\begin{aligned} \nabla(1 + \mathbf{w}_k^H \mathbf{R}\mathbf{w}_k - 2\mathbf{w}_k^H \bar{\mathbf{h}}_k) &= 2\mathbf{R}\mathbf{w}_k - 2\bar{\mathbf{h}}_k = 0 \\ \mathbf{R}\mathbf{w}_k &= \bar{\mathbf{h}}_k \\ \mathbf{w}_k &= \mathbf{R}^{-1}\bar{\mathbf{h}}_k. \end{aligned} \tag{3.17}$$

Q.E.D.

Proposition 11 ***(Subspace Method for the Blind MMSE detector):*** *The estimated information bit of the blind linear MMSE detector using the subspace method can be written as*

$$\hat{\bar{b}}_k = \mathbf{sgn}\left(\bar{\mathbf{h}}_k^H \mathbf{U}_s \Lambda_s^{-1} \mathbf{U}_s^H \mathbf{r}\right) \tag{3.18}$$

□

Proof: The solution of the subspace method for the blind linear MMSE detector can be derived by substituting the result of Lemma 4 for $\mathbf{R}$ and using the fact that $\bar{\mathbf{h}}_k^H \mathbf{U}_n = \mathbf{0}$. The inverse matrix of $\mathbf{R}$ can be derived as

$$\begin{aligned}
\mathbf{R}^{-1} &= (\mathbf{H}\mathbf{H}^H + \sigma^2\mathbf{I})^{-1} \\
&= \left([\mathbf{U}_s \mathbf{U}_n] \begin{bmatrix} \Lambda_s & \mathbf{0} \\ \mathbf{0} & \sigma^2\mathbf{I} \end{bmatrix} \begin{bmatrix} \mathbf{U}_s^H \\ \mathbf{U}_n^H \end{bmatrix}\right)^{-1} \\
&= [\mathbf{U}_s \mathbf{U}_n] \begin{bmatrix} \Lambda_s^{-1} & \mathbf{0} \\ \mathbf{0} & \sigma^{-2}\mathbf{I} \end{bmatrix} \begin{bmatrix} \mathbf{U}_s^H \\ \mathbf{U}_n^H \end{bmatrix} \\
&= \mathbf{U}_s \Lambda_s^{-1} \mathbf{U}_s^H + \sigma^{-2} \mathbf{U}_n \mathbf{U}_n^H
\end{aligned} \tag{3.19}$$

from Lemma 4.

Q.E.D.

3.3.2 Blind Linear Zero-forcing Multiuser Detector

The blind linear zero-forcing detector can be defined in the sense of the minimization problem with a constraint.

Definition 7 *The vector of the blind zero-forcing detector can be defined as*

$$\mathbf{w}_k = \arg \min_{\mathbf{w}_k \in \mathcal{C}^{Pm}} \left[(\mathbf{w}_k^H(\mathbf{H}))^2\right] \ s.t. \ \mathbf{w}_k^H \bar{\mathbf{h}}_k = 1. \tag{3.20}$$

□

Proposition 12 ***(Subspace method for the blind linear zero-forcing detector):*** *From (3.20) and Lemma 4, the estimated information bit of blind linear zero-forcing detector using subspace method is given by*

$$\hat{\bar{b}}_k = \mathbf{sgn}\left(\bar{\mathbf{h}}_k^H \mathbf{U}_s(\Lambda_s - \sigma^2\mathbf{I})^{-1}\mathbf{U}_s^H\mathbf{r}\right). \tag{3.21}$$

□

Proof: Since vector $\mathbf{w}_k \in range(\mathbf{U}_s)$, we can write $\mathbf{w}_k = \mathbf{U}_s\mathbf{c}$. By inserting $\mathbf{w}_k$ into (3.20), we obtain the minimization problem with a constraint:

$$\begin{aligned}
\mathbf{c} &= \arg \min_{\mathbf{c}\in\mathcal{C}^r} \left[((\mathbf{U}_s\mathbf{c})^H(\mathbf{H}))^2\right] \ s.t. \ (\mathbf{U}_s\mathbf{c})^H\bar{\mathbf{h}}_k = 1 \\
&= \arg \min_{\mathbf{c}\in\mathcal{C}^r} \left[(\mathbf{U}_s\mathbf{c})^H(\mathbf{H}\mathbf{H}^H)(\mathbf{U}_s\mathbf{c})\right] \ s.t. \ \mathbf{c}^H\mathbf{U}_s^H\bar{\mathbf{h}}_k = 1 \\
&= \arg \min_{\mathbf{c}\in\mathcal{C}^r} \mathbf{c}^H\left[\mathbf{U}_s^H(\mathbf{H}\mathbf{H}^H)\mathbf{U}_s\right]\mathbf{c} \ s.t. \ \mathbf{c}^H\mathbf{U}_s^H\bar{\mathbf{h}}_k = 1 \\
&= \arg \min_{\mathbf{c}\in\mathcal{C}^r} \mathbf{c}^H\left[\mathbf{U}_s^H(\mathbf{U}_s\Lambda_s\mathbf{U}_s^H + \sigma^2\mathbf{U}_n\mathbf{U}_n^H - \sigma^2\mathbf{I}_K)\mathbf{U}_s\right]\mathbf{c} \\
&\qquad s.t. \ \mathbf{c}^H\mathbf{U}_s^H\bar{\mathbf{h}}_k = 1 \\
&= \arg \min_{\mathbf{c}\in\mathcal{C}^r} \mathbf{c}^H(\Lambda_s - \sigma^2\mathbf{I}_K)\mathbf{c} \ s.t. \ \mathbf{c}^H\mathbf{U}_s^H\bar{\mathbf{h}}_k = 1
\end{aligned} \tag{3.22}$$

where $\bar{r} = \bar{K}(m + \iota)$. By the Lagrange multiplier method, the minimization problem with a constraint (3.22) can be solved as

$$\begin{aligned} \mathcal{L}(\mathbf{c}) &= \mathbf{c}^H(\Lambda_s - \sigma^2\mathbf{I}_K)\mathbf{c} - 2\mu\mathbf{c}^H\left[\mathbf{U}_s^H\bar{\mathbf{h}}_k - 1\right] \\ \nabla\mathcal{L}(\mathbf{c}) &= 2(\Lambda_s - \sigma^2\mathbf{I}_K)\mathbf{c} - 2\mu\mathbf{U}_s^H\bar{\mathbf{h}}_k = \mathbf{0} \\ \mathbf{c} &= \mu(\Lambda_s - \sigma^2\mathbf{I}_K)^{-1}\mathbf{U}_s^H\bar{\mathbf{h}}_k. \end{aligned} \tag{3.23}$$

Thus,

$$\mathbf{w}_k = \mu\mathbf{U}_s(\Lambda_s - \sigma^2\mathbf{I}_K)^{-1}\mathbf{U}_s^H\bar{\mathbf{h}}_k \tag{3.24}$$

and μ can be omitted because of the **sgn** processing for detection.

Q.E.D.

3.4 Group-Blind Multiuser Detection

Consider an asynchronous DS-CDMA cellular system which has intra-cell interference and inter-cell interference. Unlike the group-blind multiuser detectors for the synchronous system, the group-blind multiuser detection for the asynchronous system considers inter symbol interference (ISI) and multiple access interference (MAI). The channel matrix $\bar{\mathbf{H}}$ includes the multi-path channel responses and the spreading codes for known users. In this section, we assume that this channel matrix is known. In Chapter 4, we will introduce blind channel estimation.

There is another subspace concept for group-blind multiuser detectors. The basic idea is that after projection of the correlation matrix onto orthogonal subspace of $\bar{\mathbf{H}}$, we can decompose the orthogonally projected correlation matrix to signal subspace of $\tilde{\mathbf{H}}$ and noise subspace.

Lemma 5 ***(Subspace concept 4):*** *The orthogonally projected correlation matrix of the received signal can be expressed as*

$$\bar{\mathbf{P}}^{\perp}\mathbf{R}\bar{\mathbf{P}}^{\perp} = \tilde{\mathbf{U}}_s\tilde{\Lambda}_s\tilde{\mathbf{U}}_s^H + \sigma^2\tilde{\mathbf{U}}_n\tilde{\mathbf{U}}_n^H. \tag{3.25}$$

□

Proof: The projection matrix of $\bar{\mathbf{H}}$ is

$$\bar{\mathbf{P}} = \bar{\mathbf{H}}(\bar{\mathbf{H}}^T\bar{\mathbf{H}})^{-1}\bar{\mathbf{H}}^H, \tag{3.26}$$

and the orthogonal projection matrix is

$$\bar{\mathbf{P}}^{\perp} = \mathbf{I} - \bar{\mathbf{P}}. \tag{3.27}$$

Since $\bar{\mathbf{P}}^{\perp}$ projects $\mathbf{R}$ onto orthogonal subspace of $\bar{\mathbf{H}}$, only subspace of $\tilde{\mathbf{H}}$ and noise space are remained. Hence, the orthogonally projected correlation matrix can be decomposed as

$$\begin{aligned}\bar{\mathbf{P}}^{\perp}\mathbf{R}\bar{\mathbf{P}}^{\perp} &= \left[\tilde{\mathbf{U}}_s\tilde{\mathbf{U}}_n\tilde{\mathbf{U}}_o\right]\begin{bmatrix}\tilde{\Lambda}_s & \mathbf{0} & \mathbf{0}\\ \mathbf{0} & \sigma^2\mathbf{I} & \mathbf{0}\\ \mathbf{0} & \mathbf{0} & \mathbf{0}\end{bmatrix}\begin{bmatrix}\tilde{\mathbf{U}}_s^H\\ \tilde{\mathbf{U}}_n^H\\ \tilde{\mathbf{U}}_o^H\end{bmatrix}\\ &= \tilde{\mathbf{U}}_s\tilde{\Lambda}_s\tilde{\mathbf{U}}_s^H + \sigma^2\tilde{\mathbf{U}}_n\tilde{\mathbf{U}}_n^H.\end{aligned} \tag{3.28}$$

Q.E.D.

The following work has been completed by Anders Høst-Madsen and Xiaodong Wang in 1999, and these detectors have the best performance in the presence of inter-cell interference.

3.4.1 Group-Blind Linear Zero-forcing Multiuser Detection

The group-blind linear zero-forcing detector eliminates intra-cell interference and minimizes inter-cell interference using a zero-forcing technique.

Definition 8 ***(Group-blind Linear Zero-forcing Detector):*** *The vector of group-blind linear zero-forcing detector can be defined by*

$$\bar{\mathbf{d}}_k = \arg \min_{\mathbf{d} \in \mathbf{range(\bar{H})}} \left|\mathbf{d}^H \mathbf{H}\right|^2, \quad \textit{subject to} \quad \mathbf{d}^H \bar{\mathbf{H}} = \mathbf{1}_{\bar{K}\iota+k}^T. \tag{3.29}$$

□

The group-blind linear zero-forcing detector has two forms. First, form I of the detector uses subspace concept 4 (Lemma 5) with a lower calculation complexity.

Proposition 13 ***(Form I of the Group-blind Linear Zero-forcing Detector):*** *The estimated information bit of group-blind linear zero-forcing detector can be written as*

$$\hat{\bar{b}}_k = \mathbf{sgn}\left(\mathbf{1}_{\bar{K}\iota+k}^T (\bar{\mathbf{H}}^T \bar{\mathbf{H}})^{-1} \bar{\mathbf{H}}^T [\mathbf{I} - \mathbf{R}\tilde{\mathbf{U}}_s (\tilde{\Lambda}_s - \sigma^2 \mathbf{I})^{-1} \tilde{\mathbf{U}}_s^T] \mathbf{r}\right). \tag{3.30}$$

□

Proof: Assume that $\mathbf{w}_k$ has two components, $\bar{\mathbf{w}}_k \in \mathbf{range}(\bar{\mathbf{H}})$ and $\tilde{\mathbf{w}}_k \in \mathbf{range}(\tilde{\mathbf{U}}_s)$. Then $\mathbf{w}_k$ can be expressed as the summation of two components , i.e., $\mathbf{w}_k =$

$\tilde{\mathbf{w}}_k + \bar{\mathbf{w}}_k$. $\bar{\mathbf{w}}_k$ can be obtained from the constraint of (3.29) using the pseudo inverse of $\bar{\mathbf{H}}$:

$$\bar{\mathbf{w}}_k = \bar{\mathbf{H}} \left(\bar{\mathbf{H}}^H \bar{\mathbf{H}}\right)^{-1} \mathbf{1}_{\bar{K}\iota+k}. \tag{3.31}$$

Then $\mathbf{w}_k = \tilde{\mathbf{U}}_s \mathbf{c}_k + \bar{\mathbf{w}}_k$, for some $\mathbf{c}_k \in \mathcal{C}^{\tilde{r}}$ where $\tilde{r} = \tilde{K}(m+\iota)$. $\mathbf{c}_k$ can be found by inserting $\mathbf{w}_k$ to the minimization of (3.29):

$$\begin{aligned}
\mathbf{c}_k &= \arg\min_{\mathbf{c}\in\mathcal{C}^{\tilde{r}}} \left\{ \left(\tilde{\mathbf{U}}_s \mathbf{c} + \bar{\mathbf{w}}_k\right)^H \mathbf{H} \right\}^2 \\
&= \arg\min_{\mathbf{c}\in\mathcal{C}^{\tilde{r}}} \left(\tilde{\mathbf{U}}_s \mathbf{c}_k + \bar{\mathbf{w}}_k\right)^H \left(\mathbf{H}\mathbf{H}^H\right) \left(\tilde{\mathbf{U}}_s \mathbf{c}_k + \bar{\mathbf{w}}_k\right) \\
&= \arg\min_{\mathbf{c}\in\mathcal{C}^{\tilde{r}}} \left(\tilde{\mathbf{U}}_s \mathbf{c}_k + \bar{\mathbf{w}}_k\right)^H \left(\mathbf{R} - \sigma^2\mathbf{I}\right) \left(\tilde{\mathbf{U}}_s \mathbf{c}_k + \bar{\mathbf{w}}_k\right).
\end{aligned} \tag{3.32}$$

The derivative of (3.32) is

$$\bigtriangledown = 2\tilde{\mathbf{U}}_s^H \left(\mathbf{R} - \sigma^2\mathbf{I}\right) \left(\tilde{\mathbf{U}}_s \mathbf{c}_k + \bar{\mathbf{w}}_k\right) = 0. \tag{3.33}$$

By solving the above equation, we get

$$\begin{aligned}
\mathbf{c}_k &= -\left[\tilde{\mathbf{U}}_s^H \left(\mathbf{R} - \sigma^2\mathbf{I}\right) \tilde{\mathbf{U}}_s\right]^{-1} \tilde{\mathbf{U}}_s^H \left(\mathbf{R} - \sigma^2\mathbf{I}\right) \bar{\mathbf{w}}_k \\
&= -\left[\tilde{\mathbf{U}}_s^H \bar{\mathbf{P}}^{\perp} \left(\mathbf{R} - \sigma^2\mathbf{I}\right) \bar{\mathbf{P}}^{\perp} \tilde{\mathbf{U}}_s\right]^{-1} \tilde{\mathbf{U}}_s^H \left(\mathbf{R} - \sigma^2\mathbf{I}\right) \bar{\mathbf{w}}_k \\
&= -\left(\tilde{\Lambda}_s - \sigma^2\mathbf{I}\right)^{-1} \tilde{\mathbf{U}}_s^H \left(\mathbf{R} - \sigma^2\mathbf{I}\right) \bar{\mathbf{w}}_k \\
&= -\left(\tilde{\Lambda}_s - \sigma^2\mathbf{I}\right)^{-1} \tilde{\mathbf{U}}_s^H \mathbf{R} \bar{\mathbf{w}}_k
\end{aligned} \tag{3.34}$$

from the fact that $\bar{\mathbf{P}} + \bar{\mathbf{P}}^{\perp} = \mathbf{I}$, $\tilde{\mathbf{U}}_s^H \bar{\mathbf{P}} = \mathbf{0}$, and $\tilde{\mathbf{U}}_s^H \bar{\mathbf{w}}_k = \mathbf{0}$. Finally $\mathbf{w}_k$ can be written as

$$\mathbf{w}_k = \tilde{\mathbf{U}}_s \mathbf{c}_k + \bar{\mathbf{w}}_k = [\mathbf{I} - \tilde{\mathbf{U}}_s (\tilde{\Lambda}_s - \sigma^2 \mathbf{I})^{-1} \tilde{\mathbf{U}}_s^H \mathbf{R}] \bar{\mathbf{H}} (\bar{\mathbf{H}}^H \bar{\mathbf{H}})^{-1} \mathbf{1}_{\bar{K}\iota+k}. \quad (3.35)$$

Q.E.D.

Second, form II of the detector uses subspace concept 3 (Lemma 4).

Proposition 14 ***(Form II of the Group-blind Linear Zero-forcing Detector)*** *The estimated information bit of group-blind linear zero-forcing detector can be written as*

$$\begin{aligned} \hat{\bar{b}}_k &= \mathbf{sgn}\left(\mathbf{1}_{\bar{K}\iota+k}^T \left[\bar{\mathbf{H}}^H \mathbf{U}_s \left(\Lambda_s - \sigma^2 \mathbf{I} \right)^{-1} \mathbf{U}_s^H \bar{\mathbf{H}} \right]^{-1} \right. \\ &\times \left. \bar{\mathbf{H}}^H \mathbf{U}_s \left(\Lambda_s - \sigma^2 \mathbf{I} \right)^{-1} \mathbf{U}_s^H \mathbf{r} \right) \end{aligned} \quad (3.36)$$

□

Proof: We utilize the Lagrange multiplier method to solve the constrained optimization problem (3.29). Therefore, $\mathbf{w}_k$ is

$$\begin{aligned} \mathbf{w}_k &= \arg \min_{\mathbf{w}_k \in \mathbf{range(H)}} \mathbf{w}_k^H \mathbf{H} \mathbf{H}^H \mathbf{w}_k + \underline{\lambda}^H \left(\bar{\mathbf{H}}^H \mathbf{w}_k - \mathbf{1}_{\bar{K}\iota+k} \right) \\ &= \left(\mathbf{H} \mathbf{H}^H \right)^{\dagger} \bar{\mathbf{H}} \underline{\lambda}. \end{aligned} \quad (3.37)$$

By substituting (3.37) into $\bar{\mathbf{H}}^H \mathbf{w}_k = \mathbf{1}_{\bar{K}\iota+k}$, we obtain $\underline{\lambda} = [\bar{\mathbf{H}}^H (\mathbf{H}\mathbf{H}^H)^\dagger \bar{\mathbf{H}}]^{-1} \mathbf{1}_{\bar{K}\iota+k}$.

Thus, the solution for group-blind linear zero-forcing detector for user k is

$$\begin{aligned} \mathbf{w}_k &= (\mathbf{H}\mathbf{H}^H)^\dagger \bar{\mathbf{H}} \left[\bar{\mathbf{H}}^H (\mathbf{H}\mathbf{H}^H)^\dagger \bar{\mathbf{H}}\right]^{-1} \mathbf{1}_k \\ &= \mathbf{U}_s (\Lambda_s - \sigma^2 \mathbf{I})^{-1} \mathbf{U}_s^H \bar{\mathbf{H}} \left[\bar{\mathbf{H}}^H \mathbf{U}_s (\Lambda_s - \sigma^2 \mathbf{I})^{-1} \mathbf{U}_s^H \bar{\mathbf{H}}\right]^{-1} \mathbf{1}_{\bar{K}\iota+k}, \end{aligned} \quad (3.38)$$

from Lemma 4 and the fact that $\mathbf{U}_n^H \bar{\mathbf{H}} = \mathbf{0}$.

Q.E.D.

3.4.2 Group-Blind Linear Hybrid Multiuser Detection

The group-blind linear hybrid detector minimizes inter-cell interference with the MMSE method and minimizes intra-cell interference with the zero-forcing technique.

Definition 9 ***(Group-blind Linear Hybrid Detector):*** *The group-blind Linear hybrid detector can be defined as*

$$\mathbf{w}_k = \arg \min_{\mathbf{w} \in \text{range}(\bar{\mathbf{H}})} E\left\{ \left| b_k[i] - \mathbf{w}_k^H \mathbf{r}[i] \right|^2 \right\}, \text{ subject to } \mathbf{w}^H \bar{\mathbf{H}} = \mathbf{1}_{\bar{K}\iota+k}^T. \quad (3.39)$$

□

There are two forms of detector for the group-blind linear hybrid detector. Form I of the detector uses the projection method and can be proposed as follows:

Proposition 15 ***(Form I of the Group-blind Linear Hybrid Detector):*** *The estimated information bit of the group-blind linear hybrid detector can be written as*

$$\hat{\tilde{b}}_k = \mathbf{sgn}\left(\mathbf{1}_{\bar{K}\iota+k}^T(\bar{\mathbf{H}}^H\bar{\mathbf{H}})^{-1}\bar{\mathbf{H}}^H(\mathbf{I}-\mathbf{R}\tilde{\mathbf{U}}_s\tilde{\Lambda}_s^{-1}\tilde{\mathbf{U}}_s^H)\mathbf{r}\right). \tag{3.40}$$

□

Proof: Assume that $\mathbf{w}_k$ has two components, $\bar{\mathbf{w}}_k \in \mathsf{range}(\bar{\mathbf{H}})$ and $\tilde{\mathbf{w}}_k \in \mathsf{range}(\tilde{\mathbf{U}}_s)$. Then $\mathbf{w}_k$ can be expressed as the summation of two components , i.e., $\mathbf{w}_k = \tilde{\mathbf{w}}_k + \bar{\mathbf{w}}_k$. $\bar{\mathbf{w}}_k$ can be obtained from the constraint of (3.39) using the pseudo inverse of $\bar{\mathbf{H}}$:

$$\bar{\mathbf{w}}_k = \bar{\mathbf{H}}\left(\bar{\mathbf{H}}^H\bar{\mathbf{H}}\right)^{-1}\mathbf{1}_{\bar{K}\iota+k}. \tag{3.41}$$

Thus the vector for user k is $\mathbf{w}_k = \tilde{\mathbf{U}}_s\mathbf{c}_k + \bar{\mathbf{w}}_k$, for some $\mathbf{c}_k \in \mathcal{C}^{\tilde{r}}$. $\mathbf{c}_k$ can be found by inserting $\mathbf{w}_k$ to the minimization of (3.39):

$$\begin{aligned}
\mathbf{c}_k &= \arg\min_{\mathbf{c}\in\mathcal{C}^{\tilde{r}}} E\left\{\left|b_k[i] - \left(\tilde{\mathbf{U}}_s\mathbf{c}+\bar{\mathbf{w}}_k\right)^H\mathbf{r}[i]\right|^2\right\} \\
&= \arg\min_{\mathbf{c}\in\mathcal{C}^{\tilde{r}}} \left(\tilde{\mathbf{U}}_s\mathbf{c}+\bar{\mathbf{w}}_k\right)^H\mathbf{R}\left(\tilde{\mathbf{U}}_s\mathbf{c}+\bar{\mathbf{w}}_k\right) - 2\mathbf{c}^H\tilde{\mathbf{U}}_s^H\bar{\mathbf{h}}_k \\
&= -\left(\tilde{\mathbf{U}}_s^H\mathbf{R}\tilde{\mathbf{U}}_s\right)^{-1}\tilde{\mathbf{U}}_s^H\mathbf{R}\bar{\mathbf{w}}_k = -\tilde{\Lambda}_s^{-1}\tilde{\mathbf{U}}_s^H\mathbf{R}\bar{\mathbf{w}}_k,
\end{aligned} \tag{3.42}$$

from the fact that $\bar{\mathbf{P}} + \bar{\mathbf{P}}^{\perp} = \mathbf{I}$, $\tilde{\mathbf{U}}_s^H \bar{\mathbf{P}} = \mathbf{0}$,$\tilde{\mathbf{U}}_s^H \bar{\mathbf{s}}_k = \mathbf{0}$, and Lemma 5. Hence, the $\bar{\mathbf{w}}_k$ can be written as

$$\begin{aligned} \bar{\mathbf{w}}_k &= \tilde{\mathbf{U}}_s \mathbf{c}_k + \bar{\mathbf{w}}_k \\ &= (\mathbf{I}_{Pm} - \tilde{\mathbf{U}}_s \tilde{\Lambda}_s^{-1} \tilde{\mathbf{U}}_s^H \mathbf{R}) \bar{\mathbf{w}}_k \\ &= (\mathbf{I}_{Pm} - \tilde{\mathbf{U}}_s \tilde{\Lambda}_s^{-1} \tilde{\mathbf{U}}_s^H \mathbf{R}) \bar{\mathbf{H}} (\bar{\mathbf{H}}^H \bar{\mathbf{H}})^{-1} \mathbf{1}_{\bar{K}\iota+k}. \end{aligned} \tag{3.43}$$

Q.E.D.

Proposition 16 ***(Form II of the Group-blind Linear Hybrid Detector):*** *The estimated information bit of the group-blind linear hybrid detector can be expressed as*

$$\hat{\bar{b}}_k = \mathbf{sgn}\left(\mathbf{1}_{\bar{K}\iota+k}^T \left[\bar{\mathbf{H}}^H \mathbf{U}_s \Lambda_s^{-1} \mathbf{U}_s^H \bar{\mathbf{H}} \right]^{-1} \bar{\mathbf{H}}^H \mathbf{U}_s \Lambda_s^{-1} \mathbf{U}_s^H \mathbf{r} \right). \tag{3.44}$$

□

Proof: The constrained optimization problem (3.39) can be solved using the Lagrange multiplier method. Thus the problem (3.39) can be written as

$$\begin{aligned} \mathbf{w}_k &= \arg\min_{\mathbf{w} \in \mathcal{C}^{\bar{r}}} E\left\{ \left| b_k[i] - \mathbf{w}^H \mathbf{r}[i] \right|^2 \right\} + \tilde{\underline{\lambda}}^H \left(\bar{\mathbf{H}}^H \mathbf{w} - \mathbf{1}_{\bar{K}\iota+k} \right) \\ &= \arg\min_{\mathbf{w} \in \mathcal{C}^{\bar{r}}} \mathbf{w}^H \mathbf{R} \mathbf{w} - 2 \bar{\mathbf{H}}_k^H \mathbf{w} + \tilde{\underline{\lambda}}^H \left(\bar{\mathbf{H}}^H \mathbf{w} - \mathbf{1}_{\bar{K}\iota+k} \right) \\ &= \arg\min_{\mathbf{w} \in \mathcal{C}^{\bar{r}}} \mathbf{w}^H \mathbf{R} \mathbf{w} + \underline{\lambda}^H \left(\bar{\mathbf{H}}^H \mathbf{w} - \mathbf{1}_{\bar{K}\iota+k} \right) = \mathbf{R}^{-1} \bar{\mathbf{H}} \underline{\lambda}, \end{aligned} \tag{3.45}$$

where $\underline{\lambda} \triangleq \tilde{\underline{\lambda}} - 2\mathbf{1}_{\bar{K}\iota+k}$. Substituting (3.45) into the constraint that $\bar{\mathbf{H}}^H\mathbf{w}_k = \mathbf{1}_{\bar{K}\iota+k}$, we obtain $\underline{\lambda} = (\bar{\mathbf{H}}^H\mathbf{R}^{-1}\bar{\mathbf{H}})^{-1}\mathbf{1}_{\bar{K}\iota+k}$. Hence, $\mathbf{w}_k$ can be written as

$$\begin{aligned}\mathbf{w}_k &= \mathbf{R}^{-1}\bar{\mathbf{H}}\left[\bar{\mathbf{H}}^H\mathbf{R}^{-1}\bar{\mathbf{H}}\right]^{-1}\mathbf{1}_{\bar{K}\iota+k} \\ &= \mathbf{U}_s\Lambda_s^{-1}\mathbf{U}_s^{\mathbf{H}}\bar{\mathbf{H}}\left[\bar{\mathbf{H}}^{\mathbf{H}}\mathbf{U}_s\Lambda_s^{-1}\mathbf{U}_s^{\mathbf{H}}\bar{\mathbf{H}}\right]^{-1}\mathbf{1}_{\bar{\mathbf{K}}\iota+\mathbf{k}},\end{aligned} \tag{3.46}$$

using the fact that$\mathbf{U}_n^H\bar{\mathbf{H}} = \mathbf{0}$ and Lemma 4.

Q.E.D.

3.4.3 Group-Blind Linear MMSE Multiuser Detection

The group-blind linear MMSE multiuser detector minimizes inter-cell interference and intra-cell interference with the MMSE method.

Let $\bar{\mathbf{r}}[i] = \bar{\mathbf{H}}\bar{\mathbf{b}}[i] + \mathbf{v}[i]$ be the component of $\mathbf{r}[i]$, i.e., known users' signal and noise of $\mathbf{r}[i]$. Then the group-blind linear MMSE multiuser detector can be defined as follows:

Definition 10 ***(Group-blind Linear MMSE Detector):*** *The group-blind linear MMSE detector for user k can be defined as* $\mathbf{w}_k = \bar{\mathbf{w}}_k + \tilde{\mathbf{w}}_k$, *where* $\bar{\mathbf{w}}_k \in \bar{\mathbf{H}}$ *and* $\tilde{\mathbf{w}}_k \in \tilde{\mathbf{U}}_s$, *such that*

$$\bar{\mathbf{w}}_k = \arg \min_{\mathbf{w}\in\mathbf{range}(\bar{\mathbf{H}})} E\left\{\left|b_k[i] - \mathbf{w}^H\bar{\mathbf{r}}[i]\right|^2\right\}, \tag{3.47}$$

$$\tilde{\mathbf{w}}_k = \arg \min_{\mathbf{w}\in\mathbf{range}(\tilde{\mathbf{U}}_s)} E\left\{\left|b_k[i] - (\mathbf{w} + \bar{\mathbf{w}}_k)^H\mathbf{r}[i]\right|^2\right\}. \tag{3.48}$$

□

Proposition 17 ***(Form I of the Group-blind Linear MMSE Detector)*** *The estimated information bit of the group-blind linear MMSE detector can be expressed as*

$$\hat{\bar{b}}_k = \mathbf{sgn}\left(\mathbf{1}_{\bar{K}\iota+k}^T \left(\bar{\mathbf{H}}^H\bar{\mathbf{H}} + \sigma^2\mathbf{I}\right)^{-1}\bar{\mathbf{H}}^H\left(\mathbf{I} - \mathbf{R}\tilde{\mathbf{U}}_s\tilde{\Lambda}_s^{-1}\tilde{\mathbf{U}}_s^H\right)\mathbf{r}\right) \tag{3.49}$$

□

Proof: From (3.47), we can find $\bar{\mathbf{w}}_k$. We assume $\bar{\mathbf{w}}_k = \bar{\mathbf{H}}\bar{\mathbf{c}}_k$ because $\bar{\mathbf{w}}_k \in \bar{\mathbf{H}}$, and $\bar{\mathbf{H}}$ has full column rank $\bar{r} = \bar{K}(m+\iota)$. We can find $\mathbf{c}_k$ by substituting $\bar{\mathbf{w}}_k$ into (3.48):

$$\begin{aligned}
\bar{\mathbf{c}}_k &= \arg\min_{\mathbf{c}\in\mathcal{C}^{\bar{r}}} E\left\{\left|b_k[i] - \mathbf{c}^H\bar{\mathbf{H}}^H\bar{\mathbf{r}}[i]\right|^2\right\} \\
&= \arg\min_{\mathbf{c}\in\Re^{\bar{K}}} \mathbf{c}^H\left[\bar{\mathbf{H}}^H\left(\bar{\mathbf{H}}\bar{\mathbf{H}}^H + \sigma^2\mathbf{I}\right)\bar{\mathbf{H}}\right]\mathbf{c} - 2\mathbf{1}_{\bar{K}\iota+k}^H\bar{\mathbf{H}}^H\bar{\mathbf{H}}\mathbf{c} \\
&= \left[\left(\bar{\mathbf{H}}^H\bar{\mathbf{H}}\right)\left(\bar{\mathbf{H}}^H\bar{\mathbf{H}}\right) + \sigma^2\bar{\mathbf{H}}^H\bar{\mathbf{H}}\right]^{-1}\left(\bar{\mathbf{H}}^H\bar{\mathbf{H}}\right)\mathbf{1}_{\bar{K}\iota+k} \\
&= \left(\bar{\mathbf{H}}^H\bar{\mathbf{H}} + \sigma^2\mathbf{I}\right)^{-1}\mathbf{1}_{\bar{K}\iota+k}.
\end{aligned} \tag{3.50}$$

From the same derivation as (3.42), we can write $\tilde{\mathbf{w}}_k = \tilde{\mathbf{U}}_s\tilde{\mathbf{c}}_k = -\tilde{\Lambda}_s^{-1}\tilde{\mathbf{U}}_s^H\mathbf{R}\bar{\mathbf{w}}_k$,

and $\mathbf{w}_k$ is the summation of these two results:

$$\begin{aligned}\mathbf{w}_k &= \tilde{\mathbf{U}}_s\tilde{\mathbf{c}}_k + \bar{\mathbf{w}}_k = \left(\mathbf{I} - \tilde{\mathbf{U}}_s\tilde{\Lambda}_s^{-1}\tilde{\mathbf{U}}_s^H\mathbf{R}\right)\bar{\mathbf{H}}\bar{\mathbf{c}}_k \\ &= \left(\mathbf{I} - \tilde{\mathbf{U}}_s\tilde{\Lambda}_s^{-1}\tilde{\mathbf{U}}_s^H\mathbf{R}\right)\bar{\mathbf{H}}\left(\bar{\mathbf{H}}^H\bar{\mathbf{H}} + \sigma^2\mathbf{I}\right)^{-1}\mathbf{1}_{\bar{K}\iota+k}. \qquad (3.51)\end{aligned}$$

Q.E.D.

Proposition 18 ***(Form II of the Group-blind Linear MMSE Detector):*** *The estimated data of the group-blind linear MMSE detector can be written as*

$$\begin{aligned}\hat{\bar{b}}_k &= \mathbf{sgn}\Big(\mathbf{1}_{\bar{K}\iota+k}^T\left(\bar{\mathbf{H}}^H\bar{\mathbf{H}} + \sigma^2\mathbf{I}\right)^{-1}\bar{\mathbf{H}}^H \\ &\times \left[\mathbf{I} - \left(\mathbf{Q}_s\mathbf{R}_s^{-T}\right)\left(\Pi\Lambda_s\Pi^H\right)^{-1}\left(\mathbf{Q}_s\mathbf{R}_s^{-T}\right)^H\mathbf{R}\right]\mathbf{r}\Big) \qquad (3.52)\end{aligned}$$

□

Proof: With $\mathbf{U}_s$, we need to first find a basis for the $\mathsf{range}(\tilde{\mathbf{U}}_s)$. Clearly, $\mathsf{range}\left(\bar{\mathbf{P}}^{\perp}\mathbf{U}_s\right) = \mathsf{range}(\tilde{\mathbf{U}}_s)$. Consider the (rank-deficient) QR factorization of the matrix $\left(\bar{\mathbf{P}}^{\perp}\mathbf{U}_s\right)$:

$$\bar{\mathbf{P}}^{\perp}\mathbf{U}_s = \begin{bmatrix}\mathbf{Q}_s & \mathbf{Q}_o\end{bmatrix}\begin{bmatrix}\mathbf{R}_s & \mathbf{R}_o \\ \mathbf{0} & \mathbf{0}\end{bmatrix}\Pi. \qquad (3.53)$$

From the same derivation of (3.51)

$$\mathbf{w}_k = \left[\mathbf{I} - \mathbf{Q}_s \left(\mathbf{Q}_s^H \mathbf{R} \mathbf{Q}_s\right)^{-1} \mathbf{Q}_s^H \mathbf{R}\right] \bar{\mathbf{H}} \left(\bar{\mathbf{H}}^H \bar{\mathbf{H}} + \sigma^2 \mathbf{I}_{\bar{r}}\right)^{-1} \mathbf{1}_{\bar{K}t+k}. \tag{3.54}$$

Furthermore,

$$\begin{aligned}
&\mathbf{Q}_s^H \mathbf{R} \mathbf{Q}_s = \mathbf{Q}_s^H \left(\mathbf{U}_s \Lambda_s \mathbf{U}_s^H + \sigma^2 \mathbf{U}_n \mathbf{U}_n^H\right) \mathbf{Q}_s = \mathbf{Q}_s^H \left(\mathbf{U}_s \Lambda_s \mathbf{U}_s^H\right) \mathbf{Q}_s \\
&= \mathbf{Q}_s^H \left(\bar{\mathbf{P}}^{\perp} \mathbf{U}_s \Lambda_s \mathbf{U}_s^H \bar{\mathbf{P}}^{\perp}\right) \mathbf{Q}_s = \mathbf{Q}_s^H \left(\bar{\mathbf{P}}^{\perp} \mathbf{U}_s\right) \Lambda_s \left(\bar{\mathbf{P}}^{\perp} \mathbf{U}_s\right)^H \mathbf{Q}_s \\
&= \mathbf{Q}_s^H \begin{bmatrix} \mathbf{Q}_s & \mathbf{Q}_o \end{bmatrix} \begin{bmatrix} \mathbf{R}_s & \mathbf{R}_o \\ 0 & 0 \end{bmatrix} \Pi \Lambda_s \Pi^H \begin{bmatrix} \mathbf{R}_s & \mathbf{R}_o \\ 0 & 0 \end{bmatrix}^H \begin{bmatrix} \mathbf{Q}_s & \mathbf{Q}_o \end{bmatrix}^H \mathbf{Q}_s \\
&= \mathbf{R}_s \Pi \Lambda_s \Pi^H \mathbf{R}_s^H,
\end{aligned} \tag{3.55}$$

Q.E.D.

3.5 Performance Analysis

In this section, we analyze the performance of multiuser detectors. The estimated information data of a linear detector for user 1 is given by

$$\hat{\tilde{b}}_1[i] = \mathbf{sgn}\left(\mathbf{w}_1^H \mathbf{r}[i]\right). \tag{3.56}$$

From (3.4) and (3.7), the received signal is

$$\mathbf{r}[i] = \sum_{k=1}^{K} \bar{b}_k[i]\bar{\mathbf{h}}_k + \sum_{j=1}^{\tilde{K}} \tilde{b}_j[i]\tilde{\mathbf{h}}_j + \sigma\mathbf{n}. \tag{3.57}$$

Thus the output of the linear detector can be written as

$$\mathbf{w}_1^H\mathbf{r}[i] = \bar{b}_1[i]\mathbf{w}_1^H\bar{\mathbf{h}}_1 + \underbrace{\sum_{k=2}^{K} \bar{b}_k[i]\mathbf{w}_1^H\bar{\mathbf{h}}_k}_{intra-cell\ MAI} + \underbrace{\sum_{j=1}^{\tilde{K}} \tilde{b}_j[i]\mathbf{w}_1^H\tilde{\mathbf{h}}_j}_{inter-cell\ MAI} + \underbrace{\sigma\mathbf{w}_1^H\mathbf{n}}_{noise}. \tag{3.58}$$

Assuming that the user information data are independent and that the noise is independent of user information data, the signal-to-interference-plus-noise ratio(SINR) at the output of the linear detector is obtained using

$$\begin{aligned} SINR(\mathbf{w}_1) &= \frac{E\left\{\mathbf{w}_1^H\mathbf{r}[i]|\bar{b}_1[i]\right\}^2}{Var\left\{\mathbf{w}_1^H\mathbf{r}[i]|\bar{b}_1[i]\right\}} \\ &= \frac{\left(\mathbf{w}_1^H\bar{\mathbf{h}}_1\right)^2}{\sum_{k=2}^{K}\left(\mathbf{w}_1^H\bar{\mathbf{h}}_k\right)^2 + \sum_{j=1}^{\tilde{K}}\left(\mathbf{w}_1^H\tilde{\mathbf{h}}_j\right)^2 + \sigma^2||\mathbf{w}_1||^2} \end{aligned} \tag{3.59}$$

In this thesis, we assume an asynchronous system which has 6 users in the cell of interest and 4 inter-cell interfering users from adjacent cells. For simplicity, the BPSK modulation scheme is used. The processing gain is 31, the received amplitude of in-cell users is $1 + j1$, and the received amplitude of out-cell users is $1/\sqrt{2} + j1/\sqrt{2}$. Randomly generated spreading codes are used for comparison with different cross-correlation of spreading codes. The chip pulse is a raised

cosine pulse with roll-off factor 0.5. The number of paths is 3. The delay of each user d_k is uniformly distributed on $[0, 4T_c]$ and the delay of each path $\tau_{k,l}$ is uniformly distributed on $[0, 4T_c]$. The fading gain of each path is generated from a complex gaussian distribution The oversampling factor p is 2 and the smoothing factor m is 2. SINRs for each multiuser detector are obtained from (3.59). From the evaluation of the minimum SINR of the detectors, we can find the performance in the worst case, i.e., high cross-correlation between spreading codes. The bit error rate can be obtained by $Q(\sqrt{SINR})$ where Q is the Q function of the Gaussian probability density function.

Figure 3.3 shows the performance of hybrid group-blind multiuser detectors in the case of the best situation (low cross-correlation, small delays of paths, and small fading) and the worst situation (high cross-correlation, large path delays, and serious fading). The minimum SINR of the hybrid group-blind multiuser detector is better than that of the conventional detector and the partial-MMSE detector at around SNR$\geq 2dB$. However, the hybrid group-blind multiuser detector has a lower SINR than the conventional detector and the partial-MMSE detector at the low SNRs. The maximum SINRs of the hybrid group-blind multiuser detector have almost the same values as the full MMSE detector at all SNRs. In Figure 3.4, the SINRs of the group-blind MMSE multiuser detector have almost the same values as the ideal full MMSE detector and subspace based blind MMSE detector. In the worst case, the minimum SINRs of the group-blind

MMSE detector have a lower SINR difference than maximum SINRs. Figure 3.5 shows a performance comparison of group-blind multiuser detectors. We can see that the group-blind MMSE multiuser detector has the best performance compared to other group-blind multiuser detectors in the worst case. However, group-blind multiuser detectors have almost the same performance at the best case.

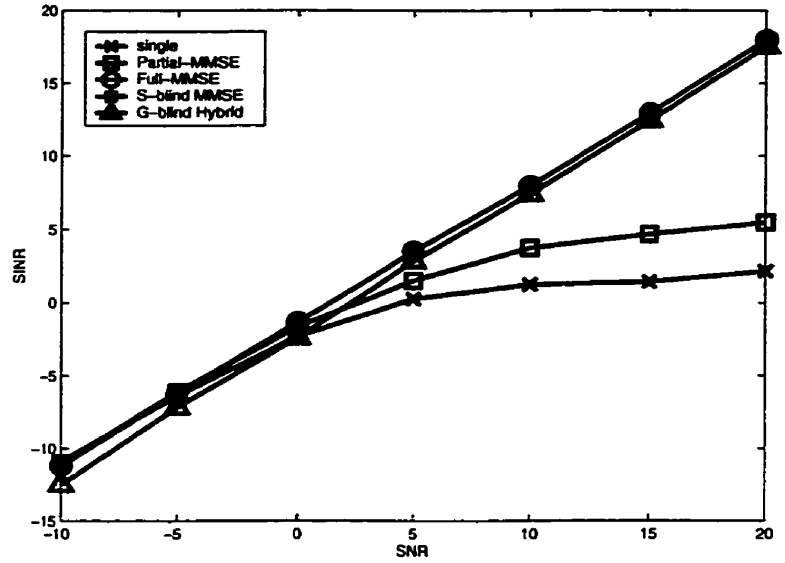

(a) Minimum SINR

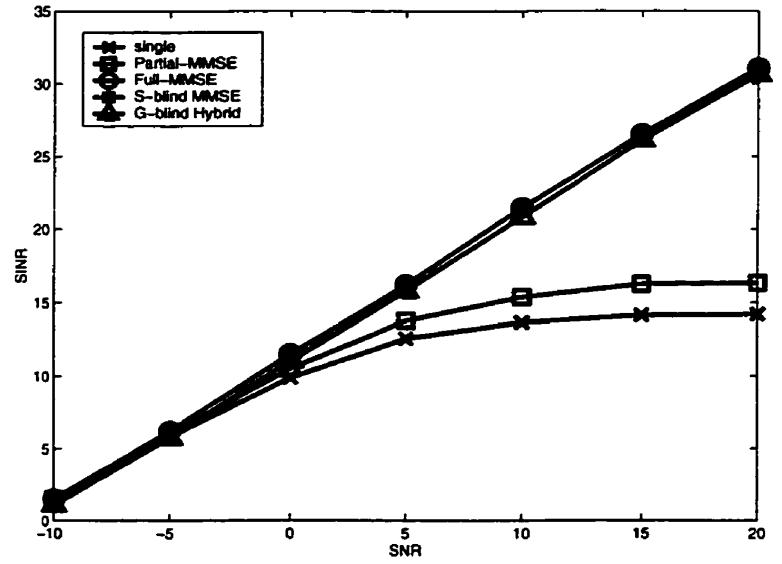

(b) Maximum SINR

Figure 3.3: Performance of the hybrid group-blind multiuser detector compared to conventional multiuser detectors (Asynchronous system, N=31, 6 known users, 4 unknown users, SIR(intra-cell)=0dB, SIR(inter-cell)=3dB, 100 ensemble)

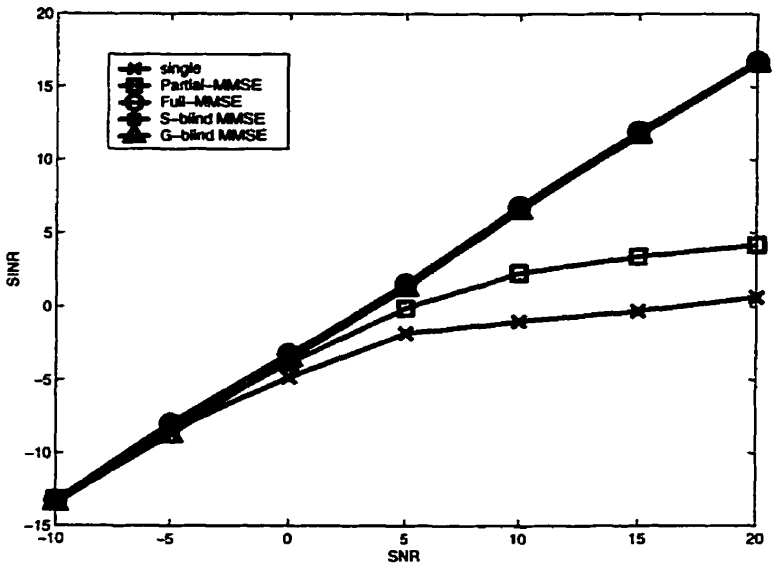

(a) Minimum SINR

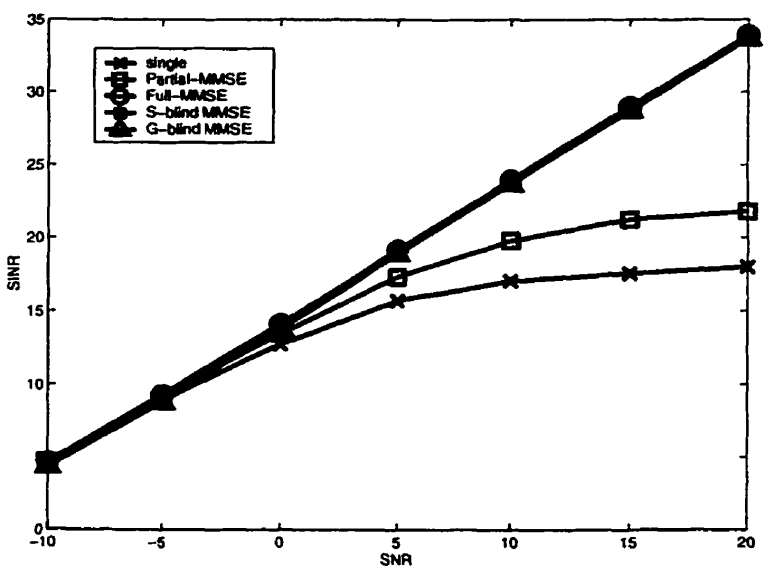

(b) Maximum SINR

Figure 3.4: Performance of the group-blind MMSE multiuser detector compared to conventional multiuser detectors (Asynchronous system, N=31, 6 known users, 4 unknown users, SIR(intra-cell)=0dB, SIR(inter-cell)=3dB, 100 ensemble)

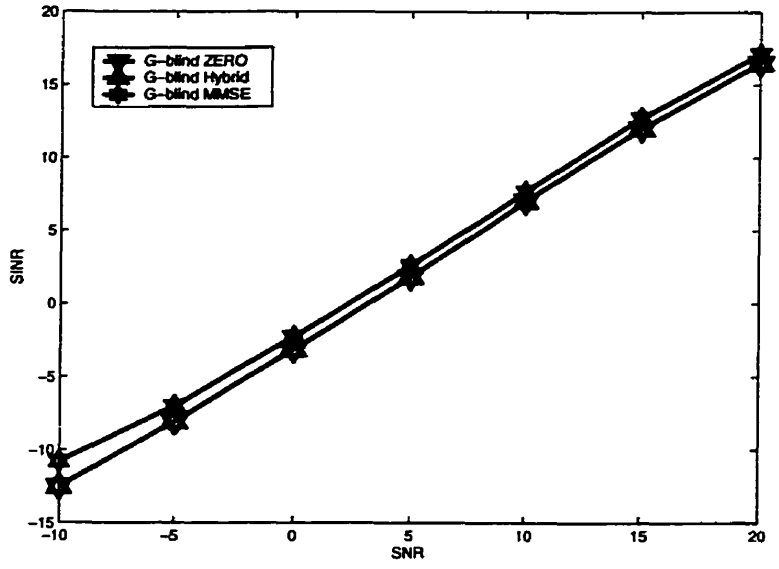

(a) Minimum SINR

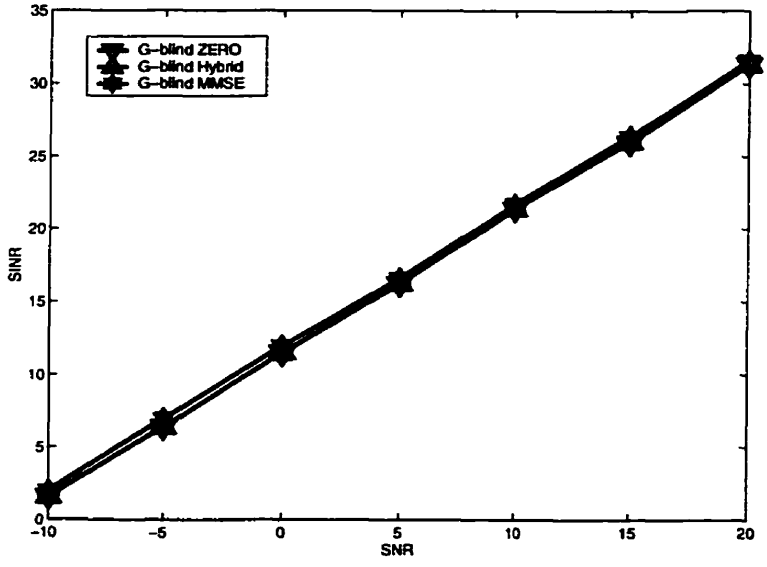

(b) Maximum SINR

Figure 3.5: Performance comparison of group-blind multiuser detectors (Asynchronous system, N=31, 6 known users, 4 unknown users, SIR(intra-cell)=0dB, SIR(inter-cell)=3dB, 100 ensemble)

Chapter 4

Estimated Detectors

4.1 Estimation of the Correlation Matrix

So far, we have assumed that the correlation matrix $\mathbf{R}$ of the received signal is known:

$$\mathbf{R} = E\left[\mathbf{r}\mathbf{r}^H\right] \tag{4.1}$$

However, in real systems, the correlation matrix of the received signal should be estimated. One way to estimate the correlation matrix is using a time average. The estimated correlation matrix of the received signal can be obtained by

$$\hat{\mathbf{R}}[n] = \frac{1}{n}\sum_{i=1}^{n}\mathbf{r}[i]\mathbf{r}[i]^H \tag{4.2}$$

The estimated correlation matrix can be decomposed to the eigen components:

$$\begin{aligned}\hat{\mathbf{R}}[n] &= \left[\hat{\mathbf{U}}_s[n]\hat{\mathbf{U}}_n[n]\right]\begin{bmatrix}\hat{\Lambda}_s[n] & \mathbf{0}\\ \mathbf{0} & \hat{\sigma}^2\mathbf{I}\end{bmatrix}\begin{bmatrix}\hat{\mathbf{U}}_s^H[n]\\ \hat{\mathbf{U}}_n^H[n]\end{bmatrix}\\ &= \hat{\mathbf{U}}_s[n]\hat{\Lambda}_s[n]\hat{\mathbf{U}}_s^H[n] + \hat{\sigma}^2\hat{\mathbf{U}}_n[n]\hat{\mathbf{U}}_n^H[n]. \qquad (4.3)\end{aligned}$$

For form I group-blind multiuser detectors, the orthogonally projected and estimated correlation matrix can be decomposed as

$$\begin{aligned}\bar{\mathbf{P}}^{\perp}\hat{\mathbf{R}}[n]\bar{\mathbf{P}}^{\perp} &= \left[\hat{\tilde{\mathbf{U}}}_s[n]\hat{\tilde{\mathbf{U}}}_n[n]\hat{\tilde{\mathbf{U}}}_o[n]\right]\begin{bmatrix}\hat{\tilde{\Lambda}}_s[n] & \mathbf{0} & \mathbf{0}\\ \mathbf{0} & \hat{\sigma}^2\mathbf{I} & \mathbf{0}\\ \mathbf{0} & \mathbf{0} & \mathbf{0}\end{bmatrix}\begin{bmatrix}\hat{\tilde{\mathbf{U}}}_s^H[n]\\ \hat{\tilde{\mathbf{U}}}_n^H[n]\\ \hat{\tilde{\mathbf{U}}}_o^H[n]\end{bmatrix}\\ &= \hat{\tilde{\mathbf{U}}}_s[n]\hat{\tilde{\Lambda}}_s[n]\hat{\tilde{\mathbf{U}}}_s^H[n] + \sigma^2\hat{\tilde{\mathbf{U}}}_n[n]\hat{\tilde{\mathbf{U}}}_n^H[n]. \qquad (4.4)\end{aligned}$$

For the group-blind MMSE multiuser detector, QR factorization of the matrix $\left(\bar{\mathbf{P}}^{\perp}\hat{\mathbf{U}}_s[n]\right)$ can factorized as

$$\bar{\mathbf{P}}^{\perp}\hat{\mathbf{U}}_s[n] = \begin{bmatrix}\hat{\mathbf{Q}}_s[n] & \hat{\mathbf{Q}}_o[n]\end{bmatrix}\begin{bmatrix}\hat{\mathbf{R}}_s[n] & \hat{\mathbf{R}}_o[n]\\ \mathbf{0} & \mathbf{0}\end{bmatrix}\hat{\Pi}[n], \qquad (4.5)$$

Figure 4.1 shows the structure of the estimated group-blind multiuser detectors. From the received signal, the correlation matrix is estimated. And by using SVD or subspace tracking, the eigen component of the correlation matrix

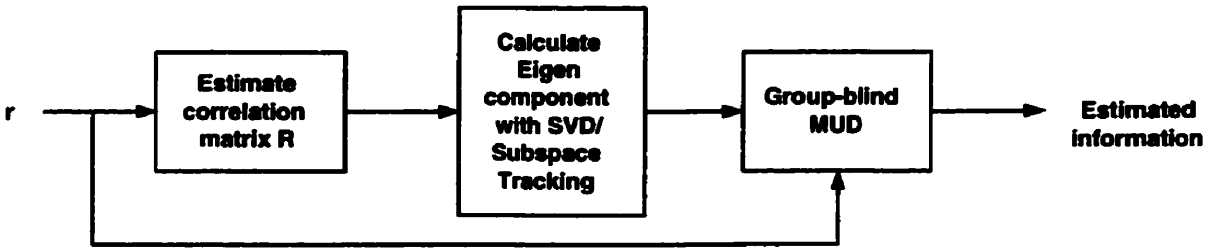

Figure 4.1: Estimated group-blind multiuser detector

is found. With the eigen component and the received signal, we can estimate the information data.

4.2 Synchronous Estimated Detectors

The estimated multiuser detectors for the synchronous system are listed as follows:

- **Blind Linear MMSE detector: Direct method**

$$\hat{\bar{b}}_k[n] = \mathbf{sgn}\left(\bar{\mathbf{s}}_k^T \hat{\mathbf{R}}^{-1}[n]\mathbf{r}[n]\right) \tag{4.6}$$

- **Blind MMSE detector: subspace method**

$$\hat{\bar{b}}_k[n] = \mathbf{sgn}\left(\bar{\mathbf{s}}_k^T \hat{\mathbf{U}}_s[n]\hat{\Lambda}_s^{-1}[n]\hat{\mathbf{U}}_s^T[n]\mathbf{r}[n]\right) \tag{4.7}$$

- **Blind Linear Zero-forcing detector: Subspace method**

$$\hat{\bar{b}}_k[n] = \mathbf{sgn}\left(\bar{\mathbf{s}}_k^T \hat{\mathbf{U}}_s[n](\hat{\Lambda}_s[n] - \hat{\sigma}^2\mathbf{I})^{-1}\hat{\mathbf{U}}_s^T[n]\mathbf{r}[n]\right) \tag{4.8}$$

- **Group-blind Linear Zero-forcing Detector: Form I**

$$\begin{aligned}\hat{\bar{b}}_k[n] &= \mathbf{sgn}\left(\mathbf{1}_k^T(\bar{\mathbf{S}}^T\bar{\mathbf{S}})^{-1}\bar{\mathbf{S}}^T\right. \\ &\times \left.[\mathbf{I} - \hat{\mathbf{R}}[n]\hat{\bar{\mathbf{U}}}_s[n](\hat{\bar{\Lambda}}_s[n] - \hat{\sigma}^2\mathbf{I})^{-1}\hat{\bar{\mathbf{U}}}_s^T[n]]\mathbf{r}[n]\right)\end{aligned} \tag{4.9}$$

- **Group-blind Linear Zero-forcing Detector: Form II**

$$\begin{aligned}\hat{\bar{b}}_k[n] &= \mathbf{sgn}\left(\mathbf{1}_k^T\left[\bar{\mathbf{S}}^T\hat{\mathbf{U}}_s\left(\hat{\Lambda}_s - \hat{\sigma}^2\mathbf{I}\right)^{-1}\right.\right. \\ &\times \left.\left.\hat{\mathbf{U}}_s^T[n]\bar{\mathbf{S}}\right]^{-1}\bar{\mathbf{S}}^T\hat{\mathbf{U}}_s[n]\left(\hat{\Lambda}_s[n] - \hat{\sigma}^2\mathbf{I}\right)^{-1}\hat{\mathbf{U}}_s^T[n]\mathbf{r}[n]\right)\end{aligned} \tag{4.10}$$

- **Group-blind Linear Hybrid Detector: Form I**

$$\begin{aligned}\hat{\bar{b}}_k[n] &= \mathbf{sgn}\left(\mathbf{1}_k^T(\bar{\mathbf{S}}^T\bar{\mathbf{S}})^{-1}\bar{\mathbf{S}}^T\right. \\ &\times \left.(\mathbf{I} - \hat{\mathbf{R}}[n]\hat{\bar{\mathbf{U}}}_s[n]\hat{\bar{\Lambda}}_s^{-1}[n]\hat{\bar{\mathbf{U}}}_s^T[n])\mathbf{r}[n]\right)\end{aligned} \tag{4.11}$$

- **Group-blind Linear Hybrid Detector: Form II**

$$\begin{aligned}\hat{\tilde{b}}_k[n] &= \mathbf{sgn}\left(\mathbf{1}_k^T\left[\bar{\mathbf{S}}^T\hat{\mathbf{U}}_s[n]\hat{\Lambda}_s^{-1}[n]\hat{\mathbf{U}}_s^T[n]\bar{\mathbf{S}}\right]^{-1}\right. \\ &\times \left.\bar{\mathbf{S}}^T\hat{\mathbf{U}}_s[n]\hat{\Lambda}_s^{-1}[n]\hat{\mathbf{U}}_s^T[n]\mathbf{r}[n]\right) \qquad (4.12)\end{aligned}$$

- **Group-blind Linear MMSE Detector: Form I**

$$\begin{aligned}\hat{\tilde{b}}_k[n] &= \mathbf{sgn}\left(\mathbf{1}_k^T\left(\bar{\mathbf{S}}^T\bar{\mathbf{S}}+\hat{\sigma}^2\mathbf{I}\right)^{-1}\bar{\mathbf{S}}^T\right. \\ &\times \left.\left(\mathbf{I}-\hat{\mathbf{R}}[n]\hat{\tilde{\mathbf{U}}}_s[n]\hat{\tilde{\Lambda}}_s^{-1}[n]\hat{\tilde{\mathbf{U}}}_s^T[n]\right)\mathbf{r}[n]\right) \qquad (4.13)\end{aligned}$$

- **Group-blind Linear MMSE Detector: Form II**

$$\begin{aligned}\hat{\tilde{b}}_k[n] &= \mathbf{sgn}\left(\mathbf{1}_k^T\left(\bar{\mathbf{S}}^T\bar{\mathbf{S}}+\hat{\sigma}^2\mathbf{I}\right)^{-1}\bar{\mathbf{S}}^T\left[\mathbf{I}-\left(\hat{\mathbf{Q}}_s[n]\hat{\mathbf{R}}_s^{-T}[n]\right)\left(\hat{\Pi}[n]\hat{\Lambda}_s[n]\hat{\Pi}^T[n]\right)^{-1}\right.\right. \\ &\times \left.\left.\left(\hat{\mathbf{Q}}_s[n]\hat{\mathbf{R}}_s^{-T}[n]\right)^T\hat{\mathbf{R}}[n]\right]\mathbf{r}[n]\right) \qquad (4.14)\end{aligned}$$

4.3 Asynchronous Estimated Detectors

The estimated multiuser detectors for the asynchronous system are as follows.

- **Blind Linear MMSE detector: Direct method**

$$\hat{\tilde{b}}_k[n] = \mathbf{sgn}\left(\bar{\mathbf{h}}_k^H\hat{\mathbf{R}}^{-1}[n]\mathbf{r}[n]\right) \qquad (4.15)$$

- **Blind MMSE detector: subspace method**

$$\hat{\bar{b}}_k[n] = \mathbf{sgn}\left(\bar{\mathbf{h}}_k^H \hat{\mathbf{U}}_s[n] \hat{\Lambda}_s^{-1}[n] \hat{\mathbf{U}}_s^H[n] \mathbf{r}[n]\right) \tag{4.16}$$

- **Blind Linear Zero-forcing detector: Subspace method**

$$\hat{\bar{b}}_k[n] = \mathbf{sgn}\left(\bar{\mathbf{h}}_k^H \hat{\mathbf{U}}_s[n] (\hat{\Lambda}_s[n] - \hat{\sigma}^2 \mathbf{I})^{-1} \hat{\mathbf{U}}_s^H[n] \mathbf{r}[n]\right) \tag{4.17}$$

- **Group-blind Linear Zero-forcing Detector: Form I**

$$\begin{aligned} \hat{\bar{b}}_k[n] &= \mathbf{sgn}\left(\mathbf{1}_{\bar{K}\iota+k}^T (\bar{\mathbf{H}}^H \bar{\mathbf{H}})^{-1} \bar{\mathbf{H}}^H \right. \\ &\times \left. [\mathbf{I} - \hat{\mathbf{R}}[n] \hat{\bar{\mathbf{U}}}_s[n] (\hat{\bar{\Lambda}}_s[n] - \hat{\sigma}^2 \mathbf{I})^{-1} \hat{\bar{\mathbf{U}}}_s^H[n]] \mathbf{r}[n]\right) \end{aligned} \tag{4.18}$$

- **Group-blind Linear Zero-forcing Detector: Form II**

$$\begin{aligned} \hat{\bar{b}}_k[n] &= \mathbf{sgn}\left(\mathbf{1}_{\bar{K}\iota+k}^T \left[\bar{\mathbf{H}}^H \hat{\mathbf{U}}_s \left(\hat{\Lambda}_s - \hat{\sigma}^2 \mathbf{I}\right)^{-1} \hat{\mathbf{U}}_s^H[n] \bar{\mathbf{H}}\right]^{-1} \right. \\ &\times \left. \bar{\mathbf{H}}^H \hat{\mathbf{U}}_s[n] \left(\hat{\Lambda}_s[n] - \hat{\sigma}^2 \mathbf{I}\right)^{-1} \hat{\mathbf{U}}_s^H[n] \mathbf{r}[n]\right) \end{aligned} \tag{4.19}$$

- **Group-blind Linear Hybrid Detector: Form I**

$$\begin{aligned} \hat{\bar{b}}_k[n] &= \mathbf{sgn}\left(\mathbf{1}_{\bar{K}\iota+k}^T (\bar{\mathbf{H}}^H \bar{\mathbf{H}})^{-1} \bar{\mathbf{H}}^H \right. \\ &\times \left. (\mathbf{I} - \hat{\mathbf{R}}[n] \hat{\bar{\mathbf{U}}}_s[n] \hat{\bar{\Lambda}}_s^{-1}[n] \hat{\bar{\mathbf{U}}}_s^H[n]) \mathbf{r}[n]\right) \end{aligned} \tag{4.20}$$

- **Group-blind Linear Hybrid Detector: Form II**

$$\begin{aligned}\hat{\tilde{b}}_k[n] &= \mathbf{sgn}\left(\mathbf{1}_{K\iota+k}^T\left[\bar{\mathbf{H}}^H\hat{\mathbf{U}}_s[n]\hat{\Lambda}_s^{-1}[n]\hat{\mathbf{U}}_s^H[n]\bar{\mathbf{H}}\right]^{-1}\right. \\ &\times \left.\bar{\mathbf{H}}^H\hat{\mathbf{U}}_s[n]\hat{\Lambda}_s^{-1}[n]\hat{\mathbf{U}}_s^H[n]\mathbf{r}[n]\right) \qquad (4.21)\end{aligned}$$

- **Group-blind Linear MMSE Detector: Form I**

$$\begin{aligned}\hat{\tilde{b}}_k[n] &= \mathbf{sgn}\left(\mathbf{1}_{K\iota+k}^T\left(\bar{\mathbf{H}}^H\bar{\mathbf{H}}+\hat{\sigma}^2\mathbf{I}\right)^{-1}\bar{\mathbf{H}}^H\right. \\ &\times \left.\left(\mathbf{I}-\hat{\mathbf{R}}[n]\hat{\tilde{\mathbf{U}}}_s[n]\hat{\tilde{\Lambda}}_s^{-1}[n]\hat{\tilde{\mathbf{U}}}_s^H[n]\right)\mathbf{r}[n]\right) \qquad (4.22)\end{aligned}$$

- **Group-blind Linear MMSE Detector: Form II**

$$\begin{aligned}\hat{\tilde{b}}_k[n] &= \mathbf{sgn}\left(\mathbf{1}_{K\iota+k}^T\left(\bar{\mathbf{H}}^H\bar{\mathbf{H}}+\hat{\sigma}^2\mathbf{I}\right)^{-1}\bar{\mathbf{H}}^T\left[\mathbf{I}-\left(\hat{\mathbf{Q}}_s[n]\hat{\mathbf{R}}_s^{-T}[n]\right)\right.\right. \\ &\times \left.\left.\left(\hat{\Pi}[n]\hat{\Lambda}_s[n]\hat{\Pi}^T[n]\right)^{-1}\left(\hat{\mathbf{Q}}_s[n]\hat{\mathbf{R}}_s^{-T}[n]\right)^H\hat{\mathbf{R}}[n]\right]\mathbf{r}[n]\right) \qquad (4.23)\end{aligned}$$

4.4 Simulation Results

In this simulation, several multiuser detectors are compared with the conventional detector, the partial-MMSE detector, and the full MMSE detector. While the partial MMSE detector can reduce only intra-cell interference, the full MMSE detector can reduce both intra-cell interference and inter-cell interference with the assumption that all spreading codes of both known and unknown users are

known.

In Figure 4.2 and 4.4, the performance of the blind MMSE multiuser detectors were evaluated. For both synchronous systems and asynchronous systems, the blind MMSE multiuser detector using the subspace method outperforms the blind MMSE multiuser detector using the direct method because it gains high resolution from the subspace decomposition. After some symbols, the SINR of the blind MMSE detector using the subspace method crosses over the partial MMSE detector and converges to the full MMSE detector. In the case of random code, it crosses over the partial MMSE detector and the conventional detector faster than in the case of gold code because the partial MMSE detector and the conventional detector have worse performance in the case of random code.

Figure 4.3 and 4.5 show performances of group-blind multiuser detectors. In most cases, the group-blind multiuser detectors outperform the blind MMSE detector using the subspace method.

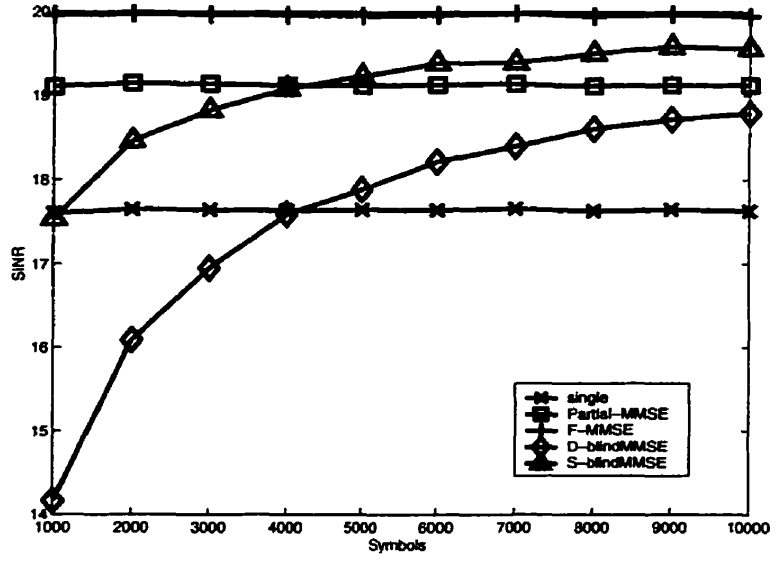

(a) gold code

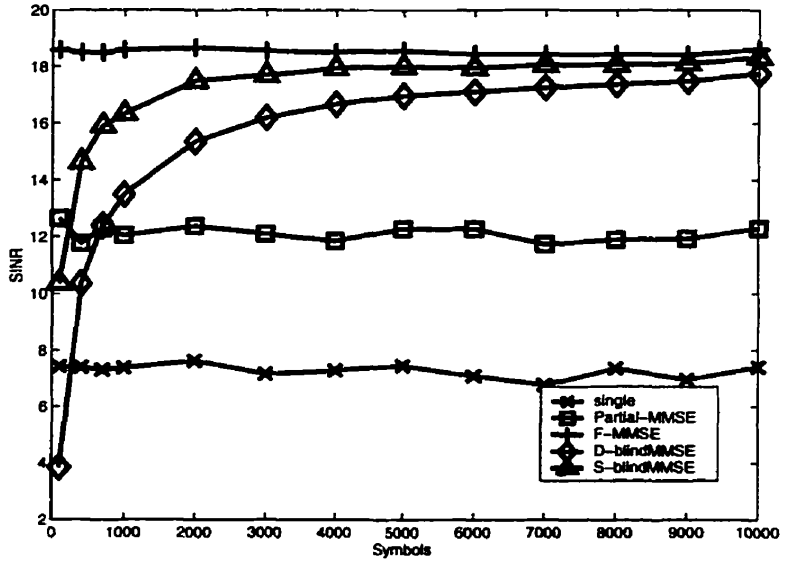

(b) random code

Figure 4.2: Estimated blind MMSE multiuser detectors in synchronous DS-CDMA systems (N=31, 6 known users, 4 unknown users, SIR=3dB, SNR=20dB)

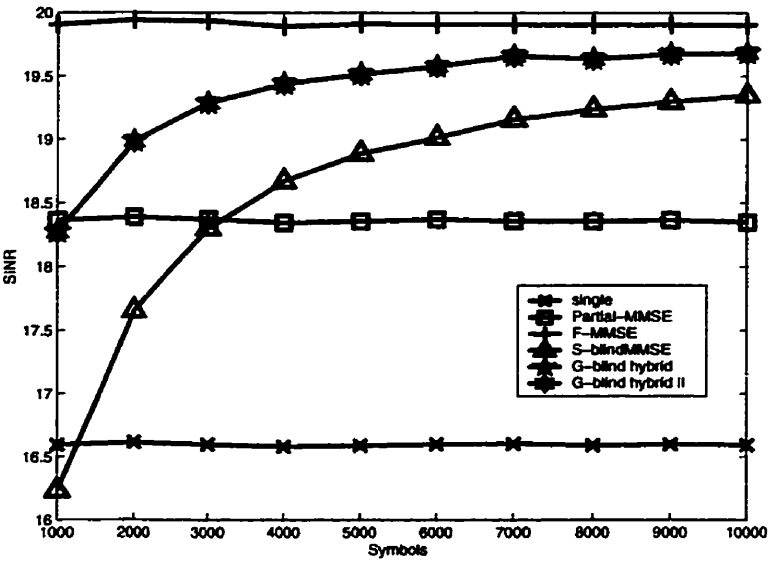

(a) gold code

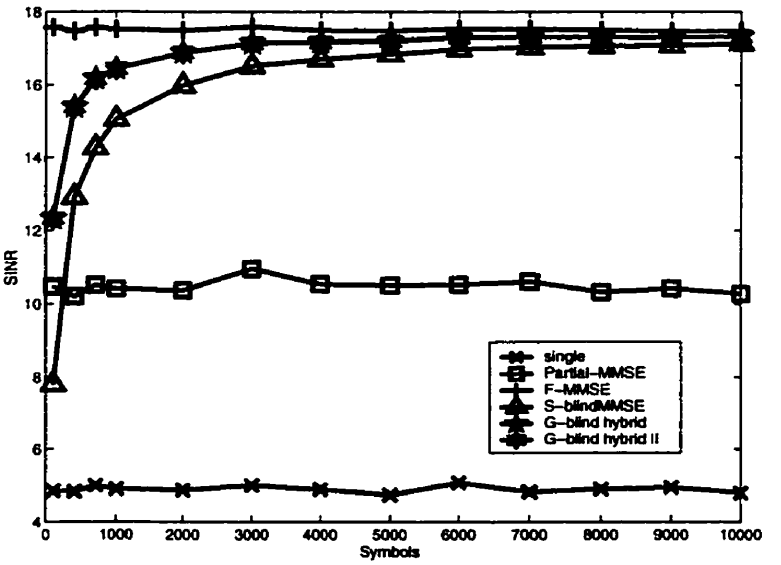

(b) random code

Figure 4.3: Estimated hybrid group-blind multiuser detectors in synchronous DS-CDMA systems (N=31, 6 known users, 4 unknown users, SIR=3dB, SNR=20dB)

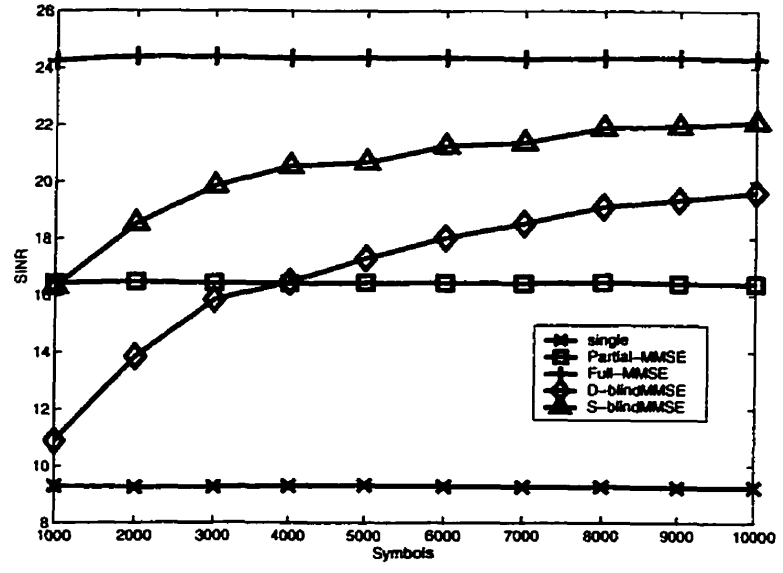

(a) gold code

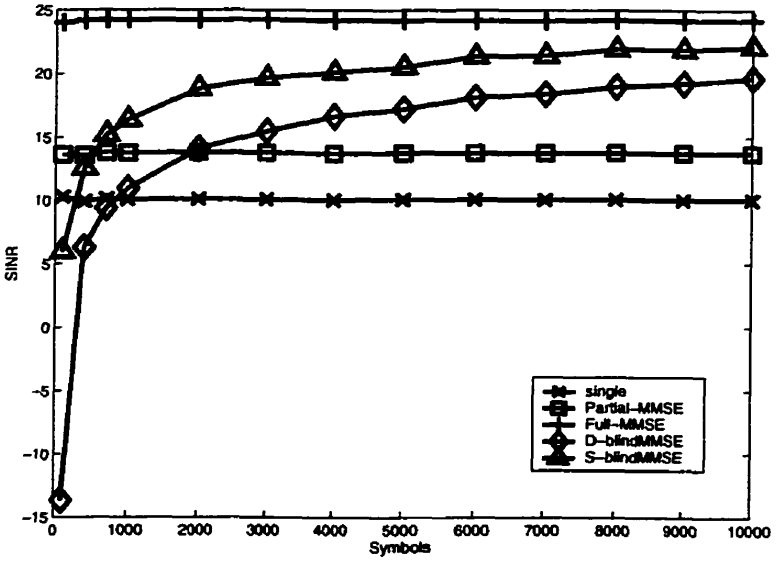

(b) random code

Figure 4.4: Estimated blind MMSE multiuser detectors in asynchronous DS-CDMA systems (N=31, 6 known users, 4 unknown users, SIR=3dB, SNR=20dB)

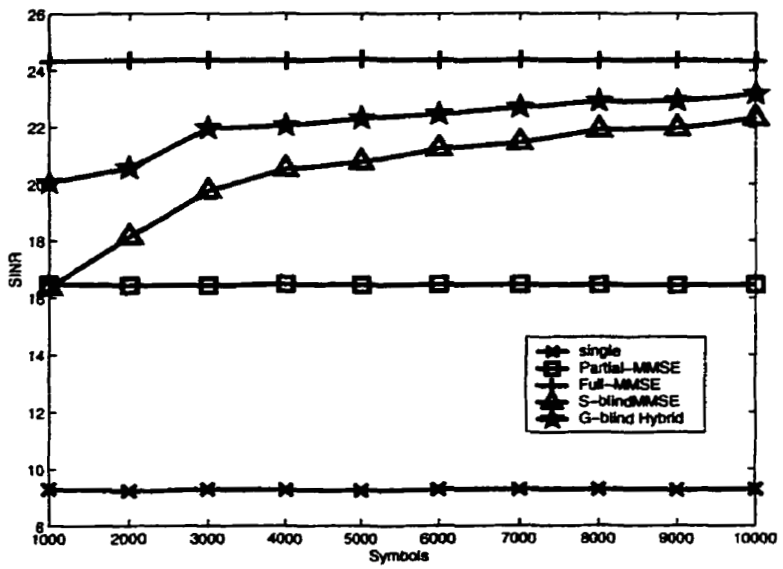

(a) gold code

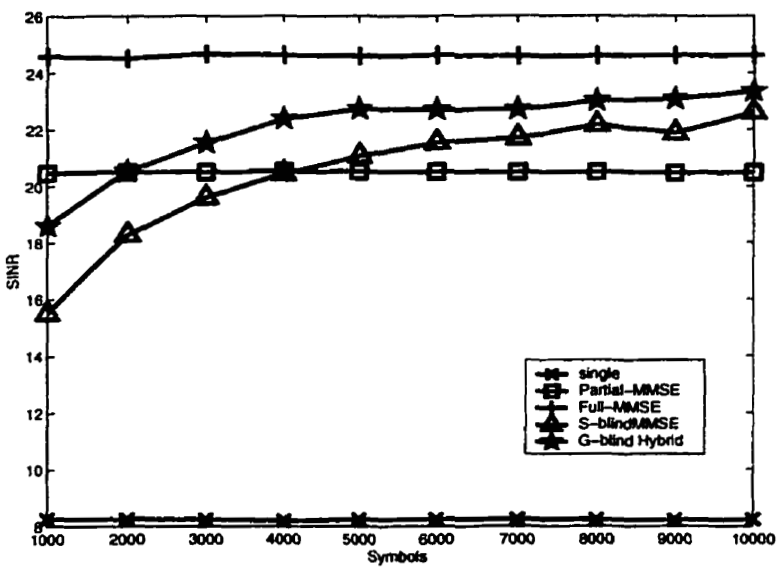

(b) random code

Figure 4.5: Estimated hybrid group-blind multiuser detectors in asynchronous DS-CDMA systems (N=31, 6 known users, 4 unknown users, SIR=3dB, SNR=20dB)

4.5 Blind Channel Estimation

In this section, we will discuss the estimation problem of the channel of a desired user in asynchronous DS-CDMA systems. The channel of a desired user can be estimated blindly with the knowledge of its own spreading code and the received signal. The performance of the blind multiuser detector and the group-blind multiuser detector will be evaluated by a simulation. To solve this problem, we introduce the discrete time channel model in 4.5.1.

4.5.1 Discrete-time Channel Model

From (3.5) and (3.9) , the n-th composite channel response during j-th symbol is given by

$$h_k[j,n] \triangleq h_k(jT+n\Delta) = \sum_{l=0}^{N-1} c_k[l]\bar{g}_k(jT+n\Delta-lT_c), \tag{4.24}$$

where $j = 0,\cdots,\iota_k;\ n = 0,\cdots,P-1$. Decimation of $h_k[j,n]$ into p sub-sequences is written as

$$\begin{aligned} & h_{k,q}[j,i] \triangleq h_k[j,q+pi] = h_k(jT+(q+pi)\Delta) \\ = & \sum_{l=0}^{N-1} c_k[l]\bar{g}_k(jT+(q+pi)\Delta-lT_c) \end{aligned} \tag{4.25}$$

From the fact that $T = NT_c$ and $T_c = p\Delta$, $h_{k,q}[j,i]$ can be given by

$$\begin{aligned} h_{k,q}[j,i] &\triangleq \sum_{l=0}^{N-1} c_k[l] \underbrace{\bar{g}_k(q\Delta + (jN+i-l)p\Delta)}_{\bar{g}_k[(jN+i-l)p+q] \triangleq \bar{g}_{k,q}(jN+i-l)} \\ &= \sum_{l=0}^{N-1} c_k[l]\bar{g}_{k,q}(jN+i-l), \qquad (4.26) \\ & \quad j = 0, \cdots, \iota_k; i = 0, \cdots, N-1; q = 0, \cdots, p-1. \end{aligned}$$

From the composite channel response $\bar{g}_k(t)$ given in (3.6), The sequence $\bar{g}_k[i]$ is obtained by sampling at rate $\frac{1}{\Delta} = \frac{p}{T_c}$:

$$\bar{g}_k[i] \triangleq \bar{g}_k(i\Delta) = A_k \sum_{l=1}^{L} \alpha_{kl}\psi(i\Delta - d_k - \tau_{kl}), \quad i = 0, \cdots, p\mu_k - 1. \quad (4.27)$$

The length $(p\mu_k)$ of the sequence $\{\bar{g}_k[i]\}$ is determined by the length of support of $\bar{g}_k(t)$. Since $\bar{g}_k(t)$ is non-zero only on the interval $[d_k + \tau_{k1}, d_k + \tau_{kL} + T_c]$, we have

$$\mu_k = \left\lceil \frac{d_k + \tau_{kL} + T_c}{p\Delta} \right\rceil = \left\lceil \frac{d_k + \tau_{kL} + T_c}{T} \cdot \frac{T}{T_c} \right\rceil \leq \iota_k N. \qquad (4.28)$$

The sequences $\bar{g}_{k,q}[i]$ in (4.27) are obtained by down-sampling the sequence $\{\bar{g}_k[i]\}$ by a factor of p, i.e., $\bar{g}_{k,q}[i] = \bar{g}_k[ip+q]$, $i = 0, \cdots, \mu_k - 1$; $q = 0, \cdots, p-1$.

From (4.27), $h_{k,q}$ can be expressed as the convolution of c_k and $\bar{g}_{k,q}$:

$$\begin{aligned} & \{h_{k,q}[0,0], \cdots, h_{k,q}[0,N-1], \cdots\cdots, h_{k,q}[\iota_k,0], \cdots, h_{k,q}[\iota_k,N-1]\} \\ = \; & \{c_k[0], \cdots, c_k[N-1]\} \star \{\bar{g}_{k,q}[0], \cdots, \bar{g}_{k,q}[\mu_k-1]\}. \end{aligned} \tag{4.29}$$

Denote

$$\underbrace{\mathbf{h}_{k,q}}_{(\iota_k+1)N\times 1} \triangleq \begin{bmatrix} h_{k,q}[0,0] \\ \vdots \\ h_{k,q}[0,N-1] \\ \vdots \\ h_{k,q}[\iota_k,0] \\ \vdots \\ h_{k,q}[\iota_k,N-1] \end{bmatrix}, \underbrace{\bar{\mathbf{g}}_{k,q}}_{\mu_k\times 1} \triangleq \begin{bmatrix} \bar{g}_{k,q}[0] \\ \vdots \\ \bar{g}_{k,q}[\mu_k-1] \end{bmatrix},$$

$$\underbrace{\mathbf{C}_k}_{(\iota_k+1)N\times\mu_k} \triangleq \begin{bmatrix} c_k[0] & & \\ c_k[1] & \ddots & \\ \vdots & \ddots & c_k[0] \\ \vdots & & c_k[1] \\ c_k[N-1] & & \vdots \\ & \ddots & \vdots \\ & & c_k[N-1] \end{bmatrix}.$$

Then (4.29) can be written in matrix form as

$$\mathbf{h}_{k,q} = \mathbf{C}_k\, \bar{\mathbf{g}}_{k,q}. \tag{4.30}$$

Finally, denote

$$\begin{aligned}
\underbrace{\mathbf{h}_k}_{(\iota_k+1)P\times 1} &\triangleq [h_k[0,0] \cdots h_k[0,P-1] \cdots h_k[\iota_k,0] \cdots h_k[\iota_k,P-1]]^T, \\
\underbrace{\bar{\mathbf{g}}_k}_{p\mu_k\times 1} &\triangleq [\bar{g}_k[0] \cdots \bar{g}_k[p\mu_k-1]]^T.
\end{aligned}$$

Then, the composite channel matrix can be written as

$$\mathbf{h}_k = \widetilde{\mathbf{C}}_k \bar{\mathbf{g}}_k, \tag{4.31}$$

where $\widetilde{\mathbf{C}}_k$ is an $(\iota_k+1)P \times p\mu_k$ matrix formed from the spreading code of k-th user. For instance, when the over-sampling factor $p=2$, we have

$$\underbrace{\widetilde{\mathbf{C}}_k}_{2(\iota_k+1)N\times 2\mu_k} = \begin{bmatrix}
c_k[0] & & & & & \\
0 & c_k[0] & & & & \\
c_k[1] & 0 & c_k[0] & & & \\
0 & c_k[1] & 0 & c_k[0] & & \\
\vdots & \ddots & \ddots & \ddots & \ddots & \\
\vdots & & \ddots & \ddots & \ddots & c_k[0] \\
c_k[N-1] & & & 0 & c_k[1] & 0 \\
 & c_k[N-1] & & & 0 & c_k[1] \\
 & & \ddots & & & 0 \\
 & & & \ddots & & \vdots \\
 & & & & \ddots & \vdots \\
 & & & & & c_k[N-1]
\end{bmatrix}.$$

For other values of p, the matrix $\widetilde{\mathbf{C}}_k$ is similarly constructed. Suppose that the

user k is the user of interest and his spreading sequence $\{c_k[0], \cdots, c_k[N-1]\}$ is known to the receiver (and therefore $\tilde{\mathbf{C}}_k$ is known). We next consider the problem of estimating the channel vector $\bar{\mathbf{g}}_k$ in (4.31) based on the received signal $\mathbf{r}[i]$ in (3.12).

4.5.2 Blind Channel Estimation in White Noise

The correlation matrix of the received signal $\mathbf{r}[t]$ can be written as

$$\begin{aligned} \mathbf{R} &= E\left\{\mathbf{r}[t]\mathbf{r}[t]^H\right\} = \mathbf{H}\mathbf{H}^H + \sigma^2\mathbf{I}_{Pm} \\ &= \mathbf{U}_s\Lambda_s\mathbf{U}_s^H + \sigma^2\mathbf{U}_n\mathbf{U}_n^H, \end{aligned} \tag{4.32}$$

where $\mathbf{U}_s$ is the signal subspace orthonormal eigenvectors, $\mathbf{U}_n$ is the noise subspace orthonormal eigenvectors, and Λ_s is the signal subspace diagonal eigenvalue matrix. From this the channel response $\mathbf{g}_k$ can be estimated from the orthogonality relationship [20]:

$$\mathbf{U}_n^H\mathbf{h}_k = \mathbf{U}_n^H\mathbf{C}_k\mathbf{g}_k = \mathbf{0}, \tag{4.33}$$

since $\mathbf{U}_n$ is orthogonal to the column space of $\mathbf{H}$, and $\mathbf{h}_k$ is in the column space of $\mathbf{H}$. Thus an estimation of the channel response $\mathbf{g}_k$ can be obtained by computing the minimum eigenvector of the matrix $\left(\mathbf{C}_k^T\mathbf{U}_n^H\mathbf{U}_n\mathbf{C}_k\right)$. We are here using Kalman tracking [28] for the channel estimation. Kalman tracking has

$\mathcal{O}(N \times \mu_k)$ complexity where μ_k is the length of the impulse response $\mathbf{g}_k$.

The estimation of the signal subspace $\mathbf{U}_s$ will be outlined below. The projected received signal $\mathbf{z}(i)$ onto the noise subspace is obtained from

$$\mathbf{z}(i) = \mathbf{U}_n\mathbf{U}_n^H\mathbf{r}(i) = \mathbf{r}(i) - \mathbf{U}_s\mathbf{U}_s^H\mathbf{r}(i) \tag{4.34}$$

from the fact that $\mathbf{U}_n\mathbf{U}_n^H = \mathbf{I} - \mathbf{U}_s\mathbf{U}_s^H$. Using (4.33), we have

$$\mathbf{g}_k^H\mathbf{C}_k^H\mathbf{z}(i) = \mathbf{0}. \tag{4.35}$$

We consider the following constrained adaptive filtering technique to estimate the channel state:

$$\begin{aligned} &\min_{\mathbf{g}_k} E\{|\mathbf{g}_k^H\mathbf{C}_k^H\mathbf{z}(i)|^2\} \\ &\textit{subject to } ||\mathbf{g}_k|| = 1. \end{aligned} \tag{4.36}$$

Among a number of algorithms that can be employed to solve the above constrained optimization problem. Here we use the following Kalman-type of algorithm[28] for channel estimation.

$$
\begin{aligned}
\mathbf{x}(i) &= \mathbf{C}_k^H \mathbf{z}(i) \\
\mathbf{p}(i) &= \mathbf{K}(i-1)\mathbf{x}(i) \\
\mathbf{q}(i) &= \mathbf{p}(i)/[\mathbf{x}^H(i)\mathbf{p}(i)] \\
\mathbf{K}(i) &= \mathbf{K}(i-1) - \mathbf{q}(i)\mathbf{p}^H(i) \\
\mathbf{g}_k(i) &= \mathbf{g}_k(i-1) - \mathbf{q}(i)\mathbf{x}^H(i)\mathbf{g}_k(i-1) \\
\mathbf{g}_k(i) &= \mathbf{g}_k(i)/||\mathbf{g}_k(i)||,
\end{aligned}
\tag{4.37}
$$

with the initial condition $\mathbf{K}(0) = \mathbf{I}$. Once an estimate of the channel state $\mathbf{g}_k$ is obtained, the composite signature waveform of the desired user is given by $\mathbf{h}_k = \mathbf{C}_k\mathbf{g}_k$.

4.6 Subspace Tracking

Due to change of multipath and moving mobile stations, the channel for a user is non-stationary in a real communications environment. SVD or EVD is need for the high resolution of estimation. However, the calculation complexity of SVD or EVD is very high ($\mathcal{O}(N^3)$, where N is the dimension of the correlation matrix of the received signal). Therefore, in a real-time implementation of the group-blind multiuser detector, a reduced complexity updating algorithm for finding the eigenvalues and eigenvectors is needed. There exist many subspace tracking algorithms in the literature with various complexities, i. e., $\mathcal{O}(NK)$, $\mathcal{O}(NK^2)$, $\mathcal{O}(N^2K)$, or $\mathcal{O}(N^2)$. A survey of subspace tracking algorithms can be founded in [29]. in the next two sections, we will briefly introduce two subspace tracking

algorithms which are well suited for the group-blind multiuser detectors.

4.6.1 FASIR Algorithm

FASIR stands for FAst Subspace Iteration with Ritz acceleration which has $\mathcal{O}(NK^2)$ complexity where N is the processing gain and K is the number of *known* users. Consider the class of matrices of rank K:

$$\hat{\mathbf{R}}^s(t) = \mathbf{U}_s(t)\Sigma_s(t)^2\mathbf{U}_s(t)^H \tag{4.38}$$

where $\mathbf{U}_s(t)$ is an N by K matrix with orthonormal columns and $\Sigma_s(t)$ is diagonal real. If $\mathbf{R}(t)$ is replaced by its low-rank approximation, then we have

$$\mathbf{R}(t)\mathbf{U}_s(t-1) \approx \hat{\mathbf{R}}^s(t)\mathbf{U}_s(t-1) = \mathbf{U}_s(t)\Sigma_s(t)^2. \tag{4.39}$$

$\mathbf{R}(t) \approx \hat{\mathbf{R}}^s(t)$ is "the FASIR approximation." This shows why the approximations of FASIR and $\mathbf{R}(t-1)\mathbf{U}_s(t-1) \approx \mathbf{U}_s(t-1)\Lambda_s(t-1)$ are equivalent if attention is restricted to the subspace iteration. A simple algorithm [29] can be

given by

$$\begin{aligned}
&\mathbf{U}_s(0) \text{ arbitrary } m \times K\,;\ \mathbf{U}_s(0)^H\mathbf{U}_s(0) = \mathbf{I};\\
&\Sigma(0) = \mathbf{I},\ \text{the identity matrix}\\
&\text{For } t = 0, 1, 2, \cdots\\
&\mathbf{W} = [\beta\mathbf{U}_s(t-1)\Sigma_s(t-1),\ \mathbf{r}(t)];\\
&\text{Compute the } N \times K \text{ and } K \times K\ matrix\mathbf{U}_s(t),\ \Sigma_s(t),\\
&\text{In the SVD } \mathbf{U}_s(t)\Sigma_s(t)\mathbf{Y}^H = \mathbf{W}\\
&\text{goto } t = t + 1,
\end{aligned} \tag{4.40}$$

where $\beta = 0.99$. The FASIR algorithm should satisfy following conditions:

- Compute only a restricted subset of K eigenpairs, in order to decrease the complexity.
- Use the estimate of the previous time step $(t-1)$ as initial guess at step t.
- If possible, compute the K left singular pairs of a matrix $\mathbf{D}$ instead, such that $\mathbf{DD^H} = \mathbf{R}$, in order to reduce rounding errors.

4.6.2 Noise Average Cross-terms Singular Value Decomposition (NA-CSVD)

Although the PASTd (Projection Approximation Subspace Tracking with deflation technique) algorithm [32] has a $\mathcal{O}(NK)$ complexity, the deflation technique causes stronger loss of orthonormality between eigen vectors and a slightly increased computational complexity if $N >> K$. On the other hand, the NA-CSVD algorithm has the advantage of maintaining the orthonormality of eigen vectors and the descending order of eigen values by careful choice of the type of Givens rotation. In addition, it has a $\mathcal{O}(NK)$ complexity. This led us to choose the NA-CSVD algorithm. The NA-CSVD algorithm can be described as follows [31].

Initialization

Initialize with$\mathbf{U}_S = \mathbf{U}_{N\times K}$, $\tilde{\Sigma} = \Sigma_{K+1\times K+1}$

For $n = 1, \ldots, \infty$

$\mathbf{x}_S = \mathbf{U}_S^H \mathbf{x}$

$\mathbf{z} = \mathbf{x} - \mathbf{U}_S \mathbf{x}_S$

$\mathbf{v}_N = \mathbf{z}/||\mathbf{z}||$ (4.41)

QR step

$\mathbf{y}^H \leftarrow [\mathbf{x}_S^H, \ ||\mathbf{z}||] \quad \tilde{\Sigma} \leftarrow \sqrt{\lambda}\tilde{\Sigma}$

for $i = 1 : d+1$

compute the angle ϕ_i to zero $\mathbf{y}(i)$ as in

$$\left[G_{\phi_i}^{1|2}\right]^H \begin{bmatrix} \sigma_{ii} \\ \mathbf{y}(i) \end{bmatrix} = \begin{bmatrix} \sigma'_{ii} \\ 0 \end{bmatrix}$$

$$\begin{bmatrix} \tilde{\Sigma} \\ \mathbf{y}^H \end{bmatrix} = \left[G_{\phi_i}^{i|K+2}\right]^H \begin{bmatrix} \tilde{\Sigma} \\ \mathbf{y}^H \end{bmatrix}$$

end

(4.42)

Refinement step

for $l = K$ downto 1

Choose the type of rotation

$$\tilde{\Sigma} \leftarrow \left[G_{\phi_l}^{l|K+1}\right]^T \tilde{\Sigma} \left[G_{\theta_l}^{l|K+1}\right]$$

$$\left[\mathbf{U}_S \quad \mathbf{v}_N\right] \leftarrow \left[\mathbf{U}_S \quad \mathbf{v}_N\right] \left[G_{\theta_l}^{l|K+1}\right]$$

end

End

(4.43)

For the hybrid group-blind multiuser detectors, (4.11) and (4.20), the input to the NA-CSVD algorithm is the projection of the received signal onto the

subspace orthogonal to subspace spanned by known users:

$$\mathbf{x}_n = \mathbf{P}^{\perp}\mathbf{r}_n. \tag{4.44}$$

In the hybrid group-blind multiuser detectors, (4.11) and (4.20), the matrix $\mathbf{U}_s(n)$ is the direct output of $\mathbf{U}(n)$ of the NA-CSVD algorithm, while $\Lambda_s(n) = \Sigma(n)^2$.

In the NA-CSVD algorithm, we assume that the number of users, i.e., the dimension of the signal subspace, is fixed and known. However, in real CDMA systems, it is possible for some users to appear and disappear. Therefore, another algorithm to find the number of users is needed. Rank estimation of the signal subspace with the NA-CSVD algorithm was developed by P. A. Pango [30] and the hybrid group-blind detector using NA-CSVD with the rank estimation could be further studied.

4.7 Simulation Results for Synchronous DS-CDMA systems

We consider CDMA systems with a variable number of both known and unknown users to compare the performance between them. The users are assigned purely random codes of length $N = 31$.

An ensemble of 50 different random code assignments for each user is gener-

ated. To investigate the subspace tracking ability, bit-by-bit detection is implemented. The mean signal to interference and noise ratio (SINR) is calculated over all known users with a moving window which has the length of 20.

Figure 4.6, Figure 4.7, and Figure 4.8 show the performance comparison among different multiuser detectors with a various number of both known and unknown users. It has previously been shown that the hybrid group-blind detector using the SVD algorithm has better performance than other detectors. In this section, the performance of the hybrid group-blind multiuser detector using the NA-CSVD is evaluated. Since the NA-CSVD algorithm has a low complexity, i.e., it is less accurate, the performance of the hybrid group-blind detector using the NA-CSVD algorithm is of course worse than when the SVD or FASIR algorithms are used. However, in all cases, it still has a better performance than the partial MMSE (non-blind MMSE) detector and has the advantage of low complexity. Also, it is better than the blind MMSE detector for the case of $\tilde{K} = 7, \tilde{K} = 4$. From the three figures, we can easily recognize that the performance of the NA-CSVD algorithm critically depends on the subspace dimension. As the subspace dimension increases, the performance decreases. As can be seen from the figures, it is obvious that the hybrid group-blind multiuser detector using the NA-CSVD has a much better performance than the blind MMSE detector using the NA-CSVD. The reason is that the hybrid group-blind detector need only track $\tilde{K}$ eigenvalues and eigenvectors, while the blind MMSE

detector must track $\bar{K} + \tilde{K}$ eigenvalues and eigenvectors.

Figure 4.9 shows the BER performance of multiuser detectors. 100 different ensembles of 10,000 bits for each user were generated. For each ensemble of 10,000 bits, the detectors were estimated over the first 300 bits. Figure 4.9 shows that the hybrid group-blind detector has better performance than the blind MMSE detector. In most cases, the hybrid group-blind detector and the blind MMSE detector using the NA-CSVD are worse than when using SVD or FASIR. However, the hybrid group-blind detector using the NA-CSVD has the advantage of low complexity. While this conclusion applies only to the NA-CSVD, it can be expected to hold true for other low complexity subspace tracking algorithms, as these seem to work best for low subspace dimensions. Thus, because of the lower subspace dimension in group-blind type algorithms, these can be expected to work considerably better than the blind algorithms.

4.8 Simulation Results for Asynchronous DS-CDMA systems

We consider an asynchronous CDMA system with 7 known users and 3 unknown users. The users are assigned purely random codes of length $N = 31$. The chip pulse is a raised cosine pulse which has roll-off factor 0.5. Each user's initial delay d_k is uniform on $[0, 4T_c]$. The channel of each user has $L = 3$ paths. The

delay of each path $\tau_{k,l}$ is uniform on $[0, 4T_c]$. Hence the maximum delay spread is $8T_c$. The fading gain of each path in each user's channel is generated from a complex Gaussian distribution and fixed over the duration of one signal frame. The path gains in each user's channel are normalized so that each user's signal arrives at the receiver with the same power. An ensemble of 50 different random code assignments for each user is generated. To investigate the subspace tracking ability, bit-by-bit detection is implemented. The mean signal to interference and noise ratio (SINR) is calculated as a moving average over all known users with a window length of 20.

Figure 4.10 shows a performance comparison for different multiuser detectors. It has previously been shown that the group-blind multiuser detector using the SVD algorithm has better performance than other detectors. Although the FASIR algorithm has low complexity, it has very good performance as can be seen in previous work [22]. But, because of the inaccuracy of the channel estimation, the performance of the group-blind multiuser detector using the FASIR algorithm is worse than when using SVD. However, in all cases, it still has a better performance than the non-blind MMSE detector and has the advantage of low complexity. Also, it is better than the blind MMSE detector in the case of $\bar{K} = 7, \tilde{K} = 3$.

Figure 4.11 shows the BER performance of multiuser detectors. 100 different ensembles of 10,000 bits for each user were generated. For each ensemble of

10,000 bits, the detectors were estimated over the first 1000 bits. As can be seen for Fig. 4.11, the group-blind multiuser detector has better performance than the blind MMSE detector. In most cases, the group-blind multiuser detector and the blind MMSE detector using the FASIR algorithm have worse performance than using SVD. However, the group-blind detector using the FASIR algorithm has the advantage of low complexity. Unlike the synchronous case [22], blind channel estimation is the main performance degradation factor in the asynchronous CDMA systems model.

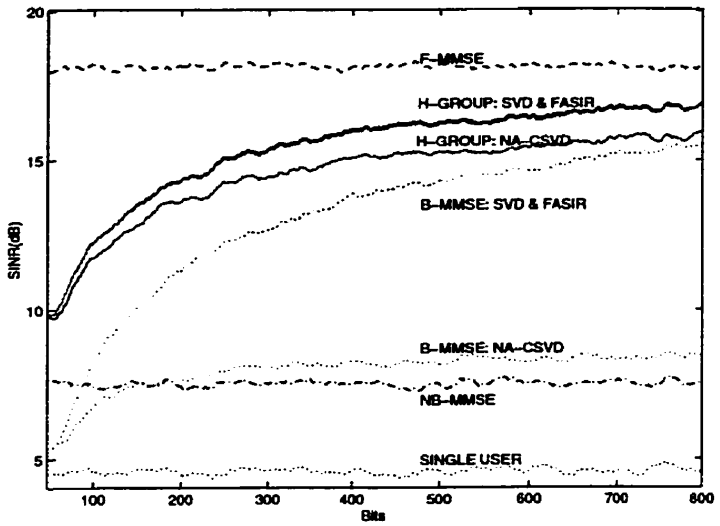

Figure 4.6: Performance comparison of multiuser detectors with respect to bits: $K = 7$, $\tilde{K} = 4$, and SNR=20dB

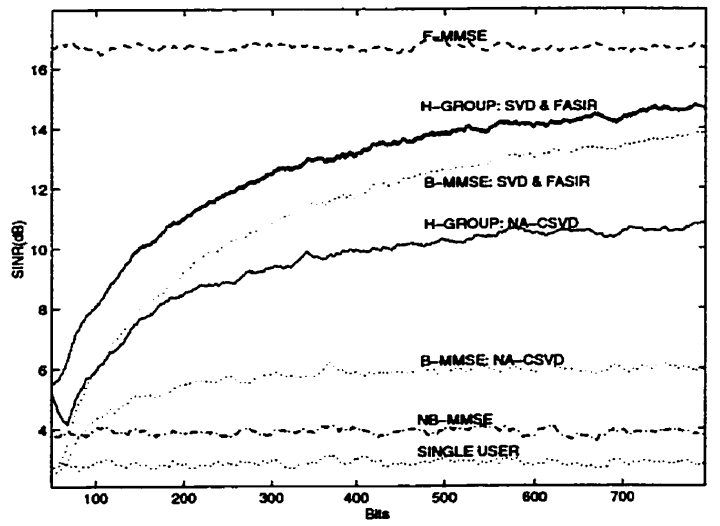

Figure 4.7: Performance comparison of multiuser detectors with respect to bits: $K = 7$, $\tilde{K} = 10$, and SNR=20dB

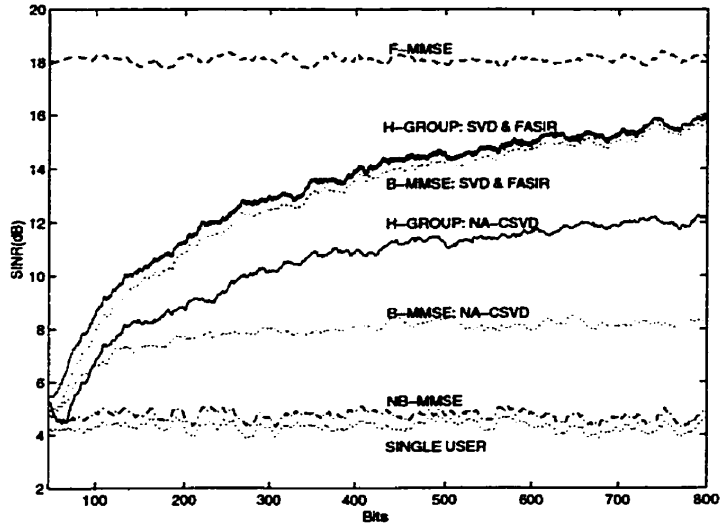

Figure 4.8: Performance comparison of multiuser detectors with respect to bits: $K = 2$, $\tilde{K} = 10$, and SNR=20dB

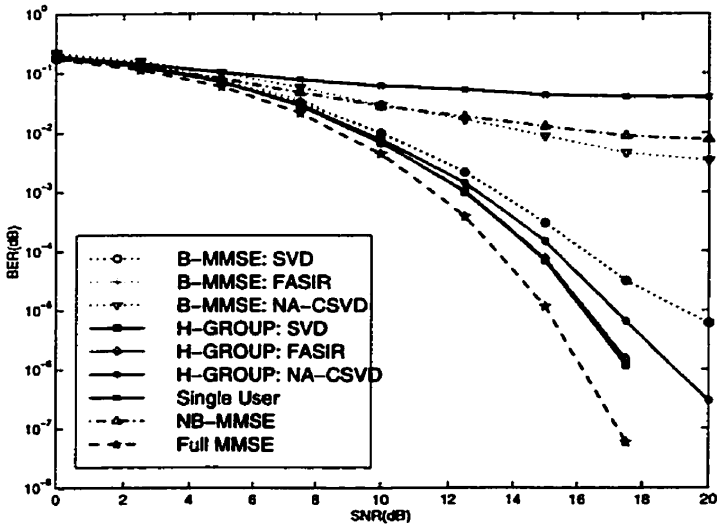

Figure 4.9: BER of multiuser detectors with respect to SNR: $K = 7$, $\tilde{K} = 4$

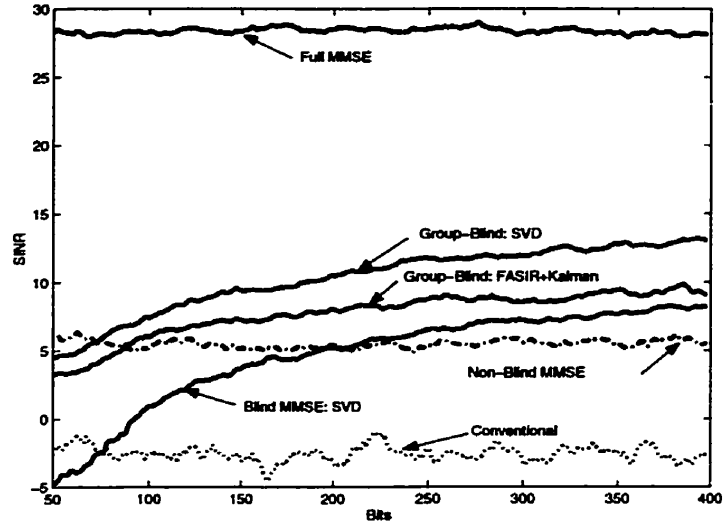

Figure 4.10: Performance of the Group-blind linear hybrid detector implemented by the FASIR algorithm and Kalman tracking: SNR=20dB, 7 known users and 3 unknown users

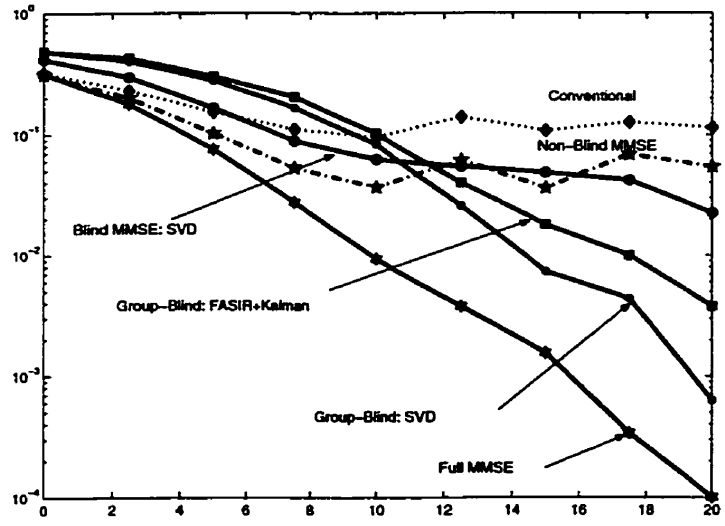

Figure 4.11: BER performance of multiuser detectors with respect to SNR: $K = 7$, $\tilde{K} = 3$

Chapter 5

Group-blind Multiuser Detection for UTRA-TDD

5.1 UMTS Terrestrial Radio Access

In the European third generation mobile radio system, Universal Mobile Telecommunications System (UMTS), there is a complex UMTS air interface called UMTS Terrestrial Radio Access (UTRA) for the requirements of different services. The UTRA consists of two modes, the UTRA-FDD (Frequency Division Duplex) [25] which uses the different frequencies for the uplink and downlink transmissions and UTRA-TDD (Time Division Duplex) [26] which uses the same frequency for the uplink and downlink transmissions. The UMTS spectrum was depicted in Figure 5.1. The basic technologies for the UTRA are wideband code

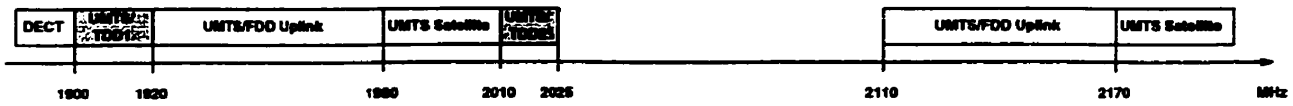

Figure 5.1: UMTS spectrum allocation

division multiple access (WCDMA) for the FDD mode and time-division CDMA (TD-CDMA) for the TDD mode as described in Figure 5.2.

Duplex Scheme	UTRA-FDD	UTRA-TDD
Multiple Access Scheme	WCDMA	TD-CDMA
Modulation	QPSK	QPSK
Frame Length	10 ms	10 ms
Pulse Shaping	Root Raise Cosine, r=0.22	Root Raise Cosine, r=0.22
Number of time slots per frame	15 slots	15 slots
Chip rate	3.84 Mchips/s	3.84 Mchips/s
Bandwidth	5 MHz	5 MHz
Multirate concept	multicode and orthogonal variable spreading factor (OVSF)	multicode , multislot and OVSF
Channel allocation	no dynamic channel allocation (DCA) required	slow and fast DCA supported
Capacity allocation between uplink and downlink	5 MHz for uplink 5 MHz for downlink	5 MHz carrier divided between uplink and downlink (2-14 out of 15 slots)

Table 5.1: Basic system parameters of UTRA-TDD and FDD

The basic system parameters of UTRA-TDD and FDD are described in Table 5.1 There are some characteristics of UTRA-TDD systems listed below.

- **Reciprocal channel:** In UTRA-FDD, the fast fading of uplink is different from down link because the fast fading is up to the frequency. However, the same frequency is employed in both uplink and downlink in UTRA-TDD, the fast fading is the same in both uplink and downlink. This enables the transceiver to estimate the fast fading for its transmission from the

received signal.

- **Unpaired band:** While UTRA-FDD requires a pair of bands, UTRA-TDD can be implemented on an unpaired band.

- **Flexible capacity allocation:** In UTRA-TDD, there exists flexible capacity allocation between the uplink and the downlink. If the capacity requirement is asymmetric between the uplink and the downlink, the capacity can be adjusted by duplex switching point.

- **Interference between uplink and downlink:** Since both uplink and downlink use the same frequency, the transmitted signal of uplink can interfere with the received signal of downlink, and vice versa.

In UTRA-TDD mode , the duration of a frame is $10ms$ and it is subdivided into 15 time slots of $625\mu s$ duration. Within each time slot, orthogonal variable spreading factor (OVSF) codes of length 16 are used for user signal separation. The TDD frame is divided into downlink and uplink parts as depicted in Figure 5.3. To change the transmit direction, the switching points (SWPs) are used. By varying the position of the SWP, asymmetrical data rates can easily be realized.

There are two benefits in UTRA-TDD mode. First, the TDD mode is well suited for microcell/picocell environment for high bit rates and low mobility applications through the use of variable asymmetric traffic. Second, the TDD mode benefits from the reciprocal nature of the channel, i.e., we can use the

impulse response of the uplink channel for the downlink channel of a user.

5.2 Interference between Uplink and Downlink in UTRA-TDD

The primary limiting factors of the TDD mode are synchronization difficulties and the associated interference problems. The asymmetric allocation of traffic leads to an interference scenario that will impact the overall spectral efficiency of a TDD mode. Figure 5.4 depicts this scenario. two neighboring cells use the same frequency and have different uplink/downlink asymmetric traffic and the MS2 is near border of cell and transmitting signal with full power. MS1 has more downlink traffic than MS2. In this case, the uplink transmission from MS2 to BS2 can block the downlink transmission from BS1 to MS1 causing the inter-cell interference. the inter-cell interference can be avoided using a dynamic resource allocation (DRA) algorithm.

5.3 Group-Blind Multiuser Detection for UTRA-TDD

In this section, we will discuss the group-blind linear hybrid multiuser detector in UTRA-TDD mode. Consider an asynchronous time duplex code division mul-

tiple access (TD-CDMA) system with $\bar{K}$ known users in a cell and $\tilde{K}$ interfering users from adjacent cells. To use QPSK modulation, complex values are used for data symbols The received signal can be expressed as

$$\mathbf{r} = \bar{\mathbf{H}}\bar{\mathbf{b}} + \tilde{\mathbf{H}}\tilde{\mathbf{b}} + \sigma\mathbf{v} \tag{5.1}$$

where $\bar{\mathbf{H}}$ and $\tilde{\mathbf{H}}$ are the channel matrices for the in-cell users and other-cell users, $\bar{\mathbf{b}}$ and $\tilde{\mathbf{b}}$ are the data symbols, $\mathbf{v}$ is the additive Gaussian noise with unit power, and σ^2 is the variance of noise. The data symbols consist of asymmetric uplink/downlink time slots as depicted in Figure 5.4. Let $\bar{\mathbf{P}}^{\perp}$ be the orthogonal projection onto the space orthogonal to the in-cell users channel matrix $\bar{\mathbf{H}}$ given by

$$\bar{\mathbf{P}}^{\perp} = \mathbf{I} - \bar{\mathbf{H}}(\bar{\mathbf{H}}^T\bar{\mathbf{H}})^{-1}\bar{\mathbf{H}}^H, \tag{5.2}$$

where $\mathbf{I}$ is the identity matrix. The orthogonal projection of the correlation matrix $\hat{\mathbf{R}} = E[\mathbf{r}\mathbf{r}^H]$ can then be decomposed as

$$\begin{aligned}\bar{\mathbf{P}}^{\perp}\mathbf{R}\bar{\mathbf{P}}^{\perp} &= \left[\tilde{\mathbf{U}}_s\tilde{\mathbf{U}}_n\tilde{\mathbf{U}}_o\right]\begin{bmatrix}\tilde{\Lambda}_s & \mathbf{0} & \mathbf{0}\\ \mathbf{0} & \sigma^2\mathbf{I} & \mathbf{0}\\ \mathbf{0} & \mathbf{0} & \mathbf{0}\end{bmatrix}\begin{bmatrix}\tilde{\mathbf{U}}_s^H\\ \tilde{\mathbf{U}}_n^H\\ \tilde{\mathbf{U}}_o^H\end{bmatrix}\\ &= \tilde{\mathbf{U}}_s\tilde{\Lambda}_s\tilde{\mathbf{U}}_s^H + \sigma^2\tilde{\mathbf{U}}_n\tilde{\mathbf{U}}_n^H\end{aligned} \tag{5.3}$$

where $\tilde{\mathbf{U}}_s$, $\tilde{\mathbf{U}}_n$, $\tilde{\mathbf{\Lambda}}_s$ are the signal subspace eigenvector matrix, the noise subspace eigenvector matrix, and the signal subspace eigenvalue matrix, respectively. The exact group-blind hybrid multiuser detector [20] is then given by

$$\hat{\bar{b}}_k = \mathbf{sgn}\left(\mathbf{1}_k^T(\bar{\mathbf{H}}^H\bar{\mathbf{H}})^{-1}\bar{\mathbf{H}}^H(\mathbf{I} - \mathbf{R}\tilde{\mathbf{U}}_s\tilde{\mathbf{\Lambda}}_s^{-1}\tilde{\mathbf{U}}_s^H)\mathbf{r}\right) \tag{5.4}$$

The group-blind linear hybrid multiuser detector can reduce intra-cell interference from the cell and the inter-cell interference from adjacent cells efficiently.

Figure 5.5 compares the performance of the exact group-blind multiuser detector with the performance of the traditional partial MMSE detector, which ignores interference from adjacent cells. It is seen that the group-blind linear hybrid multiuser detector has a better performance than the partial MMSE detector for the time slots 4-10 where the information is seriously corrupted by interfering users from adjacent cells. While the partial MMSE detector can only reduce intra-cell interference, the group-blind linear hybrid multiuser detector can reduce both intra-cell and inter-cell interference. The correlation matrix was estimated in each time slot for the estimated group-blind linear hybrid multiuser detector. The estimated group-blind linear hybrid multiuser detector can be expressed as

$$\hat{\bar{b}}_k[n] = \mathbf{sgn}\left(\mathbf{1}_k^T(\bar{\mathbf{H}}^H\bar{\mathbf{H}})^{-1}\bar{\mathbf{H}}^H(\mathbf{I} - \hat{\mathbf{R}}\hat{\tilde{\mathbf{U}}}_s[n]\hat{\tilde{\mathbf{\Lambda}}}_s^{-1}[n]\hat{\tilde{\mathbf{U}}}_s^H[n])\mathbf{r}[n]\right) \tag{5.5}$$

Figure 5.6 shows a performance of the estimated hybrid group-blind multiuser detector with respect to time slots. After time slot 5, the SINR of the estimated group-blind linear hybrid group-blind multiuser detector cross over the SINR of the partial MMSE detector. In the time slot 11-15, since there are no interfering users from adjacent cells, the group-blind linear hybrid multiuser detector is the same as the zero-forcing detector, i.e., $\hat{\bar{b}}_k[n] = \mathbf{sgn}\left(\mathbf{1}_k^T(\bar{\mathbf{H}}^H\bar{\mathbf{H}})^{-1}\bar{\mathbf{H}}^H\mathbf{r}[n]\right)$. Thus, the problem of UTRA-TDD can be solved with the group-blind linear hybrid multiuser detector.

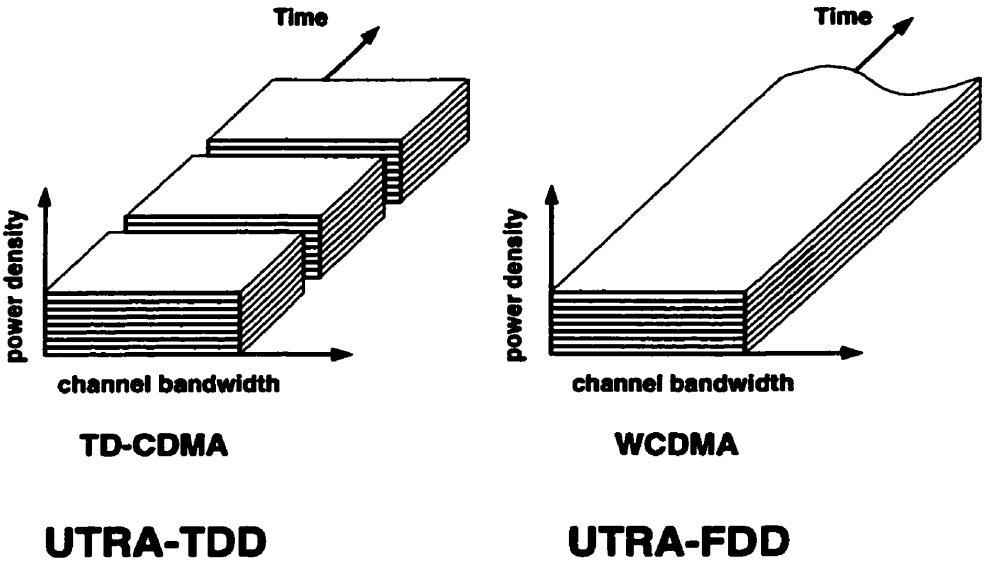

Figure 5.2: UMTS Terrestrial Radio Access (UTRA)

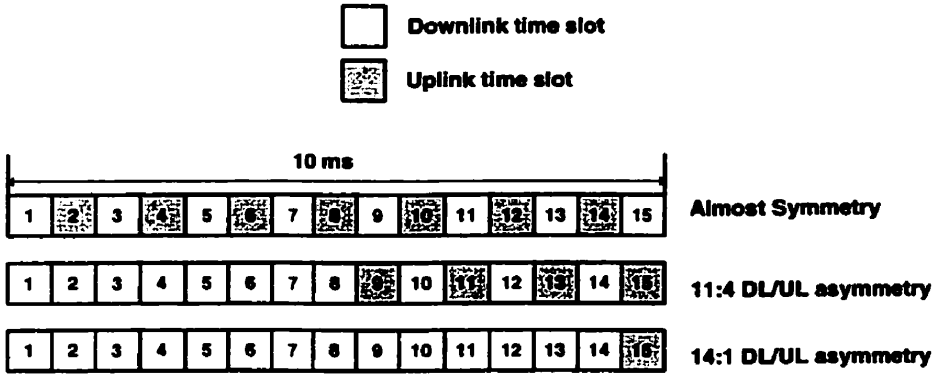

Figure 5.3: Frame structure of UTRA-TDD

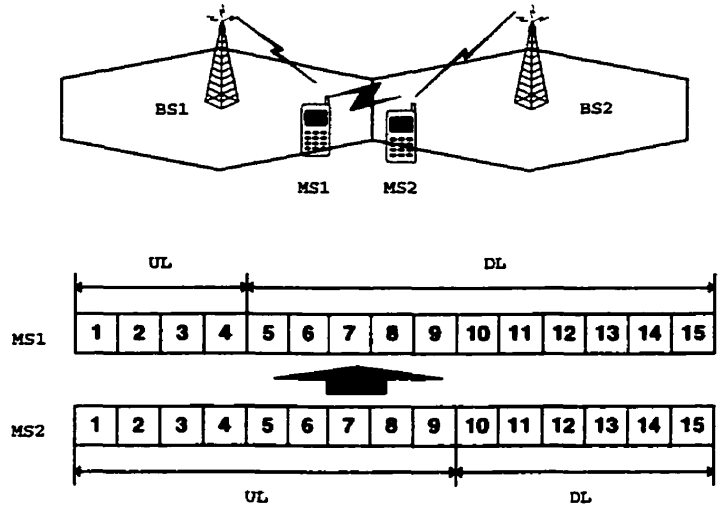

Figure 5.4: Interference scenario and UTRA-TDD frame structure

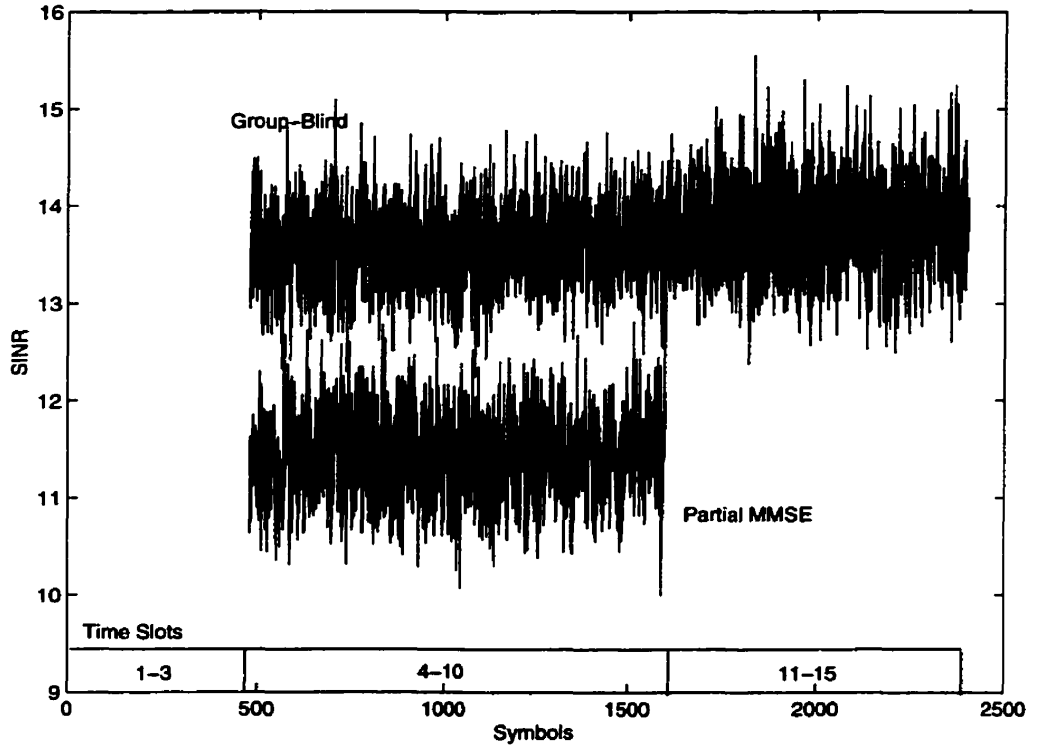

Figure 5.5: Performance of the exact group-blind linear hybrid detector in the UTRA-TDD mode with SIR=-20dB, SNR=20dB, 6 in-cell users, and 4 interfering users from adjacent cells.

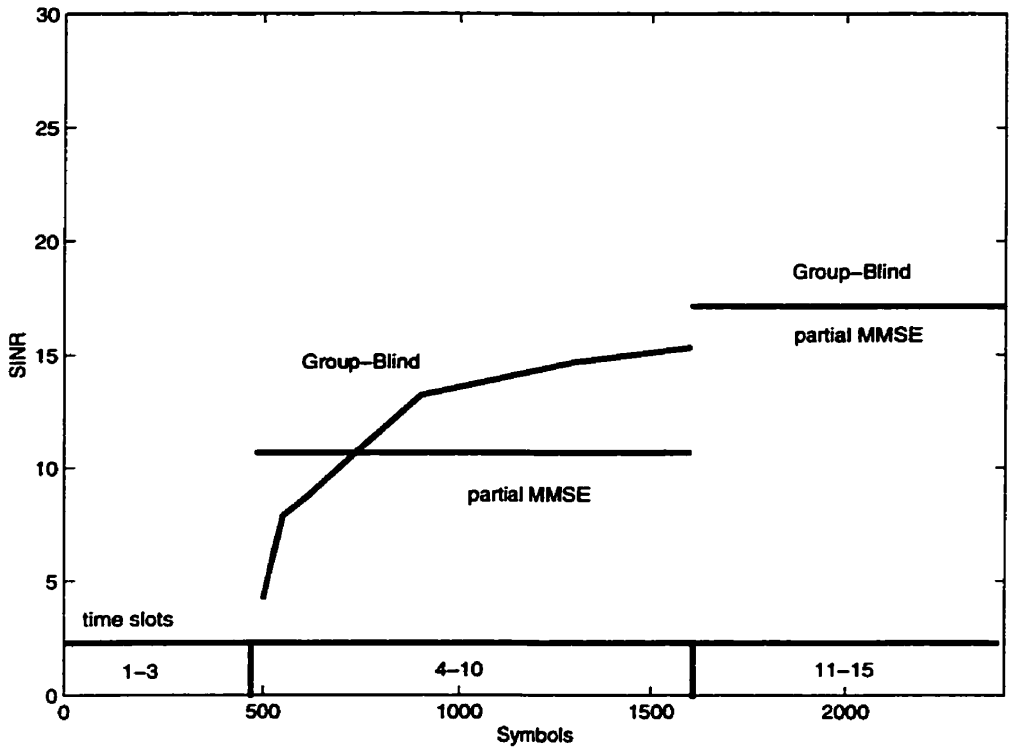

Figure 5.6: Performance of the estimated group-blind linear hybrid detector in the UTRA-TDD mode with SIR=-20dB, SNR=20dB, 6 in-cell users, and 4 interfering users from adjacent cells.

Chapter 6

Conclusion and Future Work

6.1 Conclusion

In this thesis, we have demonstrated that group-blind multiuser detectors reduce both intra-cell and inter-cell interference efficiently. The group-blind multiuser detectors were introduced and evaluated for both synchronous and asynchronous systems. In most cases, the group-blind multiuser detectors have better performance compared to traditional multiuser detectors such as the conventional detector, the blind MMSE detector, and the partial MMSE detector.

Exact group-blind multiuser detectors which use the exact correlation matrix have the same SINR as the ideal full MMSE detector when inter-cell interference occurs. However, estimated group-blind multiuser detectors need to be trained to get the exact correlation matrix with the time average method. But they

converge in performance to the ideal full MMSE detector. Blind channel estimation and subspace tracking algorithms to update the eigen components with low calculation complexities have been studied.

Because the hybrid group-blind multiuser detector has an excellent performance when the time slots are corrupted by inter-cell interference, the hybrid group-blind multiuser detector is effective for UTRA-TDD systems which suffer from serious inter-cell interference.

In this thesis, my contributions are an adaptation of two subspace tracking algorithms to group-blind multiuser detection to reduce calculation complexity, and the application of group-blind multiuser detection in UTRA-TDD.

6.2 Future Work

In this thesis, we assumed that the number of users in the received signal is known to the receiver. However, a user can appear or disappear in cellular systems. This information is very important for proper separation of the noise subspace and signal subspace in SVD or subspace tracking. An estimation of the number of users required to implement a group-blind multiuser detector should be examined.

So far, the group-blind multiuser detector considers one antenna. A performance improvement is expected when space-time signal processing with lower complexity is used. Although there are fast DSP processors available, the devel-

opment of a complexity reduced subspace tracking algorithm and an iterative implementation of the group-blind multiuser detector are suggested.

Bibliography

[1] C. Shannon, "A Mathematical Theory of Communication," Bell System Technical Journal, Vol. 27, 1948, pp. 379-423 and 623-656.

[2] "A conversation with Claude Shannon," IEEE Commun. Mag., Vol. 22, No. 5, May 1984, pp.123-126.

[3] Scholtz, "The Evolution of Spread-Spectrum Multiple-Access Communications," in Code Division Multiple Access Communications (S. G. Glisic and P. A. Leppanen, Eds., Kluwer Academic Publishers, 1995.

[4] Cooper and R. W. Nettleton, "A spread-spectrum techniques for high-capacity mobile communications," IEEE Trans. Veh. Tech., Vol. 27, No. 4, Nov. 1978, pp. 264-275.

[5] S. Verdu, "Minimum Probability of Error for Asynchronous Gaussian Multiple Access," IEEE Trans. on IT., Vol. IT-32, No. 1, Jan. 1986, pp. 85-96.

[6] H. V. Poor and S. Verdu, "Single-user detectors for multiuser channels," IEEE Trans. Commun., vol. 36, no. 1, pp. 50-60, Jan. 1988.

[7] A. M. Monk, M. Davis, L. B. Milstein, and C. W. Helstrom, "A noise whitening approach to multiple access noise rejection part I: Theory and Background," IEEE J. Select. Areas on Comm., vol. 12, no. 5, pp. 817-827, June 1994.

[8] M. Rupf, F. Tarkoy, and J. L. Massey, "User-separating demodulation for code-division multiple-access systems," IEEE J. Select. Areas on Comm., vol. 12, no. 4, pp. 786-795, May 1994.

[9] A. J. Viterbi, "Very Low Rate Convolutional Codes for Maximum Theoretical Performance of Spread-Spectrum Multiple-Access Channels," IEEE JSAC, vol. 8, no. 4, May 1990, pp. 641-49.

[10] R. Kohno et al., "Combination of an Adaptive Array Antenna and a Canceller of Interference for Direct-Sequence Spread-Spectrum Multiple-Access System," IEEE JSAC, vol. 8, no. 4, May 1990, pp. 675-82.

[11] R. Kohno et al., "An Adaptive Canceller of Cochannel Interference for Spread- Spectrum Multiple-Access Communication Networks in a Power Line," IEEE JSAC, vol. 8, no. 4, May 1990, pp. 691-99.

[12] K. S. Schneider, "Optimum Detection of Code Division Multiplexed Signals," IEEE Trans. Aerospace Elect. Sys., vol. AES-15, no., Jan. 1979, pp. 181-85.

[13] R. Lupas and S. Verdu, "Linear Multi-User Detectors for Synchronous Code-Division Multiple-Access Channels," IEEE Trans. Info. Theory, vol. 35, no. 1, Jan. 1989, pp. 123-36.

[14] R. Lupas and S. Verdu, "Near-Far Resistance of Multi-User Detectors in Asynchronous Channels," IEEE Trans. Commun., vol. 38, no. 4, Apr. 1990, pp. 496- 508.

[15] Z. Xie, R. T. Short, and C. K. Rushforth, "A Family of Suboptimum Detectors for Coherent Multi-User Communications," IEEE JSAC, vol. 8, no. 4, May 1990, pp. 683- 90.

[16] M. Honig, U. Madhow, and S. Verdu, "Blind Adaptive Multiuser Detection," IEEE Trans. Info. Theory, vol. 41, no. 4, July 1995, pp. 944-60.

[17] X. Wang and H.V. Poor, "Blind multiuser detection: A subspace approach," *IEEE Trans. Inform. Theory*, 44(2):677–691, Mar. 1998.

[18] J. R. Westlake. *A handbook of numerical matrix inversion and solution of linear equations.* John Wiley & Sons, Inc., New York, 1968., pp. 30-31

[19] Anders Hst-Madsen, "Semi-Blind Decorrelating Multi-User Detectors for CDMA: Subspace Methods," presented at PIMRC 98.

[20] X. Wang and A. Høst-Madsen, "Group-Blind Multiuser Detection for Up-

link CDMA," *IEEE Journal on Selected Areas in Communications*, vol. 17, No. 11, pp. 1971, Nov. 1999

[21] A. Høst-Madsen and Jae-Chon Yu, "Hybrid semi-blind multiuser detection: subspace tracking method," *ICASSP, IEEE International Conference on Acoustics, Speech and Signal Processing* - Proceedings, vol. 5, Mar 15-Mar 19 1999, pp. 2695-2698.

[22] Jae-Chon Yu and A. Høst-Madsen, "Subspace Tracking for Semi-Blind Multiuser Detectors," *IEEE Vehicular Technology Conference-Spring Proc.*, vol. 2, May 16-May 20 1999, pp. 1042-1046.

[23] Jae-Chon Yu, A. Høst-Madsen, and X. Wang "Subspace Tracking for Group-Blind Multiuser Detection in Asynchronous DS-CDMA Systems," *IEEE Vehicular Technology Conference-Spring Proc.*, vol. 2, May 15-May 18 2000, pp. 1042-1046.

[24] Anders Høst-Madsen and X. Wang, "Performance of Blind and Group-Blind Multiuser Detectors," submitted to *IEEE Transactions on Information Theory.*

[25] 3GPP TS 25.211 to TS 25.214 (UTRA-FDD), http://www.3gpp.org/ftp/Specs/, March 2000.

[26] 3GPP TS 25.221 to TS 25.224 (UTRA-TDD), http://www.3gpp.org/ftp/Specs/, March 2000.

[27] S. Verdú. *Multiuser Detection.* Cambridge University Press: Cambridge, UK, 1998.

[28] Y-H. Chen and C-T. Chiang. "Kalman-based estimator for DOA estimation," *IEEE Trans. Signal Proc.*, 42(12):3543-3547, Dec. 1994.

[29] P. Comon, and G.H. Golub, "Tracking a few extreme singular values and vectors," in signal processing *Proc. IEEE*, 78(8), 1327-1343, Aug. 1990.

[30] Pango, P. A. and Champagne, B., "On the issue of Rank Estimation in Subspace Tracking : the NA-CSVD Solution," *Proc. European Signal Processing Conference, EUSIPCO-1998*, Rhodes, Sept. 8-11 1998.

[31] Pango, P. A. and Champagne, B., "On the Efficient use of Givens Rotations in SVD-based Subspace Tracking," *Signal Processing* vol. 74, No. 3, May 1999 pp. 253-277.

[32] Yang, B., "Projection approximation subspace tracking," *IEEE Trans. Sig. Proc.*, vol, 44(1), pp. 95-107, Jan. 1995.